

Wireless Networks

Wei Song
Peijian Ju
A-Long Jin

Protocol Design and Analysis for Cooperative Wireless Networks

 Springer

Wireless Networks

Series Editor

Xuemin Sherman Shen
University of Waterloo, Waterloo, Ontario, Canada

More information about this series at <http://www.springer.com/series/14180>

Wei Song • Peijian Ju • A-Long Jin

Protocol Design and Analysis for Cooperative Wireless Networks

 Springer

Wei Song
Faculty of Computer Science
University of New Brunswick
Fredericton, NB, Canada

Peijian Ju
IBM Canada
Fredericton, NB, Canada

A-Long Jin
University of Waterloo
Waterloo, ON, Canada

ISSN 2366-1186

Wireless Networks

ISBN 978-3-319-47725-1

DOI 10.1007/978-3-319-47726-8

ISSN 2366-1445 (electronic)

ISBN 978-3-319-47726-8 (eBook)

Library of Congress Control Number: 2016954727

© Springer International Publishing AG 2017

This work is subject to copyright. All rights are reserved by the Publisher, whether the whole or part of the material is concerned, specifically the rights of translation, reprinting, reuse of illustrations, recitation, broadcasting, reproduction on microfilms or in any other physical way, and transmission or information storage and retrieval, electronic adaptation, computer software, or by similar or dissimilar methodology now known or hereafter developed.

The use of general descriptive names, registered names, trademarks, service marks, etc. in this publication does not imply, even in the absence of a specific statement, that such names are exempt from the relevant protective laws and regulations and therefore free for general use.

The publisher, the authors and the editors are safe to assume that the advice and information in this book are believed to be true and accurate at the date of publication. Neither the publisher nor the authors or the editors give a warranty, express or implied, with respect to the material contained herein or for any errors or omissions that may have been made.

Printed on acid-free paper

This Springer imprint is published by Springer Nature

The registered company is Springer International Publishing AG

The registered company address is: Gewerbestrasse 11, 6330 Cham, Switzerland

Preface

Cooperative wireless networks have emerged as a promising technology that allows wireless devices to take advantage of diversity and the broadcast nature of wireless medium. Nonetheless, some important issues remain to be addressed to enable practical implementation. In particular, with the fast-growing mobile traffic and rising energy costs, energy saving needs to be taken into account in the design of cooperative protocols. In addition, many designs and analyses assume that the locations of cooperative wireless nodes are deterministic or known a priori. However, due to user mobility and/or network dynamics, the node locations are spatially random. Hence, this feature should be properly incorporated into the protocol design and analysis for cooperative wireless networks.

In this book brief, we focus on the design and analysis of protocols for cooperative wireless networks, especially, at the medium access control (MAC) layer and cross-layer design between the MAC layer and the physical layer. It first provides a comprehensive review of existing studies in the literature and points out the problems that are worth further investigation. Then, it introduces several novel solutions for cooperative wireless network protocols, aiming to reduce energy consumption and address spatial random distribution of wireless nodes. For each solution, it gives a clear system model and problem formulation, details of the proposed cooperative schemes, comprehensive performance analysis, and extensive numerical and simulation results that validate the analysis and examine the performance under various conditions. At the end of this book brief, we also highlight several interesting directions on cooperative wireless networks that deserve future exploration.

Fredericton, Canada
Fredericton, Canada
Waterloo, Canada

Wei Song
Peijian Ju
A-Long Jin

Contents

1	Introduction	1
1.1	Motivations	1
1.2	Challenges	2
1.2.1	Energy Saving with Spatially Random Relays	2
1.2.2	Cooperative Diversity with Multiple Relays	2
1.3	Outline	3
	References	4
2	Related Works on Cooperative Wireless Networks	7
2.1	Cooperative Communications	7
2.2	Cooperation Scenarios	9
2.3	Three Categories of Cooperative MAC Protocols	12
2.3.1	Category-I	13
2.3.2	Category-II	15
2.3.3	Category-III	17
2.4	Research Issues for MAC-Layer Cooperation	19
2.4.1	New Categories	19
2.4.2	Cooperative Diversity	20
2.4.3	User Mobility	21
2.4.4	Energy Saving	22
	References	23
3	Energy-Efficient Uncoordinated Cooperative MAC with Uncertain Relay Distribution Intensity	27
3.1	Motivation and Overview	27
3.2	System Model and Problem Formulation	28
3.2.1	System Model	28
3.2.2	Problem Formulation	31
3.3	Relay Intensity Estimation	32
3.4	Energy-Efficient Cooperative Scheme and Its Analysis	37
3.4.1	An Energy-Efficient Cooperative Scheme	37
3.4.2	Analysis of Collision Probability	41

3.5	Numerical and Simulation Results	43
3.5.1	Relay Intensity Estimation	43
3.5.2	Energy Saving Strategy	44
3.5.3	Performance Evaluation	46
3.6	Summary	49
	Appendix A: Extended Proof of Lemma 3.2 with N Relays	49
	Appendix B: Proof of (3.34) and (3.35)	50
	References	51
4	Energy-Aware Cooperative MAC with Uncoordinated Group Relays	53
4.1	Motivation and Overview	53
4.2	System Model and Problem Formulation	54
4.2.1	System Model	54
4.2.2	Problem Formulation	56
4.3	Energy-Aware Cooperation Strategy	57
4.3.1	Cooperation Criteria	57
4.3.2	Distributed Cooperation Strategy	58
4.4	Performance Analysis	60
4.4.1	Upper Bound of Collision Probability	60
4.4.2	Lower Bound of Transmission Success Probability	63
4.4.3	Upper Bound of Transmission Success Probability	64
4.5	Numerical and Simulation Results	65
4.5.1	Transmission Success Probability	67
4.5.2	Average Delay and Delay Outage Probability	67
4.5.3	Energy Saving and Energy Balance	69
4.5.4	Scalability	71
4.6	Summary	73
	Appendix A: Proof of (4.17)	73
	Appendix B: Proof of (4.25)	74
	References	75
5	Opportunistic Cooperative Relaying with Backoff-Based Contention	77
5.1	Motivation and Overview	77
5.2	System Model	78
5.3	Cooperative Relaying Strategies	80
5.3.1	Inter-Group Backoff-Based Contention	81
5.3.2	Intra-Group Contention	81
5.4	Performance Analysis	83
5.4.1	Probability Distributions of Spatial Random Relays	84
5.4.2	Performance of Two-Level Backoff-Based Strategy	86
5.4.3	Performance of Hybrid Relaying Strategy	89
5.5	Numerical Results and Discussions	90
5.5.1	CDF of Transmission Success Probability	91
5.5.2	Performance Upper and Lower Bounds	93

- 5.5.3 Relay Success Probability 94
- 5.5.4 Backoff Delay of Relay Selection..... 98
- 5.6 Summary 100
- Appendix: Calculation of the CDF $F_{\Gamma,I}(x)$ of $\Gamma_{RD,I}$ 101
- References 103
- 6 Diversity Relaying with Spatially Random Mobile Relays 105**
 - 6.1 Motivation and Overview 105
 - 6.2 System Model 107
 - 6.2.1 Channel Model 107
 - 6.2.2 Mobility Model and Poisson Point Process 108
 - 6.2.3 Distributed Cooperative Transmission 108
 - 6.2.4 MAC for Multi-Helper Coordination 109
 - 6.2.5 MRC and Upper Bound of Total SNR 111
 - 6.3 Unconditional Success Probability and Delay 112
 - 6.3.1 Exact Unconditional PDF of SNR Upper Bound 112
 - 6.3.2 Approximate Unconditional PDF of SNR Upper Bound 114
 - 6.3.3 Approximation of Unconditional Success Probability 115
 - 6.3.4 Delay Analysis of MAC Coordination Schemes 116
 - 6.3.5 Outage-Delay Tradeoff 118
 - 6.4 Numerical and Simulation Results 119
 - 6.4.1 Analysis Validation 120
 - 6.4.2 Outage-Delay Tradeoff 123
 - 6.5 Summary 124
 - Appendix: Proof of Lemma 6.1 125
 - References 126
- 7 Conclusions and Future Directions 129**
 - 7.1 Conclusions 129
 - 7.2 Future Work 130

Chapter 1

Introduction

1.1 Motivations

In the past decade, wireless networks have been widely studied and used. However, wireless communications face several challenging issues which are not imposed in wired networks, such as mobility, power consumption, interference and reliability. Besides, signal fading is often a problem in wireless networks, which is caused by multipath propagation and shadowing. To deal with these challenges, attractive techniques, such as multiple input and multiple output (MIMO) and cooperative communications [4, 7], have been developed by exploiting spatial diversity. Nonetheless, due to the size, cost and energy limitations of mobile devices, it can be infeasible to deploy multiple antennas in some wireless terminals. In order to meet the needs of future wireless networks, user cooperation [13] is studied as a promising low-cost technique to provide spatial diversity. Taking advantage of the inherent broadcasting nature of the wireless medium, the nodes with good channel conditions can forward the overheard data to facilitate the transmission between source (S) and destination (D).

Originally, most of the research works focus on the physical layer cooperation [4, 7], where the cooperative schemes pay more attention to the various methods of signal processing at the relay node and signal combination at the destination node. With physical layer cooperation, either diversity or multiplexing can be achieved, which improves the quality of communications in the upper layers. Since multiple cooperative nodes are available during packet transmission, it is vital to coordinate these nodes to access the channel in a cooperative fashion. To achieve the cooperation gain at upper layers, considerable research attention has been attracted to the medium access control (MAC) layer [6, 9]. Different from physical layer cooperation, MAC layer cooperation needs to figure out *when to cooperate* and *whom to cooperate with*.

While centralized solutions [2, 5, 6] can rely on a central controller to determine the best relays, distributed solutions also attract considerable research attention

due to lightweight signaling and good scalability. In the probability-based schemes [10–12], each relay that successfully overhears the data from the source independently determines a forwarding probability by synthesizing a variety of factors. In the backoff-based schemes [1, 8], each relay makes use of local information to tune a backoff time so that a best relay with a smallest backoff time wins the contention to forward the overheard data. Although cooperative MAC has been widely studied, many practical issues remain to be addressed.

1.2 Challenges

1.2.1 *Energy Saving with Spatially Random Relays*

With rising energy costs and rigorous environmental standards, green communications become a new research trend in recent years, especially, to accommodate the fast-growing multimedia services in wireless networks, since mobile devices are usually energy-constrained. Hence, how to reduce energy consumption is a critical issue for MAC layer cooperation. Besides, many existing works assume that the network topology is known a priori [10] and focus on the throughput perspective [6]. It is vital to relax the assumption of deterministic known topology and take into account relaying nodes that are randomly distributed in a spatial area.

1.2.2 *Cooperative Diversity with Multiple Relays*

As motivated by diversity and MIMO, cooperative relay links and the direct link can be used to transmit the same packet to achieve diversity. A key problem is to choose a good criterion to start cooperation. Cross-layer techniques can be employed to dynamically estimate the channel condition. If a transmission failure is very likely to happen with a poor direct link condition, cooperative diversity transmission is initiated to satisfy certain QoS requirements [2]. Whether the source should always enable diversity transmission or only activate it on demand depends on factors such as the energy consumption and availability of helpers.

Another essential question to exploit diversity gain is the selection of a single optimal helper or multiple uncorrelated helpers with limited interference and power consumption. From the physical-layer standpoint, multiple helpers can improve diversity to achieve a higher signal-to-noise ratio (SNR) and better performance. However, from the link layer's point of view, multiple relays may not perform better than a single best relay, because of the overhead to coordinate multiple relays and manage transmissions. Intuitively, the more helpers, the more complex the coordination. Besides, multiple helpers may increase energy consumption and possibilities of collisions (e.g., due to the hidden terminal and exposed terminal problems).

On the other hand, a single best relay requires less complex coordination and can achieve the full diversity order (selection diversity) [3]. Nonetheless, it is challenging to identify a single best relay in real time since the information available to the source may be out-of-date quickly when nodes are moving fast. As a result, it is necessary to balance a tradeoff between the performance gain and coordination overhead when we decide to choose multiple helpers or a single best helper [9, 13]. This is a slightly different view from that of the physical layer, where more relays can provide better performance.

1.3 Outline

In this book brief, Chap. 2 first reviews the background and related works on the physical layer and the MAC layer of cooperative wireless networks. After that, we present several state-of-the-art solutions which can well address the above challenges.

In Chaps. 3 and 4, we focus on energy saving for cooperative MAC with spatially random relays. In Chap. 3, we first introduce an algorithm to estimate the unknown intensity of relay distribution, which is critical to properly engage cooperating nodes. The convergence and accuracy of the estimation algorithm are theoretically justified. Considering a backoff-based distributed relay scheme, we further incorporate an energy saving scheme to minimize energy consumption while maintaining satisfactory transmission success probability. The performance of the proposed cooperative scheme, particularly the collision probability, is analytically evaluated, since it determines the transmission success probability and thus the average energy consumption. The simulation results validate the analysis and demonstrate that the proposed cooperative scheme outperforms the uncoordinated reference scheme with respect to transmission performance and energy saving.

In Chap. 4, extending the single S-D pair cooperation scenario, we consider a new framework where multiple S-D pairs share a group of relays with energy constraint. To satisfy the QoS requirements of multimedia services in a green manner, we introduce an energy-aware distributed cooperation scheme based on the backoff timer. Also, its performance is evaluated analytically with respect to the theoretical bounds of the collision probability and the transmission success probability. Extensive simulations are conducted to compare the performance of different distributed schemes and the analytical bounds. The theoretical and simulation results demonstrate that the proposed scheme is preferable for the delay-sensitive multimedia services and achieves significant energy saving.

In Chap. 5, we focus on an opportunistic relaying scenario and develop two distributed cooperation strategies. Both adopt a backoff-based inter-group coordination, while the intra-group contention is based on either the forwarding probability or the backoff timer. In particular, we employ *stochastic geometry* to address the impact of spatial distribution of relays. Considering a Poisson point process for random relays, we derive the probability distributions of the average received

SNR and transmission success probability of potential relays. Making use of such statistics and location information, each relay can independently determine its contention parameters such as a backoff time and/or a forwarding probability. We analytically evaluate the relaying performance and validate the accuracy with simulations. The results demonstrate the improvement over a pure probabilistic scheme and the gap to the upper bound of a centralized scheme with the pre-selected best relay.

In Chap. 6, we investigate a wireless diversity system with distributed cooperation and spatially random helpers subject to random direction (RD) mobility. To enable opportunistic relaying with multiple helpers, we consider an ALOHA-like MAC scheme and a timer-based random backoff scheme for multi-helper coordination. Particularly, we analyze the upper bound of combined SNR and unconditional success probability with multi-helper cooperation. We also provide numerical approximations for the delay of the two MAC schemes. To characterize the tradeoff between the success probability and delay, we further define a success/delay ratio, which can be maximized by adapting the intensity of selected helpers. The numerical and simulation results validate the analysis accuracy and demonstrate insightful observations. Finally, in Chap. 7, we conclude the discussions on cooperative wireless networks and point out future directions to explore.

References

1. Bletsas, A., Khisti, A., Reed, D.P., Lippman, A.: A simple cooperative diversity method based on network path selection. *IEEE J. Sel. Areas Commun.* **24**(3), 659–672 (2006)
2. Du, Q., Zhang, X.: QoS-aware base-station selections for distributed MIMO links in broadband wireless networks. *IEEE J. Sel. Areas Commun.* **29**(6), 1123–1138 (2011)
3. Ikki, S.S., Ahmed, M.H.: Performance analysis of generalized selection combining for amplify-and-forward cooperative-diversity networks. In: *Proceedings of IEEE ICC, Dresden (2009)*
4. Laneman, J.N., Tse, D.N.C., Wornell, G.W.: Cooperative diversity in wireless networks: efficient protocols and outage behavior. *IEEE Trans. Inf. Theory* **50**(12), 3062–3080 (2004)
5. Li, Y., Wang, P., Niyato, D., Zhuang, W.: A hierarchical framework of dynamic relay selection for mobile users and profit maximization for service providers in wireless relay networks. *Wirel. Commun. Mob. Comput.* **14**(12), 1113–1126 (2014)
6. Liu, P., Tao, Z., Narayanan, S., Korakis, T., Panwar, S.S.: CoopMAC: a cooperative MAC for wireless LANs. *IEEE J. Sel. Areas Commun.* **25**(2), 340–354 (2007)
7. Nosratinia, A., Hunter, T.E., Hedayat, A.: Cooperative communication in wireless networks. *IEEE Commun. Mag.* **42**(10), 74–80 (2004)
8. Shan, H., Cheng, H., Zhuang, W.: Cross-layer cooperative MAC protocol in distributed wireless networks. *IEEE Trans. Wirel. Commun.* **10**(8), 2603–2615 (2011)
9. Shan, H., Zhuang, W., Wang, Z.: Distributed cooperative MAC for multihop wireless networks. *IEEE Commun. Mag.* **47**(2), 126–133 (2009)
10. Song, W., Zhuang, W.: Performance analysis and enhancement of cooperative retransmission strategy for delay-sensitive real-time services. In: *Proceeding IEEE GLOBECOM, Honolulu (2009)*

11. Xiong, L., Libman, L., Mao, G.: Uncoordinated cooperative communications in highly dynamic wireless networks. *IEEE J. Sel. Areas Commun.* **30**(2), 280–288 (2012)
12. Zhai, C., Zhang, W., Mao, G.: Uncoordinated cooperative communications with spatially random relays. *IEEE Trans. Wirel. Commun.* **11**(9), 3126–3135 (2012)
13. Zhuang, W., Ismail, M.: Cooperation in wireless communication networks. *IEEE Wirel. Commun. Mag.* **19**(2), 10–20 (2012)

Chapter 2

Related Works on Cooperative Wireless Networks

2.1 Cooperative Communications

Given the broadcast nature of the wireless medium, data transmission from a source terminal can be overheard by other terminals. As a result, it is possible for the source to cooperate with these overhearing terminals to form a virtual MIMO system [49, 50]. Cooperation at the physical layer is often considered as the foundation of cooperative MAC protocols because of the following reasons:

- The main purpose of a cooperative MAC protocol is to fulfill the cooperation agreement. After the agreement, cooperative protocols at the physical layer are often used to implement the actual non-diversity or diversity packet relaying.
- In the design of a cooperative MAC protocol, cross-layer design is often used, and the exact boundary of layers becomes vague.

Most cooperative transmission schemes at the physical layer involve two phases of transmission [43]: *phase I* and *phase II*, also known as the coordination phase and the cooperation phase, respectively. In phase I, the nodes exchange their own data and control messages with each other and/or the destination. In phase II, the nodes cooperatively retransmit the overheard data from others to the destination. Among all the physical cooperative strategies, the most well-known ones are: decode-and-forward (DF) and amplify-and-forward (AF) [34]. Besides DF and AF, there are other protocols, such as coded-cooperation (CC) [20–22] and compress-and-forward (CF) [19].

- ***Decode-and-forward (DF)***. Originally proposed in [34], the basic idea of DF is as follows: During phase I, the source node transmits its signal to both the relay node and the destination node; during Phase II, if the relay can decode the overheard signal, it will regenerate and transmit it to the destination node. It is possible that the overall received signal is just the relayed version from the relay node which is a non-diversity relaying scenario as introduced in Sect. 2.2.

The works on this scenario often focus on how to select an optimal helper, which ultimately becomes a cross-layer relay selection problem. We will discuss this in more details in Sect. 2.3.

On the other hand, if diversity is used, which is called the diversity relaying scenario as in Sect. 2.2, the signals from both the source node and the relay node will be considered. The maximal ratio combiner (MRC) or selective combiner (SC) can be employed to produce the overall received SNR. Works in this direction often assume that helpers are pre-selected and focus on the signal processing and analysis [7, 40, 55, 57].

In [7, 55], the outage probability of DF is analyzed for the Rayleigh fading channel and Nakagami- m fading channel respectively. A multi-helper DF cooperative diversity protocol is analyzed in [40] from a power allocation point of view. An optimal power allocation scheme is proposed to minimize the outage probability while the total power consumption is guaranteed to be within a certain constraint. In [57], the diversity order is analyzed when cooperative MRC (C-MRC) is used to combine the DF relayed signals. It is shown that C-MRC achieves the full diversity order.

- **Amplify-and-forward (AF).** The basic idea of AF is similar to that of DF but in a simpler way [34]: During phase I, the source node transmits its signal to both the relay and the destination node; during phase II, instead of decoding and regenerating the message, the relay just amplifies the overheard signal (thus noise is boosted as well) and forwards it to the destination. AF can work in either a non-diversity way or a diversity way. Like DF, the works on the non-diversity scenario often focus on how to select an optimal helper, while the essential problem for the diversity scenario is how to process the received signals [4, 25, 58, 59]

In [4], a multiple amplifying relay diversity system is analyzed and the exact average symbol error rate is derived for the Rayleigh-fading channel. Tight bounds on the probability of error show that the cooperative system in [4] achieves full diversity order. A power allocation scheme is proposed in [58] to minimize the outage probability of an AF system and it further proposes a scheme to choose several best relays to achieve good performance instead of choosing all relays. In [59], the authors extend [58] by providing an asymptotic analysis of the symbol error rates of the AF system. A more systematic work to examine AF can be found in [25], which jointly considers a burst traffic at the application layer, an auto repeated request (ARQ)-based error recovery mechanism at the link layer and an AF cooperation scheme at the physical layer. Using Markov analysis, [25] derives a sufficient condition which ensures improved packet delivery by adjusting of the physical-layer, ARQ and traffic parameters.

- **Coded-cooperation (CC).** Coded cooperation is proposed in the serial works [20–22] where cooperation is achieved through channel coding methods instead of a direct relay or repetition as in AF and DF. Specifically, CC assumes each user has K_{cc} information bits per block, and N_{cc} coded bits per block, so that the code rate is $R_{cc} = K_{cc}/N_{cc}$. N_{cc} coded bits are expanded into two successive time segments with length N_{cc1} and N_{cc2} , where $N_{cc1} + N_{cc2} = N_{cc}$. Then a sub-codeword of rate $R_{cc1} = K_{cc}/N_{cc1}$ is broadcast by the source. Each node will

thus receive a noisy version of the coded message. If a node can correctly decode the message by the cyclic redundancy check (CRC), it will compute and transmit the message by the cyclic redundancy check (CRC), it will compute and transmit the N_{cc2} bits for the source. Otherwise, N_{cc2} additional parity bits for the users' own data will be transmitted. There is not a clear-cut boundary in CC for the non-diversity scenario and the diversity scenario, because it really depends on if the relay can decode the overheard codeword subset.

Some extension works on CC can be found in [23, 26]. In [23], the authors analyze the outage performance and BER of CC. It provides the general outage expressions for arbitrary SNR and reveals that CC benefits from diversity in the order of the number of cooperating partners. Two extensions are provided in [26] to the CC framework. Firstly, it increases the diversity of CC in the fast-fading scenario. Secondly, turbo code is applied to the CC framework. Bounds for the BER and block-error rates are also developed.

- **Compress-and-forward (CF)**. CF is originally proposed in [13] and also called estimate-and-forward, observe-and-forward [33] or quantize-and-forward [30]. The general idea is that a relay transmits a quantized and compressed version of its overheard signal to the destination, and the destination decodes by combining with the signal from the source. It is obvious that CF can only be used in the diversity scenario and the relays use Wyner-Ziv source coding to exploit side information at the destination [32]. In [31], the authors investigate the achievable diversity-multiplexing tradeoff of CF when the relay is constrained to make use of non-Wyner-Ziv source coding. In [3], a discrete memoryless state-dependent relay channel with non-causal channel state information (CSI) is considered where perfect channel states can be known only to the source, only to the relay or both. The channel capacity is investigated for these three cases. In [53], CF is analyzed with a cooperative time division duplex (TDD) relaying in the multiple-antenna case with full CSI. It provides an analytical expression for the optimum Wyner-Ziv coding rates and also proposes an iterative procedure to perform this optimization.

2.2 Cooperation Scenarios¹

A typical cooperation topology is shown in Fig. 2.1, in which there are multiple nodes within the coverage of a destination node which can be an access point (AP) or a base station (BS). If a node decides to cooperate with others for its data transmission, there are several communication entities involved in this cooperation:

¹Reprinted with permission, from IET Communications (2013) 7(9), "Survey on cooperative medium access control protocols," by P. Ju, W. Song, and D. Zhou [29].

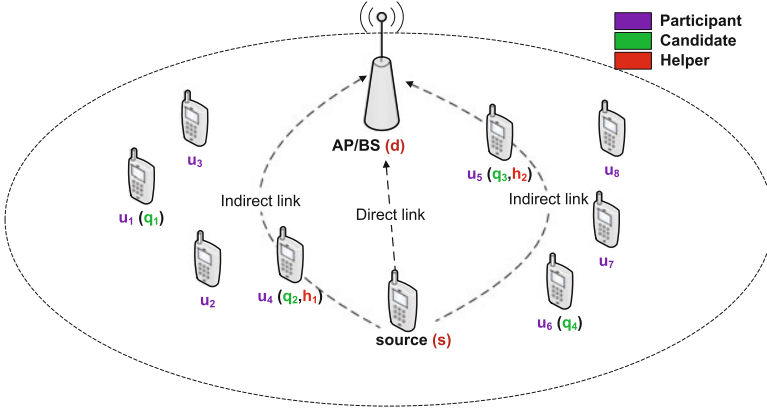
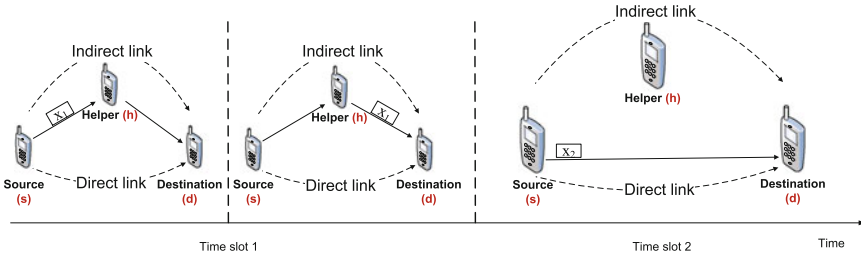


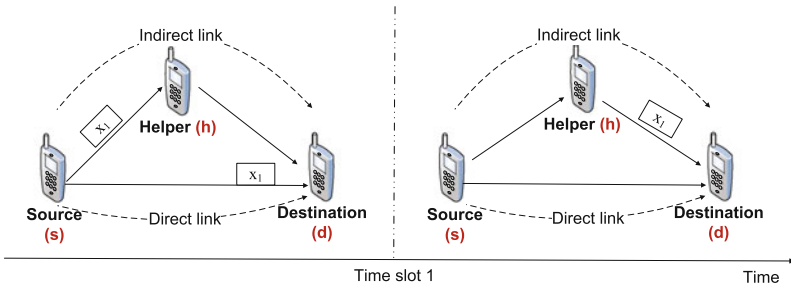
Fig. 2.1 A general cooperation topology

- **Source.** The source s is the node who has a data packet to be transmitted through cooperative relaying as shown in Fig. 2.1. The source s is also the node who initiates the cooperation request.
- **Destination.** The destination d is the receiver for the data packet from s and it can be an AP, a BS, or just a peer wireless node in ad-hoc networks.
- **Helper.** The wireless node who is selected to relay the data packet of s is called a *helper*. All the selected helpers form the helper set \mathbb{H} with size H , which are labelled by h_1 and h_2 in Fig. 2.1. Helpers are the winners of helper selection and take part in the final cooperative transmission.
- **Candidate.** Helper candidates, shortened as *candidates*, are the wireless nodes from which the helpers are selected. Candidates are potential helpers who know that they are qualified helpers and are ready to relay once selected and provided with incentive. Candidates form set \mathbb{Q} with size Q . Fig. 2.1 shows several example candidates, including q_1 , q_2 , q_3 and q_4 .
- **Participant.** The wireless nodes who can overhear the transmission of the ongoing data packet is called a *participant*. Participants are potential candidates. If a participant reveals itself to s or to other wireless nodes, it becomes a candidate. All the participants form set \mathbb{P} . In Fig. 2.1, we show a few participants, u_1, u_2, \dots, u_8 . The relation between \mathbb{H} , \mathbb{Q} and \mathbb{P} is: $\mathbb{H} \subseteq \mathbb{Q} \subseteq \mathbb{P}$. In the literature, \mathbb{Q} and \mathbb{P} are the same in many works, but some cooperative MAC protocols indeed differentiate them.

Accordingly, two types of links can be formed in this topology among the above entities: (1) the direct link between s and d , which is used for data transmission if no cooperation is activated; and (2) the indirect link involving the helpers. More than one indirect link can be involved in cooperative transmission. As shown in Fig. 2.1, two helpers are selected to form two indirect links over two hops. A multiple-hop indirect link is also possible. Depending on how the direct link and the indirect link contribute to the data transmission, two typical cooperation scenarios are shown in Fig. 2.2:



(a) Non-diversity scenario.



(b) Diversity scenario.

Fig. 2.2 Typical cooperation relaying scenarios. (a) Non-diversity scenario. (b) Diversity scenario

- **Non-diversity scenario.** In this case, only the better link, either the direct link or the indirect link, is selected to transmit a packet. As seen in Fig. 2.2a, in time slot 1, the indirect link is chosen to first send packet x_1 to h and then h forwards x_1 to d . In time slot 2, the direct link is selected to transmit packet x_2 .
- **Diversity scenario.** In this case, both the direct link and the indirect link are involved in each packet transmission. Thus, diversity gain can be achieved with spatial diversity. As shown in Fig. 2.2b, in time slot 1, two independently faded replicas of packet x_1 are received by both h and d in the first subslot and d keeps this packet for future processing. In the second subslot, h relays another copy of x_1 to d . At the end of time slot 1, d can choose a strategy such as maximal ratio combining (MRC) [17, 36] or selective combining (SC) [48, 54] to process the two copies of x_1 for the best receiving performance.

According to the number of helpers that the source actually chooses from the candidates, two scenarios can be developed from Fig. 2.1:

- **Single-helper scenario.** In this case, the handshake procedure is straightforward since the source already chooses its partner and the partner just has to decide to accept the cooperation request or not based on its own judgement, e.g., incentive

that the source offers. There is no need to consider a coordination scheme for this scenario, and it is often jointly used with non-diversity because of its simplicity.

- **Multiple-helper scenario.** This case is more complicated than the single-helper scenario because coordination among the chosen helpers needs to be considered. It is often jointly used with diversity because multiple helpers can take advantage of spatial diversity. Thus, a careful choice is required to determine the number of helpers, because the more chosen helpers, the higher spatial diversity, and the more complicated the coordination.

2.3 Three Categories of Cooperative MAC Protocols²

In traditional wireless networks, the primary task of the MAC layer is to coordinate multiple nodes sharing the wireless medium. Channel allocation is a typical way to share the wireless medium. It partitions the wireless channel resource in a certain dimension, e.g., time, frequency, or spreading code. Correspondingly, there are time division multiple access (TDMA), frequency division multiple access (FDMA), and code division multiple access (CDMA).

Another big family of MAC protocols are contention-based random access, such as ALOHA and carrier sensing multiple access with collision avoidance (CSMA/CA) used in IEEE 802.11. In CSMA/CA, the transmitting node senses the channel before sending a packet to avoid collision. Due to the hidden terminal problem and the exposed terminal problem, even when the channel is sensed idle from the transmitting node side, a collision may still occur. A virtual carrier sensing approach can be used by including a handshake before the actual data transmission. The key idea is to have the sender broadcast a request-to-send (RTS) frame to reserve the channel and have the receiver respond a clear-to-send (CTS) frame to confirm the reservation. The other terminals who overhear the RTS and/or CTS should defer their transmission for a period of time indicated by the network allocation vector (NAV).

Both the contention-based random access and channel allocation-based MAC can be extended to a cooperative scenario. For example, cooperative ALOHA is analyzed theoretically in [12, 17, 18]. There is also interesting research on cooperative MAC based on TDMA [45, 56] and CDMA [41]. Due to the complexity concern with channel management, channel allocation-based cooperative MAC is not as popular as contention-based MAC. In this brief, we focus on the contention-based MAC, which has attracted most research attention. In addition, the cooperative MAC protocol should address several fundamental problems [62, 63]:

- **When to cooperate? (Q1)** The nature of this question is to find the conditions when cooperation can be enabled, or the regions where cooperation is beneficial.

²Reprinted with permission, from IET Communications (2013) 7(9), "Survey on cooperative medium access control protocols," by P. Ju, W. Song, and D. Zhou [29].

Table 2.1 Categories of cooperative MAC protocols

Category	Q1 is addressed by	Q2		A typical example
		(a) is addressed by	(b) is addressed by	
I	Source	Source	Source	CoopMAC [38]
II	Source	Participants	Source	rDCF [61]
III	Source	Candidates	Candidates	Shan-MAC [51]

- **Whom to cooperate with? (Q2)** To answer this question, the cooperative MAC protocol should determine who are the available helpers and who is (are) the optimal helper(s) that the source is going to cooperate with.

More generally, we call Q1 and Q2 together as the matter of *relay selection*. Specifically, Q1 is to find the conditions when cooperation can be enabled. These conditions to trigger cooperation can be straightforward, e.g., less transmission time [16, 38, 39, 64], or as complex as the cooperative region [51].

To answer Q2, there are two aspects to address: (a) *potential relay contention*, in which available potential relay nodes compete to become a helper candidate in the helper candidate list of the source; and (b) *helper selection*, in which the optimal helpers are selected according to certain criteria and decision mechanism from the candidates. It is worth noting that some cooperative MAC protocols address Q2(a) and Q2(b) in one process, such as CoopMAC [38] and Shan-MAC [51]. Nonetheless, some protocols indeed handle them in different processes by different entities, such as rDCF [61]. While apparently Q2(a) should be addressed before Q2(b), there is no predetermined order of addressing Q1 and Q2. In Shan-MAC [51], Q1 is answered before Q2, while rDCF [61] deals with Q2(a) first, followed by Q1 and Q2(b). According to which entity addresses Q1 and/or Q2, we propose the categorization of contention-based cooperative MAC protocols in Table 2.1 [29].

2.3.1 Category-I

For the cooperative MAC protocols of Category-I, the source addresses both Q1 and Q2. Typical examples include Ahmed-MAC [24], CoopMAC [38], ADC-MAC [60]. These protocols generally follow a common procedure as follows:

- The source acquires the knowledge of other nodes such as the transmission rate and transmission time. Such information is usually obtained by overhearing, e.g., in CoopMAC [38], or periodical broadcast indicator packets, e.g., in ADC-MAC [60]. The collected information of the candidates is generally maintained in a table, known as CoopTable in CoopMAC and ADC-MAC.
- Based on the information of candidates, the source needs to answer the questions Q1 and Q2. For this category of cooperative MAC protocols, some address Q1 first while others address Q2 first. The source checks if the cooperation

Table 2.2 Category-I cooperative MAC protocols

Protocol	Knowledge collection	Solving order	Cooperation condition
Ahmed-MAC [24]	–	Q2, Q1	$(\beta_{s,d}/\beta_{\max}) > \text{threshold}$
CoopMAC [38, 39]	Overhearing	Q1, Q2	Less transmission time
ADC-MAC [60]	Broadcasting	Q2, Q1	SNR meets requirement
C-MAC [5]	Broadcasting	Q2, Q1	Lower transmit power
CD-MAC [46]	Overhearing	Q2, Q1	Once a transmission fails
Protocol	Helper selection	Scenario	
Ahmed-MAC [24]	Highest β function value	Diversity	
CoopMAC [38, 39]	Highest transmission rate	Non-diversity	
ADC-MAC [60]	Highest transmission rate	Non-diversity	
C-MAC [5]	Lowest transmitting power	Diversity	
CD-MAC [46]	Highest SINR	Diversity	

conditions are met and selects a best helper among the candidates. It is worth emphasizing that the source makes the selection decision and the best helper is not elected with competition.

- Once the source decides to initiate cooperation with the selected helper, it sends a cooperation request to the helper and starts the cooperative transmission based on the feedback from the helper.

We list in Table 2.2 some typical Category-I MAC protocols and will briefly introduce them in the following. The cooperative proposal in [24] is referred to as Ahmed-MAC for reference convenience. Ahmed-MAC addresses Q2 firstly and Q1 secondly. Since the source has the knowledge of all available potential relays, it chooses an optimal one according to a modified harmonic mean function β . The helper with the maximum β is selected. Whether to initiate cooperative transmission or not depends on the ratio $\beta_{s,d}/\beta_{\max}$, where $\beta_{s,d}$ is the modified harmonic mean function of the channel between the source and the destination, and β_{\max} is that of the optimal helper. If the ratio falls below a threshold, the source only uses direct transmission. Otherwise, cooperative transmission is involved. Nonetheless, Ahmed-MAC does not specify the handshake procedure or how the source obtains the knowledge of the potential relays.

CoopMAC proposed in [38, 39] further addresses these problems. The source acquires the overall knowledge of potential relays by overhearing their transmission. This is feasible for reciprocal channels between the source and the helper. The source maintains the information of the helpers obtained from overheard packets in CoopTable. CoopMAC addresses Q1 first by comparing the transmission time of the direct link and the indirect link, which is calculated by the transmission rate and handshake time. Cooperation is only enabled when the indirect transmission time is shorter. To answer Q2, the source looks up the CoopTable and selects the helper with the highest indirect transmission rate. If multiple helpers have the same highest indirect transmission rate, the source chooses the one with the most recent update and the least number of failures. Compared with Ahmed-MAC, CoopMAC

is a more complete solution. It proposes the triangle handshake to reserve an optimal helper and uses the triangle transmission to relay data. However, the reciprocal channel assumption to enable overhearing may not hold when the channel is fast time-varying or different frequencies are used for the uplink and downlink. Also, there must be sufficient packets overheard, so that the source can obtain accurate and up-to-date information for the CoopTable. Moreover, the triangle handshake and transmission procedures are still dependent on the direct link. As a result, CoopMAC cannot deal with the circumstances where the direct link is unavailable.

The adaptive distributed cooperative MAC protocol (ADC-MAC) in [60] collects the information of the helpers in a way different from that of CoopMAC. In CoopMAC, the source overhears the packet transmission of a potential relay and infers its information accordingly. In ADC-MAC, a potential relays periodically broadcasts a heartbeat frame, which contains not only the received signal strength indication (RSSI) but also the information about its neighbors. As such, the source maintains a global knowledge of the network in a CoopTable. Based on the CoopTable, ADC-MAC addresses Q2 first by applying a shortest path routing algorithm (e.g., the Dijkstra's algorithm) to determine the most appropriate indirect path. The optimal helper is then selected. The MAC address of this selected helper is included in the RTS frame to reserve the channel. If this helper is available, it acknowledges with an acceptance packet indicating its availability. After the source confirms the eligibility of the helper, cooperative transmission is initiated. Different from CoopMAC, ADC-MAC designs a pure two-hop transmission to avoid using the direct path. This mode is more feasible than CoopMAC when the direct path is not available.

Because the source has complete knowledge of all other nodes in the network, it is possible for it to (a) decide whether cooperation is necessary and then selects a helper (Q1-Q2); or (b) predetermine a helper and then decide whether to initiate cooperation or not based on the feedback of this helper (Q2-Q1). Which addressing sequence performs better depends on the networking scenario to apply the cooperation protocol. For example, a Category-I protocol in a Q2-Q1 sequence can perform better in a mobile network, in that the cooperation decision can be further confirmed by the helper feedback to ensure an up-to-date decision, such as ADC-MAC in [60]. On the other hand, the Category-I solutions in a Q1-Q2 sequence may have an easier implementation by means of extending current 802.11-based protocols and better fit a more static network topology. Such solutions do not require complicated decision algorithms or handshake control packets to guarantee a timely cooperation decision.

2.3.2 *Category-II*

In this category of cooperative MAC protocols, the source addresses Q1 and Q2(b), which means the source proposes to cooperate and selects an optimal helper from a candidate list. The candidate list is first obtained via contention in a distributed

manner when Q2(a) is being addressed. The number of helper candidate to consider can be reduced when Q2(a) is answered. The addressing sequence of Q1 and Q2(b) can be the same as the Q1-Q2 sequence and the Q2-Q1 sequence discussed in Category-I. The Category-II of cooperative MAC protocols shares the following common features:

- First, all potential relays compete with each other and the winners are qualified for the candidate list of the source. In one way, the nodes are aware of each other before competing through certain mechanism. For all the existing work surveyed in this section, broadcast is used to accomplish this task. Another is a pure distributed approach, which allows potential relays not aware of each other. The distributed timer algorithm in [9] is a good option.
- Although cooperative transmission is still initiated by the source, the source only has partial knowledge of the network, which is different from Category-I. The helper candidate list obtained by the source is only the result of contention.

In the following, we present and compare a few typical Category-II protocols in Table 2.3, such as rDCF in [61], ErDCF in [1, 2], RAMA in [64], and EMR in [44]. rDCF [61] is one of the earliest classic cooperative MAC protocols. It creates innovative concepts such as CoopTable and broadcast information frame. The fundamental cooperation questions are addressed in the order of Q2(a), Q1 and Q2(b). A node decides whether it can help a pair of source and destination nodes by checking the overheard RTS and CTS between them. If it is able to improve their transmission by cooperating, it adds this pair into its willing list and broadcasts its willing list periodically. To content with other potential relays and answer Q2(a), each node keeps listening to others' willing lists and checking the source and destination pairs contained in their willing lists. If the number of the overheard willing lists that contain the same pair exceeds a certain threshold, the node stops advertising itself. Through this contention, the source maintains its CoopTable.

Table 2.3 Category-II cooperative MAC protocols

Protocol	Solving order	Helper contention	Cooperation condition
rDCF [61]	Q2(a), Q1, Q2(b)	Broadcast to overhear M peers	Non-empty CoopTable
ErDCF [1, 2]	Q2(a), Q1, Q2(b)	Broadcast to overhear M peers	Non-empty CoopTable
RAMA [64]	Q2(a), Q1, Q2(b)	Random backoff contention	Less transmission time
EMR [44]	Q2(a), Q1, Q2(b)	Priority-based contention	Higher effective throughput
Protocol	Helper selection	Scenario	
rDCF [61]	Random by source	Non-diversity	
ErDCF [1, 2]	Random by source	Non-diversity	
RAMA [64]	Highest rate	Non-diversity	
EMR [44]	Highest throughput	Non-diversity	

If the transmission time via cooperation is shorter, the source sends a cooperation request to the helper who provides the shortest cooperative transmission time.

The relay-aided medium access (RAMA) control protocol [64] has a similar idea. The difference is that RAMA broadcasts the information frame in a random manner rather than periodically. If a node succeeds in accessing the channel first, it starts to broadcast its frame while others stop broadcasting and keep silent. Although RAMA [64] and rDCF [61] can be easily extended from an 802.11-based protocol, the competition among the nodes cannot guarantee that the most capable nodes appear in the short-list of helper candidates of the source. In RAMA, nodes compete via random backoff so that those whose backoff timers run out earlier become winners and qualified helper candidates. Similarly, in rDCF, a node stops broadcasting its willing list if the same source and destination pair has appeared in more than a threshold. As a consequence, it is likely that a more capable node may not be even considered as a helper candidate, if it broadcasts its willing list less frequently than other less capable nodes.

The efficient multi-rate relaying (EMR) MAC protocol [44] addresses this problem with a simple but reasonable solution. It defines the effective throughput as the criterion to evaluate a node. A *priority number* is assigned to each node according to the effective throughput and broadcast in its indicator frame. Any other who overhears this frame compares the priority number with its own and stops broadcasting if the overheard priority number is greater. Although the broadcast frame is a simple solution to helper contention, excessive overhead traffic is brought into the network.

2.3.3 Category-III

In Category-III, all the potential relays are helper candidates and Q2, including both Q2(a) and Q(b), is addressed by the same entity as in Category-I. The difference is that Q2 is addressed by helper candidates in a distributed manner rather than by the source in a centralized manner in Category-I. In this category, the source only handles the question Q1 and does not know who are the helper candidates to select. Once the source determines that cooperative transmission is beneficial, the source can propose cooperation to its overhearing neighbors. Then, it is up to the neighbors to make the ultimate cooperation decision. Different from Category-I and Category-II, we believe that Q2 cannot be addressed ahead of Q1 in Category-III. For one thing, the helper entity must have received a cooperation proposal signal to start the helper contention and selection procedure. On the other hand, if Q2 were addressed before Q1, it would be unnecessary to re-evaluate the cooperation timing since the distributed contention and selection procedure could provide an up-to-date helper.

Although there are few protocols that fall into this category, Table 2.4 shows three examples, i.e., the Feeney-MAC [16], OR [8, 9] and Shan-MAC [51]. Feeney-MAC is a very simple and naive MAC. If there is a possibility that the transmission time over an indirect path is shorter, the source initiates cooperative transmission

Table 2.4 Category-III cooperative MAC

Protocol	Solving order	Helper contention	Cooperation condition
Feeney-MAC [16]	Q1, Q2	Random backoff	Less transmission time
OR [8, 9]	–	Timer-based	–
Shan-MAC [51]	Q1, Q2	Distributed grouping, timer-based	Cooperation region exists
Protocol	Helper selection		Scenario
Feeney-MAC [16]	Highest rate		Non-diversity
OR [8, 9]	Highest SNR		Diversity
Shan-MAC [51]	Highest rate		Non-diversity

assuming that certain node may help. If there indeed exist some nodes that are able to help, the one that captures the channel first after random access contention will relay packets for the source. The other nodes will cancel their competition. However, in the absence of proper handshake, Feeney-MAC simply assumes the existence of a helper candidate and cannot guarantee successful cooperation. The channel access can neither ensure that the optimal helper is selected.

In [8, 9], an opportunistic relaying (OR) protocol is proposed. All the helpers estimate the “instantaneous channel conditions” based on RTS and CTS frames and set a corresponding timer based on the channel condition. Two policies to set the timer are evaluated in [8]. Basically, the better the channel condition, the shorter the timer. As a result, the optimal helper will time out first and transmit a flag packet to claim itself. After receiving the packet from both the source and the helper, the destination uses maximal ratio combining to decode the message. Strictly speaking, OR is not a complete Category-III solution, since it assumes implicitly that cooperation starts once a helper is selected. That is, the question Q1 is not explicitly addressed. Important factors such as energy and security also need to be considered to evaluate if cooperation is really beneficial.

The distributed MAC proposed in [51] is a mature solution and we refer to it as Shan-MAC. To answer Q1, a new metric called cooperation region (CR) is defined in Shan-MAC and the acquisition of CR is formulated as an optimization problem. By solving the optimization problem, the source starts cooperation if CR exists and uses direct transmission otherwise. To answer Q2, a distributed timer-based selection scheme is specified in Shan-MAC. The key idea is similar to the timer algorithm in [9], in which a better candidate is indicated by less channel access time. Thus, the first responding helper is expected to be the optimal one. Hence, no information broadcast is required for the candidates to be aware of other competitors, which alleviates the network from broadcast traffic. To enable the timer-based selection scheme, appropriate synchronization is necessary among the helpers.

2.4 Research Issues for MAC-Layer Cooperation³

2.4.1 New Categories

Most existing contention-based cooperative MAC protocols fall into the three categories in Table 2.1. In particular, Category I has received most research attention. This is mainly because the idea is straightforward and close to the popular cooperative physical-layer protocols. Also, this category of MAC protocols can be easily implemented by extending the mainstream 802.11 MAC. However, there can be a large overhead for the source as the decision entity to maintain the overall knowledge of other nodes (e.g., in CoopTable) when there are a great number of helpers around the source. Overhearing of packet transmissions from helpers is required under the reciprocal channel assumption although overhearing is power consuming. Meanwhile, the broadcast of information frames involves additional traffic. On the other hand, it may be challenging to keep up-to-date accurate information in CoopTable in a highly varying environment, such as with node mobility. Efficient search algorithm is also essential to identify an optimal helper in a large-sized CoopTable.

The solutions of Categories II and III balance the decision intelligence of the source with the helper entities. Category II includes helper contention to reduce the size of CoopTable so that the source makes a cooperation decision among less helper candidates. In Category III, helper selection is taken over by the helpers. Thus, a major challenge for Categories II and III is to design a reliable and efficient helper contention and/or selection algorithm for the helpers. Also, a handshake procedure can be designed for the helpers to exchange information with each other, or between the source and the helper to inform the source of the selected optimal helper.

If we follow the categorization logic in Table 2.1, we see that, there exist other potential categories as shown in Table 2.5. Although not all of them are reasonable such as Category V, some are quite promising, such as Category VIII. Category VIII is a pure distributed cooperative MAC approach, in which the source

Table 2.5 Other possible categories of cooperative MAC protocols

Category	Q1 is addressed by	Q2	
		(a) is addressed by	(b) is addressed by
IV	Source	Source	Helper(s)
V	Helper(s)	Source	Source
VI	Helper(s)	Source	Helper(s)
VII	Helper(s)	Helper(s)	Source
VIII	Helper(s)	Helper(s)	Helper(s)

³Reprinted with permission, from IET Communications (2013) 7(9), “Survey on cooperative medium access control protocols,” by P. Ju, W. Song, and D. Zhou [29].

is not aware of how Q1 and Q2 are resolved. In this case, each cooperation decision is made by the helpers. As long as a good contention algorithm is designed, the decision is up-to-date to ensure a high success rate of cooperation. The source is informed of the selected thereafter if cooperative transmission is found beneficial. Since a cooperation decision should be made for each packet transmission, the contention overhead needs to be effectively balanced. In addition, Category IV may include some promising solutions as well. For example, the source can overhear its neighbors and list some potential helpers based on gathered information to address Q2(a). As a result, when cooperation is triggered to answer Q1, a control packet can be sent to potential helpers instead of all nodes as in Category III. If helper selection is initiated afterwards only among potential helpers in a distributed manner to answer Q2(b), the complexity of distributed selection can be decreased with a smaller number of participating helpers.

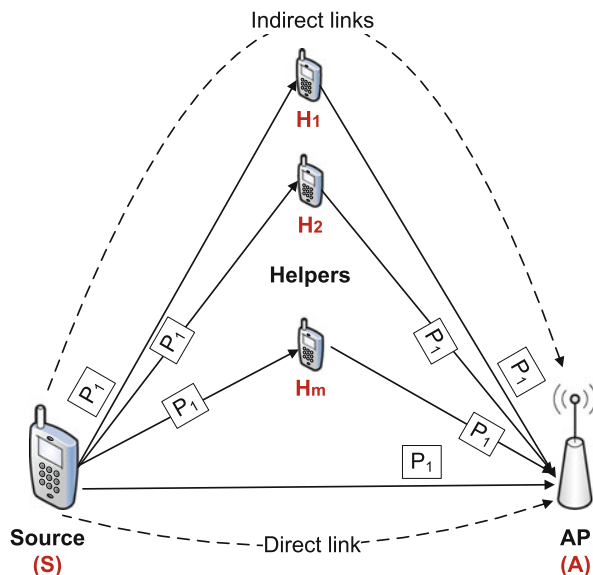
2.4.2 Cooperative Diversity

As mentioned in Sect. 2.2, a cooperative relay link and the direct link can be used to transmit the same packet in the diversity scenario, or different packets in the non-diversity scenario. From the discussion in Sect. 2.3, we can see that most existing cooperative MAC designs focus on the non-diversity scenario [1, 2, 16, 24, 38, 42, 44, 51, 60, 61, 64], and only a few protocols [5, 8, 46] consider the diversity gain with cooperation. There are the *single-helper diversity scenario*, as shown in Fig. 2.2b, and the *multiple-helper diversity scenario*, as shown in Fig. 2.3. In the latter case, orthogonal distributed space-time coding can be applied to enable that multiple helpers transmit over the same channel [35, 47]. In the diversity scenario, the source and the helpers form a virtual antenna array (VAA) system. The helpers become the virtual external antennas of the source. The study of the physical-layer capacity of VAA system can be found in [14].

From the MAC-layer perspective, many issues remain unsolved. As considered in [46], one possible cooperation criterion may be the minimization of transmission failures. Cross-layer techniques can be employed to dynamically estimate the channel condition, so that cooperative diversity transmission is initiated to satisfy certain quality-of-service (QoS) requirements [15] if a transmission failure is very likely to happen with a poor channel condition. Whether the source should always enable diversity transmission or only activate it on demand depends on factors such as the energy consumption and availability of helpers.

In the non-diversity scenario in Fig. 2.2a, adaptive modulation and coding (AMC) can be enabled at the physical layer to adapt transmission rates with varying channel conditions. As such, the capacity of the selected optimal link can be fully exploited. Conversely, in a diversity scenario in Fig. 2.2b, multiple possible links can be utilized at the same time to make a good use of spatial diversity, which is different from choosing an optimal link at the MAC layer in the non-diversity scenario. As a

Fig. 2.3 Multiple-helper diversity scenario



consequence, it is challenging to enable AMC simultaneously for multiple links experiencing different channel conditions.

One essential question to exploit diversity gain is the selection of a single optimal helper or multiple uncorrelated helpers with limited interference and power consumption. There is a different perspective at the physical layer and the link layer regarding whether more relays can provide better performance. From the physical-layer standpoint, multiple helpers can improve diversity to achieve a higher signal-to-noise ratio (SNR). However, more relays introduce higher complexity, larger coordination overhead, and even increased energy consumption. Hence, a challenging issue is how to balance the tradeoff between performance gain and coordination overhead when choosing multiple helpers or a single best helper [52, 62].

2.4.3 User Mobility

Although mobility support is an attractive feature of wireless networks, node mobility may lead to high channel variation. In such a dynamic environment, it is challenging to guarantee an accurate and up-to-date decision on initiating cooperation and/or selecting the optimal helper(s). In a non-diversity scenario, the out-of-date information is a most pronounced problem brought by mobility. Beyond that, the mobility of nodes can increase the correlation (mainly spatial correlation) between the channel coefficients of the cooperating entities, which reduces diversity gain [62] and is particularly detrimental to the diversity scenario.

To ensure a high success rate of cooperation, one possible solution is to apply advanced cooperation criteria which can involve the history profile of helpers [28]. For example, unstable helpers can be excluded from cooperation candidates by using analysis of history data. In addition, the cooperative MAC protocols in Table 2.5, such as Category VIII that enables cooperation in a pure decentralized manner, can also be a promising approach to address node mobility. Furthermore, the impact of node mobility on the performance of cooperative MAC protocols may vary with the specific mobility patterns. Good surveys on mobility models can be found in [6, 10]. The widely used mobility models include the random way point model [27], Chiang's model [11] and Gauss-Markov model [37]. The impact of different mobility patterns on cooperation performance needs further study.

2.4.4 Energy Saving

Mobile nodes are usually portable devices powered with batteries. The energy consumption is an important factor to consider for a cooperative wireless network, since the helpers invest power resources to assist the source in forwarding packets rather than remain idle otherwise. Most existing work on cooperative MAC protocols focuses on performance improvement in terms of system throughput. There are few studies that well address the energy concern in cooperative transmission.

As demonstrated in the study of CoopMAC in [38, 42], energy consumption of cooperative transmission in terms of Joule per bit is even lower than that with only direct transmission. If a helper can provide a sufficiently high transmission rate to forward a large packet, the helper may wait for less time for other nodes to finish their transmission. Eventually, it is likely that the helper has a less idling time by helping others. Consequently, the decrease of the energy spent in idling can compensate for the additional energy spent in forwarding for others. As a result, the total energy consumption of the network is saved under the saturated assumption [42]. However, this analysis actually does not consider the energy cost of the overhearing scheme to maintain the knowledge of helper nodes. The energy consumption analysis in [1, 2] for rDCF [61] and enhanced rDCF (ErDCF) also concludes that there is a significant energy saving with the two cooperative MAC protocols. Similar observation is also found in [64] for RAMA. To come up with a more realistic cooperation solution, it is necessary to include the energy consumption as a critical factor in decision making [5] rather than a bonus feature in addition to throughput improvement as most previous work did.

References

1. Ahmad, R.: Performance analysis of relay based cooperative MAC protocols. Ph.D. thesis, Victoria University (2010)
2. Ahmad, R., Zheng, F., Driberg, M., Olafsson, S.: An enhanced relay-enabled medium access control protocol for wireless ad hoc networks. In: Proceedings of IEEE VTC Spring, Melbourne (2006)
3. Akhbari, B., Mirmohseni, M., Aref, M.R.: Compress-and-forward strategy for the relay channel with non-causal state information. In: Proceedings of IEEE International Symposium on Information Theory, Seoul, pp. 1169–1173 (2009)
4. Anghel, P.A., Kaveh, M.: Exact symbol error probability of a cooperative network in a Rayleigh-fading environment. *IEEE Trans. Wirel. Commun.* **3**(5), 1416–1421 (2004)
5. Azgin, A., Altunbasak, Y., AlRegib, G.: Cooperative MAC and routing protocols for wireless ad hoc networks. In: Proceedings of IEEE GLOBECOM, St. Louis, Missouri (2005)
6. Bai, F., Helmy, A.: A survey of mobility models in wireless adhoc networks. In: Safwat, A. (ed.) *Wireless Ad Hoc and Sensor Networks*, pp. 1–30. Springer (2006). ISBN: 978-0-387-25483-8
7. Beaulieu, N.C., Hu, J.: A closed-form expression for the outage probability of decode-and-forward relaying in dissimilar Rayleigh fading channels. *IEEE Commun. Lett.* **10**(12), 813–815 (2006)
8. Bletsas, A., Khisti, A., Reed, D.P., Lippman, A.: A simple cooperative diversity method based on network path selection. *IEEE J. Sel. Areas Commun.* **24**(3), 659–672 (2006)
9. Bletsas, A., Lippman, A., Reed, D.P.: A simple distributed method for relay selection in cooperative diversity wireless networks, based on reciprocity and channel measurements. In: Proceedings of IEEE VTC Spring, vol. 3, Stockholm, pp. 1484–1488 (2005)
10. Camp, T., Boleng, J., Davies, V.: A survey of mobility models for ad hoc network research. *Wirel. Commun. Mob. Comput.* **2**(5), 483–502 (2002)
11. Chiang, C.C.: Wireless network multicasting. Ph.D. thesis, University of California (1998)
12. Chiang, Y., Chen, K.: Optimal cooperative ALOHA multiple access in fading channels. *IEEE Commun. Lett.* **14**(8), 779–781 (2010)
13. Cover, T., Gamal, A.E.: Capacity theorems for the relay channel. *IEEE Trans. Inf. Theory* **25**(5), 572–584 (1979)
14. Dohler, M.: Virtual antenna arrays. Ph.D. thesis, University of London (2003)
15. Du, Q., Zhang, X.: QoS-aware base-station selections for distributed MIMO links in broadband wireless networks. *IEEE J. Sel. Areas Commun.* **29**(6), 1123–1138 (2011)
16. Feeney, L.M., Cetin, B., Hollos, D., Kubisch, M., Mengesha, S., Karl, H.: Multi-rate relaying for performance improvement in IEEE 802.11 WLANs. In: Proceedings of 5th International Conference on Wired/Wireless Internet Communications, Coimbra (2007)
17. Gokturk, M.S., Ercetin, O., Gurbuz, O.: Throughput analysis of ALOHA with cooperative diversity. *IEEE Commun. Lett.* **12**(6), 468–470 (2008)
18. Hong, Y.W., Lin, C.K., Wang, S.H.: On the stability region of two-user slotted ALOHA with cooperative relays. In: Proceedings of IEEE International Symposium on Information Theory, San Diego, pp. 356–360 (2007)
19. Hu, R., Li, J.: Practical compress-and-forward in user cooperation: Wyner-Ziv cooperation. In: Proceedings of IEEE International Symposium on Information Theory, Chengdu. pp. 489–493 (2006)
20. Hunter, T., Nosratinia, A.: Cooperative diversity through coding. In: Proceedings of IEEE International Symposium on Information Theory, Lausanne, p. 220 (2002)
21. Hunter, T.E., Nosratinia, A.: Coded cooperation under slow fading, fast fading, and power control. In: Proceedings of Asilomar Conference on Signals, Systems and Computers, vol. 1, Pacific Grove, pp. 118–122 (2002)
22. Hunter, T.E., Nosratinia, A.: Diversity through coded cooperation. *IEEE Trans. Wirel. Commun.* **5**(2), 283–289 (2006)

23. Hunter, T.E., Sanayei, S., Nosratinia, A.: Outage analysis of coded cooperation. *IEEE Trans. Inform. Theory* **52**(2), 375–391 (2006)
24. Ibrahim, A.S., Sadek, A.K., Su, W., Liu, K.J.R.: Cooperative communications with relay-selection: when to cooperate and whom to cooperate with? *IEEE Trans. Wirel. Commun.* **7**(7), 2814–2827 (2008)
25. Issariyakul, T., Krishnamurthy, V.: Amplify-and-forward cooperative diversity wireless networks: model, analysis, and monotonicity properties. *IEEE/ACM Trans. Netw.* **17**(1), 225–238 (2009)
26. Janani, M., Hedayat, A., Hunter, T.E., Nosratinia, A.: Coded cooperation in wireless communications: space-time transmission and iterative decoding. *IEEE Trans. Signal Process.* **52**(2), 362–371 (2004)
27. Johnson, D.B., Maltz, D.A.: Dynamic source routing in ad hoc wireless networks. *Mobile Comput.* pp. 153–181 (1996)
28. Ju, P., Song, W., Zhou, D.: An enhanced cooperative MAC protocol based on perceptron training. In: *Proceedings of IEEE WCNC, Shanghai* (2013)
29. Ju, P., Song, W., Zhou, D.: Survey on cooperative medium access control protocols. *IET Commun.* **7**(9), 893–902 (2013)
30. Khojastepour, M., Sabharwal, A., Aazhang, B.: Lower bounds on the capacity of Gaussian relay channel. In: *Proceedings of annual conference on information sciences and systems, Big Island*, pp. 597–602 (2004)
31. Kim, T., Skoglund, M., Caire, G.: Quantifying the loss of compress-forward relaying without Wyner-Ziv coding. *IEEE Trans. Inform. Theory* **55**(4), 1529–1533 (2009)
32. Kramer, G., Gastpar, M., Gupta, P.: Cooperative strategies and capacity theorems for relay networks. *IEEE Trans. Inform. Theory* **51**(9), 3037–3063 (2005)
33. Laneman, J.N.: Cooperative diversity in wireless networks: algorithms and architectures. Ph.D. thesis, Massachusetts Institute of Technology (2002)
34. Laneman, J.N., Tse, D.N.C., Wornell, G.W.: Cooperative diversity in wireless networks: efficient protocols and outage behavior. *IEEE Trans. Inf. Theory* **50**(12), 3062–3080 (2004)
35. Laneman, J.N., Wornell, G.W.: Distributed space-time-coded protocols for exploiting cooperative diversity in wireless networks. *IEEE Trans. Inform. Theory* **49**(10), 2415–2425 (2003)
36. Li, Y., Wang, P., Niyato, D., Zhuang, W.: A dynamic relay selection scheme for mobile users in wireless relay networks. In: *Proceedings of IEEE INFOCOM Workshop, Shanghai* (2011)
37. Liang, B., Haas, Z.J.: Predictive distance-based mobility management for PCS networks. In: *Proceedings of IEEE INFOCOM*, vol. 3, pp. 1377–1384 (1999)
38. Liu, P., Tao, Z., Narayanan, S., Korakis, T., Panwar, S.S.: CoopMAC: a cooperative MAC for wireless LANs. *IEEE J. Sel. Areas Commun.* **25**(2), 340–354 (2007)
39. Liu, P., Tao, Z., Panwar, S.: A cooperative MAC protocol for wireless local area networks. In: *Proceedings of IEEE ICC*, vol. 5, St Louis, pp. 2962–2968 (2005)
40. Luo, J., Blum, R.S., Cimini, L.J., Greenstein, L.J., Haimovich, A.M.: Decode-and-forward cooperative diversity with power allocation in wireless networks. *IEEE Trans. Wirel. Commun.* **6**(3), 793–799 (2007)
41. Moon, Y., Syrotiuk, V.R.: A cooperative CDMA-based multi-channel MAC protocol for mobile ad hoc networks. *Comput. Commun.* **32**(17), 1810–1819 (2009)
42. Narayanan, S., Panwar, S.S.: To forward or not to forward – that is the question. *Wirel. Pers. Commun.* **43**(1), 65–87 (2007)
43. Nosratinia, A., Hunter, T.E., Hedayat, A.: Cooperative communication in wireless networks. *IEEE Commun. Mag.* **42**(10), 74–80 (2004)
44. Pathmasuritharam, J.S., Das, A., Gupta, A.K.: Efficient multi-rate relaying (EMR) MAC protocol for ad hoc networks. In: *Proceedings of IEEE ICC*, vol. 5, St Louis, pp. 2947–2951 (2005)
45. Sadek, A.K., Liu, K.J.R., Ephremides, A.: Collaborative multiple-access protocols for wireless networks. In: *Proceedings of IEEE ICC*, vol. 10, Setúbal, pp. 4495–4500 (2006)

46. Sangman, M., Chansu, Y., Seung-Min, P., Heung-Nam, K., Jiwon, P.: CD-MAC: cooperative diversity MAC for robust communication in wireless ad hoc networks. In: Proceedings of IEEE ICC, Glasgow, pp. 3636–3641 (2007)
47. Scutari, G., Barbarossa, S.: Distributed space-time coding for regenerative relay networks. *IEEE Trans. Wirel. Commun.* **4**(5), 2387–2399 (2005)
48. Sediq, A.B., Yanikomeroğlu, H.: Performance analysis of selection combining of signals with different modulation levels in cooperative communications. *IEEE Trans. Veh. Technol.* **60**(4), 1880–1887 (2011)
49. Sendonaris, A., Erkip, E., Aazhang, B.: User cooperation diversity—Part I: system description. *IEEE Trans. Commun.* **51**(11), 1927–1938 (2003)
50. Sendonaris, A., Erkip, E., Aazhang, B.: User cooperation diversity—Part II: implementation aspects and performance analysis. *IEEE Trans. Commun.* **51**(11), 1939–1948 (2003)
51. Shan, H., Cheng, H., Zhuang, W.: Cross-layer cooperative MAC protocol in distributed wireless networks. *IEEE Trans. Wirel. Commun.* **10**(8), 2603–2615 (2011)
52. Shan, H., Zhuang, W., Wang, Z.: Distributed cooperative MAC for multihop wireless networks. *IEEE Commun. Mag.* **47**(2), 126–133 (2009)
53. Simoens, S., Muoz-Medina, O., Vidal, J., Coso, A.D.: Compress-and-forward cooperative MIMO relaying with full channel state information. *IEEE Trans. Signal Process.* **58**(2), 781–791 (2010)
54. Song, W., Ju, P., Zhou, D.: Performance of cooperative relaying with adaptive modulation and selection combining. In: Proceedings of International Conference on Computing, Networking and Communications (ICNC), San Diego (2013)
55. Suraweera, H.A., Smith, P.J., Armstrong, J.: Outage probability of cooperative relay networks in Nakagami- m fading channels. *IEEE Commun. Lett.* **10**(12), 834–836 (2006)
56. Yang, Z., Yao, Y.D., Li, X., Zheng, D.: A TDMA-based MAC protocol with cooperative diversity. *IEEE Commun. Lett.* **14**(6), 542–544 (2010)
57. Yi, Z., Kim, I.: Diversity order analysis of the decode-and-forward cooperative networks with relay selection. *IEEE Trans. Wirel. Commun.* **7**(5), 1792–1799 (2008)
58. Zhao, Y., Adve, R., Lim, T.: Improving amplify-and-forward relay networks: optimal power allocation versus selection. In: Proceedings of IEEE International Symposium on Information Theory, Seattle, pp. 1234–1238 (2006)
59. Zhao, Y., Adve, R., Lim, T.: Symbol error rate of selection amplify-and-forward relay systems. *IEEE Commun. Lett.* **10**(11), 757–759 (2006)
60. Zhou, T., Sharif, H., Hempel, M., Mahasukhon, P., Wang, W., Ma, T.: A novel adaptive distributed cooperative relaying MAC protocol for vehicular networks. *IEEE J. Sel. Areas Commun.* **29**(1), 72–82 (2011)
61. Zhu, H., Cao, G.: rDCF: A relay-enabled medium access control protocol for wireless ad hoc networks. *IEEE Trans. Mobile Comput.* **5**(9), 1201–1214 (2006)
62. Zhuang, W., Ismail, M.: Cooperation in wireless communication networks. *IEEE Wirel. Commun. Mag.* **19**(2), 10–20 (2012)
63. Zhuang, W., Zhou, Y.: A survey of cooperative mac protocols for mobile communication networks. *J. Internet Technol.* **14**(4), 541–560 (2013)
64. Zou, S., Li, B., Wu, H., Zhang, Q., Zhu, W., Cheng, S.: A relay-aided media access (RAMA) protocol in multirate wireless networks. *IEEE Trans. Veh. Technol.* **55**(5), 1657–1667 (2006)

Chapter 3

Energy-Efficient Uncoordinated Cooperative MAC with Uncertain Relay Distribution Intensity

3.1 Motivation and Overview¹

To enable cooperative transmission, the centralized solutions [4, 8, 9] rely on a central controller to determine the best relays, while distributed solutions often have each relay make an independent decision, thus involving light signaling and offering good scalability. In the probability-based strategies [14, 16, 17], each relay that successfully overhears the data from the source independently determines a forwarding probability by synthesizing a variety of factors. In the backoff-based strategies [1, 13], each relay makes use of local information to tune a backoff time so that a best relay with a smallest backoff time wins the contention to forward the overheard data.

Many studies on distributed cooperative strategies assume that the number of relays or the intensity of relay distribution is fixed and known [5, 14]. The forwarding probability or the backoff time can thus be determined accordingly. Unfortunately, such information may not be available in practice, e.g., when a network is newly set up or the network topology dynamically changes. Besides, the energy constraint becomes another primary concern to accommodate green communications with the rising energy cost and rigid environmental standards. Nonetheless, the existing cooperative strategies may suffer a high energy consumption, because of the signalling exchange in the centralized solutions, or excessive packet retransmissions resulting from a bounded transmission success probability of the probability-based strategies. Since only few relays having good channel conditions are important to be ready for packet forwarding, the energy can be wasted unnecessarily to place all relays standby for transmission. Hence, a cooperative

¹Copyright © IEEE (2015). Some content of this chapter is reprinted with permission, from IEEE Transactions on Vehicular Technology (2015) 64(2), 677–688 “An energy-efficient uncoordinated cooperative scheme with uncertain relay distribution intensity,” by A. Jin, W. Song, P. Ju, and D. Zhou [6].

relaying scheme needs to be properly integrated with an effective energy saving strategy. Although there are many studies on energy saving, e.g., for ad hoc and sensor networks with sleeping nodes [18], these solutions may not be directly applicable or too heavy for a two-hop cooperative scenario.

In this chapter, we first develop an algorithm to estimate the unknown intensity of relay distribution, which is critical to properly engage cooperating nodes. The convergence and accuracy of the estimation algorithm are theoretically justified. Considering a backoff-based distributed relay scheme, we further incorporate an energy saving strategy to minimize energy consumption while maintaining satisfactory transmission success probability. The performance of the proposed cooperative solution, particularly the collision probability, is analytically evaluated, since it determines the transmission success probability and thus the average energy consumption. The numerical and simulation results validate our analysis and demonstrate that the proposed cooperative solution outperforms the uncoordinated reference scheme with respect to the transmission performance and energy saving.

3.2 System Model and Problem Formulation

3.2.1 System Model

Consider a wireless network where nodes are randomly distributed in a given region, following a homogeneous Poisson point process (PPP) with an *unknown* intensity λ . We assume that the node distribution is time-stationary and ergodic, which is generally valid under broad assumptions, e.g., for random direction mobility models [2]. The source (S) is referred to the node that generates data traffic; the destination (D) is the node that receives the data. Relay nodes have no intrinsic traffic demands, and the *potential relays* are referred to those nodes that correctly overhear the packet from the source.

We focus on the cooperative transmission of packets from S to D of a distance L in between, as illustrated in Fig. 3.1. Although the direct transmission from S to D may not definitely fail, the success probability can be very low when L is large. Focusing on this challenging scenario, we aim to improve the forwarding performance via spatially random relays, especially the energy efficiency of the cooperative relaying scheme. Hence, we assume that the source has to communicate with the destination via the relays. In practice, the overall success probability can be even higher further considering the direct transmission.

Figure 3.2 illustrates how the cooperative relay protocol works. Here, the time is slotted and each time slot is divided into two mini-slots. The source transmits the packet in the first mini-slot. It is assumed that the source always has a packet to transmit, which can be a new packet when the previous packet has been successfully delivered or a retransmitted packet when the previous packet is corrupted. At the beginning of the second mini-slot, the potential relays start the channel access

Fig. 3.1 An illustration of the system model for cooperative transmission. In addition to S and D , there are potential relays represented by *black nodes*, while the *white nodes* indicate other relay nodes

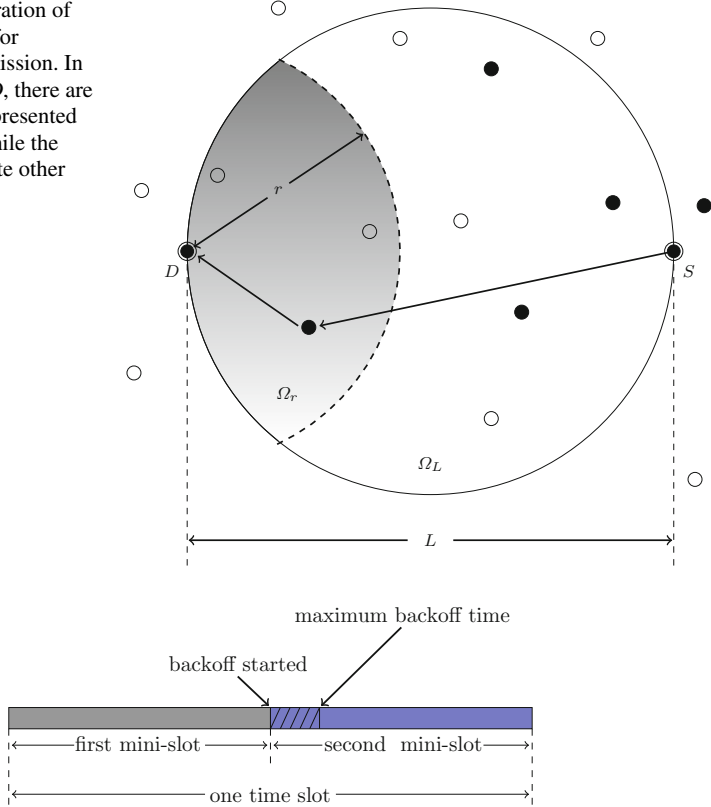


Fig. 3.2 The source transmits the packet in the first mini-slot, and the potential relays start channel access contention with different backoff time at the beginning of the second mini-slot. Whenever a relay wins the contention, it will forward the overheard packet immediately. If no relaying starts within the maximum backoff time, the packet transmission fails and a retransmission is required in the next time slot

contention with different backoff time. Whenever the backoff timer of a relay expires and no packet relaying is sensed, the relay forwards the overheard packet to the destination immediately. If no relaying happens by the maximum backoff time, the current transmission attempt fails and a retransmission is required in the next time slot.

We assume that each node knows its own location, which can be obtained either from a localization technique based on signal strength, time-of-arrival or angle-of-arrival measurements with nearby nodes [3, 10], or through a GPS receiver which becomes increasingly ubiquitous in mobile devices. Further, the location of D can also be obtained in advance via prior handshaking. By piggybacking the locations within the transmitted packets, the relay nodes can obtain this information from the overheard packets. It should be noted that S does not have the knowledge of the

locations of relay nodes, and one relay does not have the location information of other relays either. Besides, we assume that the locations of all nodes in the network do not change significantly during the short cooperative transmission period, which is a typical assumption that generally holds.

For the data transmission between a transmitter located at x and a receiver located at y , the SNR of the received signal can be written as

$$\gamma_{xy} = \frac{P_0}{N_0} h_{xy} g_{xy} \quad (3.1)$$

where P_0 is the transmit power, N_0 is the power of additive white Gaussian noise (AWGN), and h_{xy} denotes the small-scale channel fading which is exponentially distributed with unit mean. The path-loss effect is captured by $g_{xy} = \|x - y\|^{-\alpha}$, where $\|x - y\|$ is the Euclidean distance, and α is the path-loss exponent. The receiver is able to successfully decode the received signal only when the instantaneous SNR is no less than a threshold T_0 [17]. The probability of correctly decoding a packet is given by

$$P_{xy} = \text{P}[\gamma_{xy} \geq T_0] = e^{-K\|x-y\|^\alpha} \quad (3.2)$$

where $K = T_0 N_0 / P_0$. Thus, the one-hop transmission success probability with $\alpha = 2$ is given by

$$P_{SD} = e^{-KL^2}.$$

With the assistance of a relay node, the two-hop transmission success probability is

$$P_{SRD} = e^{-KL_{SR}^2} \cdot e^{-KL_{RD}^2} = e^{-K(L_{SR}^2 + L_{RD}^2)}$$

where L_{SR} is the distance between S and a relay, and L_{RD} is that of the relay and D . To achieve the cooperation gain, we should have

$$\begin{aligned} \frac{P_{SRD}}{P_{SD}} &= e^{-K(L_{SR}^2 + L_{RD}^2 - L^2)} \\ &= e^{-2KL_{SR}L_{RD} \cos(\angle SRD)} \geq 1 \end{aligned}$$

which requires that $\cos(\angle SRD) \leq 0$. Therefore, we only focus on the relays within the region Ω_L , which is the circle with a diameter L , as shown in Fig. 3.1.

3.2.2 Problem Formulation

Cooperative wireless communications have been widely studied and various techniques are proposed for different layers. At the physical layer, a cooperative diversity technique can be used at the relays to forward the received signal from the source in an analog or digital fashion, such as amplify-and-forward (AF) and decode-and-forward (DF) [7]. Then, the destination uses combining techniques such as maximal ratio combining or selective combining to process the contributions from multiple relays. Although such physical-layer techniques can improve the receiving performance, an effective MAC scheme is still needed to coordinate the transmissions from multiple relays. Furthermore, when more relays are engaged, there is a longer delay as well as a higher overall energy consumption to incorporate all relay transmissions (e.g., in orthogonal time slots). In this chapter, we aim to enhance cooperative transmission and minimize the energy consumption from the MAC perspective. The relay selection and channel access mechanisms are the main aspects to be addressed in the cooperative MAC design.

In general, a centralized relay selection protocol aims to identify the best relay(s) by exploiting a global view of the network so as to maximize the transmission success probability and minimize the collision probability. However, because such protocols require additional time to exchange channel state information, the incurred overhead and delay are often large, as well as the energy consumption. On the other hand, due to the high collision probability, the transmission success probability of probability-based uncoordinated protocols is bounded by $1/e \approx 0.368$ [12, 16]. Thus, the energy consumption is also high because of packet retransmission. Besides, it becomes difficult to figure out the optimal forwarding probabilities for the potential relays when the network scales up.

Based on the above observations, we can see that the backoff-based cooperative scheme is more energy-efficient, because of its distributed nature and low collision probability. According to (3.2), we know that the potential relay with a closer distance to the destination has a higher transmission success probability over the relay-to-destination channel. To prioritize such relays closer to the destination, we consider a simple distributed backoff-based cooperative scheme, in which each relay sets the backoff timer to

$$T_i = \frac{r_i}{L} \quad (3.3)$$

where r_i is the distance of the relay R_i to the destination, L is the distance between the source and destination, and the maximum backoff time is taken to be one unit time. As such, the nearest potential relay has the shortest backoff time and forwards the packet to D . If the first two or more relays time out within a certain interval c , a collision will happen [1]. This is generally a valid assumption for MAC-layer study and has been widely considered in the literature [1, 9, 16, 17].

It is worth mentioning that the setting of backoff timer in (3.3) cannot guarantee maximization of the throughput of the source. We see in (3.2) that the distance

determines the transmission success probability over the relay-to-destination channel. In other words, the distance actually captures average channel state information in the long term. Hence, the potential relay with the smallest distance to the destination only has the highest transmission success probability on average. It is possible that there exist other potential relays that experience better instantaneous channel conditions than the relay with the smallest distance to the destination. However, more signalling overhead will be incurred to collect instantaneous channel state information, so as to identify the optimal potential relay with the best instantaneous channel quality. This deviates from our primary design goal, which is to improve the energy efficiency of the cooperative solution while maintaining a high throughput for the source.

To reduce the energy consumption, we further propose an energy saving strategy working together with the backoff-based cooperative scheme. At the beginning of each time slot, each relay determines its on/off status according to a sleeping probability. This sleeping probability is independently decided by each relay in a distributed manner based on a variety of factors. Intuitively, when the relays are deployed sparsely with a low intensity, the sleeping probabilities should be relatively small to ensure that a sufficient number of relays are available to achieve the required performance. In contrast, when the relay intensity is high, the relays can be put to sleep at relatively large probabilities to save energy. As seen, the estimation of relay intensity is important to achieve a high energy efficiency. Meanwhile, the local channel condition of the relay should be considered so that the relays having a good relay-destination channel end up with a low sleeping probability in order to balance energy consumption and transmission performance.

3.3 Relay Intensity Estimation

As discussed in Sect. 3.2.2, the efficiency of the energy saving strategy depends on appropriate setting of the sleep probability of the relay, which in turn varies with the relay intensity. In practice, the relay intensity is often unknown in advance or dynamically changing. Hence, in this section, we first introduce an accurate algorithm to estimate the relay intensity, which is further used in the energy saving strategy presented in Sect. 3.4 for cooperative transmission.

Given the system model in Sect. 3.2.1, the relays are distributed as a homogeneous PPP. Nonetheless, because the receiving success probability of each relay is location-dependent, the distribution of the *potential relays* that correctly overhear the packet from the source is not a homogeneous PPP. To facilitate the relay intensity estimation, we consider a simple node sleeping strategy, which is different from the energy saving strategy used with the cooperative scheme in Sect. 3.4. According to the backoff scheme in (3.3), the relay closer to the source but farther from the destination sets a longer backoff time, which results in a smaller probability to win the contention and to be selected as the forwarding node. Based on this observation, we initialize the sleeping probability of a relay R_i with a distance L_i towards S to

$$\eta_i = 1 - \frac{e^{-KL^2}}{e^{-KL_i^2}}. \quad (3.4)$$

Thus, the spatial distribution of the potential relays can be viewed as the result of a $p(x)$ -thinning process [15]. The $p(x)$ -thinning is a generalized operation that defines a retention probability $p(x)$ for each point of a PPP and yields a thinned point process by deleting the point with a probability $1 - p(x)$. Here, the retention probability for a relay R_i of a distance L_i to S is given by $P_{SR_i} \cdot (1 - \eta_i) = e^{-KL^2}$. Therefore, the distribution of the potential relays is not only a PPP according to Prekopa's Theorem [15], but also homogeneous with the intensity given by

$$\lambda' = \lambda \cdot e^{-KL^2}. \quad (3.5)$$

Then, we can obtain the intensity measure of the potential relays in the region Ω_r (the gray region in Fig. 3.1), which is part of the circle centered at D of a radius r ($0 \leq r \leq L$) within Ω_L :

$$\Lambda'_r = \lambda' \cdot A_r \quad (3.6)$$

where A_r is the area of region Ω_r , given by

$$A_r = r^2 \arccos\left(\frac{r}{L}\right) + \frac{L^2}{2} \arcsin\left(\frac{r}{L}\right) - \frac{L \cdot r}{2} \sqrt{1 - \left(\frac{r}{L}\right)^2}. \quad (3.7)$$

Let $r_{(1)}$ and $r_{(2)}$ be the distance of the nearest and second nearest potential relays to D , receptively. If only the nearest potential relay lies within a distance $[r, r + \Delta r]$ to D , we have the occurrence probability

$$\mathbb{P}[r \leq r_{(1)} \leq r + \Delta r] = \frac{1}{1 - e^{-\Lambda'_L}} \cdot e^{-\Lambda'_r} \cdot \Lambda'_{\Delta r} e^{-\Lambda'_{\Delta r}} \quad (3.8)$$

where $1 - e^{-\Lambda'_L}$ is the probability that there is at least one potential relay within Ω_L , and $\Lambda'_{\Delta r}$ is given by

$$\Lambda'_{\Delta r} = \lambda' \cdot (A_{r+\Delta r} - A_r).$$

Similarly, the probability that the nearest two potential relays both fall into $[r, r + \Delta r]$ is given by

$$\begin{aligned} & \mathbb{P}[r \leq r_{(1)} \leq r + \Delta r, r \leq r_{(2)} \leq r + \Delta r] \\ &= \frac{1}{1 - e^{-\Lambda'_L} - \Lambda'_L e^{-\Lambda'_L}} e^{-\Lambda'_r} \frac{(\Lambda'_{\Delta r})^2}{2} e^{-\Lambda'_{\Delta r}} \\ &= o(\Delta r). \end{aligned} \quad (3.9)$$

Here, a function $\mathcal{Y}(\Delta r)$ is said to be $o(\Delta r)$ if $\lim_{\Delta r \rightarrow 0} \frac{\mathcal{Y}(\Delta r)}{\Delta r} = 0$. Similarly, the probability that there are more than two potential relays within $[r, r + \Delta r]$ is also $o(\Delta r)$. Therefore, we can obtain the probability density function (PDF) of $r_{(1)}$ as

$$\begin{aligned} f(r) &= \lim_{\Delta r \rightarrow 0} \frac{\mathbb{P}[r \leq r_{(1)} \leq r + \Delta r] + o(\Delta r)}{\Delta r} \\ &= \lambda' \frac{e^{-\Lambda'_r}}{1 - e^{-\Lambda'_L}} 2r \arccos\left(\frac{r}{L}\right). \end{aligned} \quad (3.10)$$

The corresponding cumulative distribution function (CDF) is given by

$$F(r) = \frac{1 - e^{-\Lambda'_r}}{1 - e^{-\Lambda'_L}}. \quad (3.11)$$

When $e^{-\Lambda'_L} \rightarrow 0$, we can approximate the CDF as follows:

$$F(r) \approx 1 - e^{-\Lambda'_r} = 1 - e^{-\lambda A_r e^{-KL^2}}. \quad (3.12)$$

In (3.12), the relay intensity λ is directly related to $F(r)$, which can be easily observed from the packets forwarded by the relays. Table 3.1 presents the details of our estimation algorithm for λ . As seen in Line 1 to Line 10, each relay initializes its sleeping probability according to (3.4) and an awake relay R_i that overhears a packet from S sets its backoff time based on (3.3). To collect statistics for $F(r)$, the relay piggybacks its location when forwarding the packet to D . Thus, the destination can obtain the estimated CDF of the distance of the nearest potential relay to D , denoted by $\tilde{F}(r)$.

Supposing that the estimated $\tilde{F}(r)$ involves an error ΔF , we have

$$\begin{aligned} \tilde{F}(r) &= F(r) + \Delta F \\ &= 1 - e^{-\lambda A_r e^{-KL^2}} + \Delta F. \end{aligned} \quad (3.13)$$

Denoting the intensity estimated from $\tilde{F}(r)$ by $\tilde{\lambda}$, we define $\tilde{\lambda} = \lambda + \Delta\lambda$, where $\Delta\lambda$ indicates the estimation error of the intensity. Then, we rewrite $\tilde{F}(r)$ as

$$\begin{aligned} \tilde{F}(r) &= 1 - e^{-\tilde{\lambda} A_r e^{-KL^2}} \\ &= 1 - e^{-\lambda A_r e^{-KL^2}} \cdot e^{-\Delta\lambda A_r e^{-KL^2}}. \end{aligned} \quad (3.14)$$

Combining (3.13) and (3.14), we obtain

$$\begin{aligned}\Delta\lambda &= \frac{-1}{A_r e^{-KL^2}} \ln(1 - \Delta F \cdot e^{\lambda A_r e^{-KL^2}}) \\ &\approx \frac{e^{\lambda A_r e^{-KL^2}}}{A_r e^{-KL^2}} \cdot \Delta F.\end{aligned}\tag{3.15}$$

Since $\Delta\lambda$ is a function of A_r (as well as r), we have

$$\frac{d\Delta\lambda}{dA_r} = \frac{\Delta F}{e^{-KL^2}} \cdot \frac{e^{\lambda A_r e^{-KL^2}} \cdot (\lambda A_r e^{-KL^2} - 1)}{A_r^2}.\tag{3.16}$$

If the estimation error ΔF is bounded, $\Delta\lambda$ is minimized when

$$A_r = \frac{1}{\lambda e^{-KL^2}}.\tag{3.17}$$

Table 3.1 Intensity estimation algorithm

-
- 1: **for** $i = 1 : N_o$ **do** $\triangleright N_o$ packets are transmitted to estimate λ
 - 2: The source node transmits a packet;
 - 3: **for** all the relays **do**
 - 4: Set the sleeping probability according to (3.4);
 - 5: **if** a relay is awake and correctly receives the packet **then**
 - 6: Set its backoff time according to (3.3);
 - 7: **end if**
 - 8: **end for**
 - 9: The destination node records the distance of the first potential relay that forwards the packet;
 - 10: **end for**
 - 11: Initialize r_1 and calculate A_{r_1} according to (3.7);
 - 12: **for** $i = 1 : I_o$ **do** $\triangleright I_o$ iterations are run to estimate λ
 - 13: The destination node estimates $\tilde{F}(r_i)$ according to the record obtained above;
 - 14: Calculate $\tilde{\lambda}_i$ from $\tilde{F}(r_i)$ according to (3.12);
 - 15: Calculate $A_{r_{i+1}}$ according to (3.17) by using $\tilde{\lambda}_i$;
 - 16: Calculate r_{i+1} from $A_{r_{i+1}}$ according to (3.7);
 - 17: **end for**
 - 18: Return $\tilde{\lambda}$;
-

Since the A_r and the corresponding r that satisfies (3.17) are unknown, we use the iterative algorithm in Table 3.1 to approach the exact intensity λ so as to minimize the estimation error. As seen in Line 11 to Line 17, an intensity estimate $\tilde{\lambda}_i$ is obtained from the observed $\tilde{F}(r_i)$ in the i th round. Then, $A_{r_{i+1}}$ and r_{i+1} are updated for the $(i + 1)$ th round by applying $\tilde{\lambda}_i$ to (3.17). The following lemma proves that the iterative algorithm approaches to the optimal r that satisfies (3.17) and minimizes the estimation error $\Delta\lambda$.

Lemma 3.1. *For any $\epsilon > 0$, there exists an I_o so that, when the number of iterations $I > I_o$, we have $|r_i - r_o| < \epsilon$, where r_o is the achievable distance that approaches the minimum estimation error $\Delta\lambda$, given that the estimation error of $F(r)$ is bounded by F_B , i.e., $0 \leq |\Delta F| \leq F_B \ll F(r_o)$.*

Proof. According to (3.17), we need to show that $A_{r_i}e^{-KL^2}$ converges to $A_{r_o}e^{-KL^2} \triangleq x_o$, so as to prove that r_i is updated with the iterative algorithm in a manner so that it converges to r_o . Letting λ_o denote the optimal estimation of λ , we have $x_o = \frac{1}{\lambda_o}$. For the i th iteration, we define the iterative term $x_i = A_{r_i}e^{-KL^2}$. Given $-F_B \leq \Delta F \leq F_B$, if $\Delta F > 0$, we would have $x_i < x_o = \frac{1}{\lambda_o} < \frac{1}{\tilde{\lambda}}$ after very few iterations. Then, we define the estimation errors of any two adjacent rounds as follows:

$$\begin{aligned}\Delta x_i &= x_o - x_i > 0 \\ \Delta x_{i+1} &= x_o - x_{i+1} = x_o - \frac{1}{\tilde{\lambda}_i} > 0.\end{aligned}$$

From (3.13) and (3.14), we have

$$F(r_i) + \Delta F = 1 - e^{-\tilde{\lambda}_i A_{r_i} e^{-KL^2}} = 1 - e^{-\tilde{\lambda}_i x_i}. \quad (3.18)$$

Therefore, we have

$$\begin{aligned}\Delta x_{i+1} - \Delta x_i &= x_i - \frac{1}{\tilde{\lambda}_i} = \frac{-1}{\tilde{\lambda}_i} \cdot \ln \left[1 - F(r_i) - \Delta F \right] - \frac{1}{\tilde{\lambda}_i} \\ &\approx \frac{-1}{\tilde{\lambda}} \cdot \left[\ln(1 - F(r_i)) + 1 \right] \\ &= \frac{-1}{\tilde{\lambda}_i} \cdot \left[\ln(e^{-\lambda x_i}) + 1 \right] \\ &= \frac{-1}{\tilde{\lambda}_i} \cdot (-\lambda \cdot x_i + 1) \\ &= \frac{\lambda}{\tilde{\lambda}_i} \cdot \left(x_i - \frac{1}{\lambda} \right) < 0.\end{aligned}$$

For other cases of ΔF , it can be shown similarly that x_i converges to x_o . Thus, r_i can converge to r_o to approach the minimum estimation error $\Delta\lambda$. \blacksquare

3.4 Energy-Efficient Cooperative Scheme and Its Analysis

The estimation algorithm in Sect. 3.3 can be used to obtain the relay intensity. In this section, we further propose an energy-efficient cooperative scheme, which exploits such information so as to satisfy the required transmission performance while reducing the energy consumption. The performance of the proposed scheme is also analytically evaluated.

3.4.1 An Energy-Efficient Cooperative Scheme

For the backoff-based cooperative schemes, each individual relay determines its backoff time, so that a good relay ends up with a short backoff time, while there is a small probability that more than one relay times out within an indistinguishable interval and results in a collision. There are many studies on the determination of the backoff time such as [1]. In this chapter, we more focus on the energy efficiency of the cooperative scheme and consider the simple design in (3.3), where each relay sets the backoff time based on its distance to D . To reduce the energy consumption, each relay R_i independently decides its on/off status at the beginning of a slot according to a sleeping probability η_i . Intuitively, a relay closer to D should choose a lower sleeping probability, since such relays have a smaller backoff time according to (3.3) and their forwarding transmission can succeed with a higher probability. Thus, there will be less retransmissions and lower energy consumption.

Lemma 3.2. *Assume perfect relaying over the relay-to-destination channel. To minimize energy consumption, the active probability $\zeta_i = 1 - \eta_i$ of a relay R_i in the region Ω_L should be either 0 or 1.*

Proof. The extended proof for the general case with N relays is given in [Appendix A: Extended Proof of Lemma 3.2 with \$N\$ Relays](#). In the following, we present the proof for a special case with two relay nodes for easy comprehension. Consider two arbitrary relay nodes R_1 and R_2 in the region Ω_L , as illustrated in Fig. 3.3, where p_1 and p_2 are their corresponding successful receiving probabilities from S . Let ζ_1 and ζ_2 be the active probabilities of R_1 and R_2 , respectively. Assume that the energy consumption for transmitting a packet, and that for listening to and receiving a packet are both constants, denoted by E_t and E_r , respectively. Obviously, the overall transmission success probability depends on the available relay candidates. Generally, the more relay candidates, the greater total energy consumption, and the higher transmission success probability. Intuitively, more collisions are involved with more relays and degrade the transmission success probability. On the other hand, the opportunity of locating a good relay also increases with the number of relays, which reduces packet loss caused by poor channel condition. Moreover, the collision probability of the backoff-based cooperative scheme is very low and increases slowly with the number of relays,

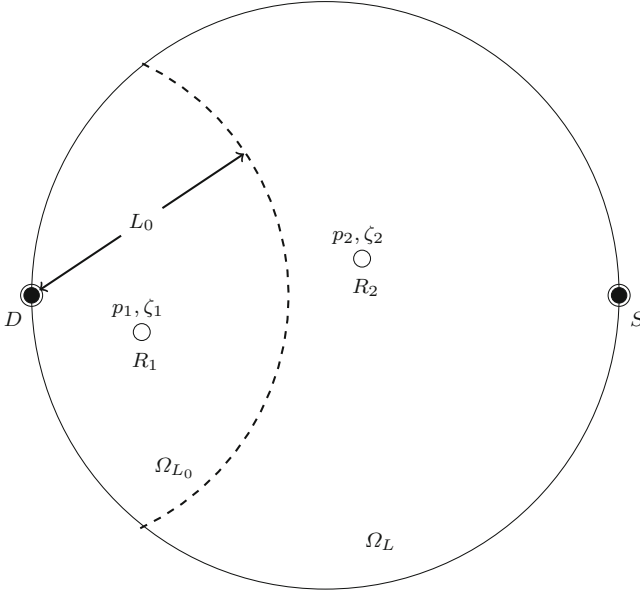


Fig. 3.3 An illustration of sleeping scheduling for relays

as illustrated in Sect. 3.5.3. Hence, the transmission success probability is not lowered with more relays. The trade-off between the energy consumption and the transmission success probability will be discussed in depth in Sect. 3.5.2. Here, we first focus on the energy consumption and assume perfect forwarding from the relays. The average energy consumption of a packet transmission is then given by

$$\begin{aligned}
 E &= \zeta_1 \zeta_2 \left[2E_r + p_1 E_t + (1 - p_1) p_2 E_t + (1 - p_1)(1 - p_2) E \right] \\
 &\quad + \zeta_1 (1 - \zeta_2) \left[E_r + p_1 E_t + (1 - p_1) E \right] \\
 &\quad + (1 - \zeta_1) \zeta_2 \left[E_r + p_2 E_t + (1 - p_2) E \right] \\
 &\quad + (1 - \zeta_1)(1 - \zeta_2) E.
 \end{aligned} \tag{3.19}$$

In (3.19), the first term gives the total energy consumption if both R_1 and R_2 are active during the packet transmission, which includes the listening and receiving energy consumption of the two nodes, the transmission energy consumption with a forwarding priority to R_1 , and the retransmission energy consumption if both nodes fail to successfully receive the packet. The other three terms define the energy consumption when only one node or none correctly overhears the packet. We can simplify (3.19) to

$$E = E_t + \frac{\zeta_1 + \zeta_2}{1 - (1 - p_1 \zeta_1)(1 - p_2 \zeta_2)} \cdot E_r. \quad (3.20)$$

Equation (3.20) provides a physical interpretation of the average energy consumption, which is the transmission energy consumption plus the normalized average energy consumption for listening and receiving. Here, the normalization factor is the probability that at least one active relay among R_1 and R_2 correctly overhears the packet from the source.

Assuming that p_1 , p_2 and ζ_1 are known, we next determine ζ_2 so as to minimize the energy consumption. Thus, we consider

$$\frac{dE}{d\zeta_2} = \frac{p_1 \zeta_1 - (1 - p_1 \zeta_1)p_2 \zeta_1}{\left[1 - (1 - p_1 \zeta_1)(1 - p_2 \zeta_2)\right]^2} \cdot E_r \quad (3.21)$$

and obtain the active probability ζ_2 of R_2 according to p_1 , p_2 and ζ_1 as

$$\zeta_2 = \begin{cases} 0, & \text{if } p_2 \leq P_\zeta \\ 1, & \text{if } p_2 > P_\zeta \end{cases} \quad (3.22)$$

where P_ζ is derived by setting $\frac{dE}{d\zeta_2} = 0$ and given by

$$P_\zeta = \frac{1}{\zeta_1} \cdot \left(\frac{1}{1 - p_1 \zeta_1} - 1 \right). \quad (3.23)$$

As seen, to minimize the energy consumption, the active probability of the relay R_2 is either 0 or 1, depending on its successful receiving probability p_2 and the status of other relays captured by P_ζ . ■

Based on the conclusion of Lemma 3.2, we assume that there exists a distance L_0 such that any relay R_i in the region Ω_L and with a distance less than L_0 to D has an active probability $\zeta_i = 1$, and all the other relays have $\zeta_i = 0$. Extending (3.20), we write the average energy consumption for the above energy saving strategy as

$$E = E_t + \frac{\iint_{\Omega_{L_0}} 1 \cdot \lambda r d\theta dr}{1 - e^{-\Lambda_{L_0}}} \cdot E_r \quad (3.24)$$

where Ω_{L_0} denotes the region within Ω_L and with a distance less than L_0 to D , and Λ_{L_0} is the intensity measure of the potential relays in Ω_{L_0} , given by

$$\Lambda_{L_0} = \iint_{\Omega_{L_0}} e^{-K(L^2 + r^2 - 2Lr \cos \theta)} \lambda r d\theta dr.$$

Hence, the probability that at least one relay in Ω_{L_0} correctly overhears the packet is given by

$$P_{1+} = 1 - e^{-\Lambda L_0} \quad (3.25)$$

which is actually the upper bound of the transmission success probability. Following an approach similar to (3.21), (3.22), and (3.23), we can take the first-order derivative of E with respect to L_0 and determine L_0 that minimizes the energy consumption by setting $\frac{dE}{dL_0} = 0$. The threshold L_0 should satisfy

$$\bar{P}_{L_0} = P_\zeta \quad (3.26)$$

where \bar{P}_{L_0} is the average successful receiving probability of the relays on the separating arc of Ω_{L_0} as illustrated in Fig. 3.3, given by

$$\bar{P}_{L_0} = \frac{\int_0^{\arccos(\frac{L_0}{L})} e^{-K(L^2 + L_0^2 - 2LL_0 \cos \theta)} d\theta}{\arccos(\frac{L_0}{L})} \quad (3.27)$$

and P_ζ captures the status of the relays in Ω_{L_0} , given by

$$P_\zeta = \frac{1}{\iint_{\Omega_{L_0}} 1 \cdot \lambda r d\theta dr} \cdot \left(\frac{1}{e^{-\Lambda L_0}} - 1 \right) = \frac{1}{\lambda A_{L_0}} \cdot \left(\frac{1}{e^{-\Lambda L_0}} - 1 \right). \quad (3.28)$$

As seen, the proposed energy saving strategy is distributed, since the active probability is determined individually by each relay according to its distance to D and the relay intensity λ . The relay intensity can be estimated by the destination with the algorithm in Table 3.1 and obtained by each relay via prior handshaking. Intuitively, if the relay intensity is overvalued, the threshold L_0 will be underestimated, and P_{1+} will be too small. Consequently, the energy consumption will be high due to retransmissions, since the transmission success probability is bounded by P_{1+} at a low level. If the relay intensity is underestimated, the threshold L_0 will be overvalued and more relays will be involved unnecessarily in the cooperative transmission. As a result, the energy consumption will also be high. Thus, the accuracy of the estimated relay intensity λ becomes important to properly determine L_0 . In Sect. 3.5.2, we will provide a numerical example to further discuss the impact of L_0 on the tradeoff between the transmission success probability and the energy consumption.

It is worth mentioning that the proposed strategy is not optimal since we set bias for the relays close to D due to their high transmission success probability. In fact, it is very difficult to find the optimal ζ_i for all the relays in Ω_L , because the global information of the relays will be required. We leave that to future work. Although the proposed strategy is not optimal, it is highly efficient due to the distributed nature, which is validated by the results in Sect. 3.5.3.

3.4.2 Analysis of Collision Probability

Since collisions are a main concern with distributed cooperative solutions, we evaluate the collision probability of the backoff-based cooperative scheme with energy saving in this section. A collision happens when the first two or more potential relays time out within an indistinguishable time interval c . As discussed in [1], this uncertainty interval depends on factors such as radio switch time between the receive and transmit modes, and different signal propagation time in the wireless medium. Although an explicit time synchronization protocol among the relays is usually not required for the backoff-based schemes, the packet reception from the source can initiate a “crude” timing process at each relay. To account for the asynchronization among contending relays, we can consider a sufficiently large value for the interval c . Then, the performance is assessed in a worst-case scenario since the higher the uncertainty interval, the higher the collision probability. For analysis purposes, we further map the time interval c to a distance interval w , which means that two potential relays nearest to the destination are spaced less than w apart. According to (3.3), the backoff time of a potential relay is linearly related to its distance to the destination. As a result, the time interval c is linearly mapped to the distance interval w , which also captures the relay differences as well as the synchronization margin.

Provided that at least two potential relays lie in Ω_{L_0} with a probability

$$P_{2+} = 1 - e^{-\Lambda_{L_0}} - \Lambda_{L_0} \cdot e^{-\Lambda_{L_0}} \quad (3.29)$$

we next obtain the joint distribution of the distance of the first and second nearest potential relays to D . Let $r_{(1)}$ and $r_{(2)}$ denote the distance of the two nearest potential relays to D , where $r_{(1)} \leq r_{(2)}$. We consider two cases depending on whether the two potential relays fall into the same sufficiently small area. In the first case, the first nearest potential relay is located in the region $[r_1, r_1 + \Delta r]$, while the second nearest potential relay falls into the region $[r_2, r_2 + \Delta r]$, where $r_1 < r_2 \leq L_0$. The corresponding occurrence probability is given by

$$\begin{aligned} & \text{P}[r_1 \leq r_{(1)} \leq r_1 + \Delta r, r_2 \leq r_{(2)} \leq r_2 + \Delta r] \\ &= \frac{e^{-\Lambda_{r_1}} \cdot \Lambda_{\Delta r_1} e^{-\Lambda_{\Delta r_1}} \cdot e^{-(\Lambda_{r_2} - \Lambda_{r_1 + \Delta r_1})} \cdot \Lambda_{\Delta r_2} e^{-\Lambda_{\Delta r_2}}}{P_{2+}} \\ &= \frac{\Lambda_{\Delta r_1} \cdot \Lambda_{\Delta r_2} \cdot e^{-\Lambda_{\Delta r_2}} \cdot e^{-\Lambda_{r_2}}}{P_{2+}} \end{aligned} \quad (3.30)$$

where

$$\Lambda_{\Delta r_1} = 2 \int_{r_1}^{r_1 + \Delta r} \int_0^{\arccos(\frac{r}{L})} e^{-K(L^2 + r^2 - 2Lr \cos \theta)} \lambda r d\theta dr$$

$$\Lambda_{\Delta r_2} = 2 \int_{r_2}^{r_2 + \Delta r} \int_0^{\arccos(\frac{r}{L})} e^{-K(L^2 + r^2 - 2Lr \cos \theta)} \lambda r d\theta dr$$

$$\Lambda_{r_2} = 2 \int_0^{r_2} \int_0^{\arccos(\frac{r}{L})} e^{-K(L^2 + r^2 - 2Lr \cos \theta)} \lambda r d\theta dr.$$

Therefore, we obtain the joint PDF as

$$\begin{aligned} & g(r_1, r_2) \\ &= \lim_{\Delta r \rightarrow 0} \frac{\mathbb{P}[r_1 \leq r_{(1)} \leq r_1 + \Delta r, r_2 \leq r_{(2)} \leq r_2 + \Delta r]}{(\Delta r)^2} \\ &= \frac{e^{-\Lambda_{r_2}}}{P_{2+}} \cdot \left[2\lambda r_1 e^{-K(L^2 + r_1^2)} \int_0^{\arccos(\frac{r_1}{L})} e^{2KLr_1 \cos \theta} d\theta \right] \\ & \quad \left[2\lambda r_2 e^{-K(L^2 + r_2^2)} \int_0^{\arccos(\frac{r_2}{L})} e^{2KLr_2 \cos \theta} d\theta \right]. \end{aligned} \quad (3.31)$$

In the second case, the two potential relays lie in the same sufficiently small region $[r_1, r_1 + \Delta r]$, which occurs with a probability

$$\begin{aligned} & \mathbb{P}[r_1 \leq r_{(1)} \leq r_1 + \Delta r, r_1 \leq r_{(2)} \leq r_1 + \Delta r] \\ &= \frac{1}{P_{2+}} \cdot e^{-\Lambda_{r_1}} \cdot \frac{(\Lambda_{\Delta r_1})^2}{2} e^{-\Lambda_{\Delta r_1}}. \end{aligned} \quad (3.32)$$

The PDF for the second case is then

$$\begin{aligned} h(r_1) &= \lim_{\Delta r \rightarrow 0} \frac{\mathbb{P}[r_1 \leq r_{(1)} \leq r_1 + \Delta r, r_1 \leq r_{(2)} \leq r_1 + \Delta r]}{\Delta r} \\ &= \lim_{\Delta r \rightarrow 0} \frac{o(\Delta r)}{\Delta r} = 0. \end{aligned} \quad (3.33)$$

According to the distributions of the distance of the two nearest potential relays to D , we obtain the conditional collision probability given that at least two potential relays lie in Ω_{L_0} as follows:

$$P_c = 1 + \frac{\Lambda_{L_0-w} \cdot e^{-\Lambda_{L_0}}}{P_{2+}} - \frac{1}{P_{2+}} \int_0^{L_0-w} e^{-\Lambda_{r_1}} \cdot e^{-\Lambda_{\Delta w}} d\Lambda_{r_1} \quad (3.34)$$

where

$$\Lambda_{\Delta w} = 2 \int_{r_1}^{r_1+w} \int_0^{\arccos(\frac{r}{L})} e^{-K(L^2 + r^2 - 2Lr \cos \theta)} \lambda r d\theta dr$$

$$\Lambda_{L_0-w} = 2 \int_0^{L_0-w} \int_0^{\arccos(\frac{r}{L})} e^{-K(L^2 + r^2 - 2Lr \cos \theta)} \lambda r d\theta dr.$$

The derivation of (3.34) is given in [Appendix B: Proof of \(3.34\) and \(3.35\)](#). An upper bound is also obtained for P_c in [Appendix B: Proof of \(3.34\) and \(3.35\)](#), given by

$$P_c \leq 1 + \frac{\Lambda_{L_0-w} \cdot e^{-\Lambda_{L_0}}}{P_{2+}} - \frac{e^{-\Psi}}{P_{2+}} \cdot (1 - e^{-\Lambda_{L_0-w}}) \triangleq P_c^U \quad (3.35)$$

where

$$\begin{aligned} \Psi &= \max\{\Lambda_{\Delta w}\} \\ &= 2 \int_{L_0-w}^{L_0} \int_0^{\arccos(\frac{r}{L})} e^{-K(L^2+r^2-2Lr\cos\theta)} \lambda r d\theta dr. \end{aligned}$$

3.5 Numerical and Simulation Results

In this section, numerical and simulation results are first presented to demonstrate the accuracy of the estimation algorithm for relay intensity introduced in Sect. 3.3. Then, we validate our theoretical analysis in Sect. 3.4.2 for the cooperative scheme with energy saving. The proposed scheme is also compared with an uncoordinated probability-based scheme. Table 3.2 lists the default system parameters.

3.5.1 Relay Intensity Estimation

Because the relay intensity estimation depends on the collected statistics of $F(r)$, we first validate the analysis of $F(r)$. As seen in Fig. 3.4, the simulation results and theoretical results match well, which confirms the analysis accuracy for $F(r)$. The simulation results of the estimated intensity $\tilde{\lambda}$ are shown in Fig. 3.5. As seen, the estimated $\tilde{\lambda}$ is of high accuracy, which demonstrates the effectiveness of our proposed estimation algorithm.

Table 3.2 System parameters

Symbol	Value	Definition
P_0/N_0	40 dB	SNR of the transmitter
T_0	5	SNR threshold of signal decoding
α	2	Path-loss exponent
L	70 m	Distance between source and destination
λ	$10^{-2} \sim 10^{-1}$	Relay distribution intensity
w	0.5 m	Collision window (distance interval)

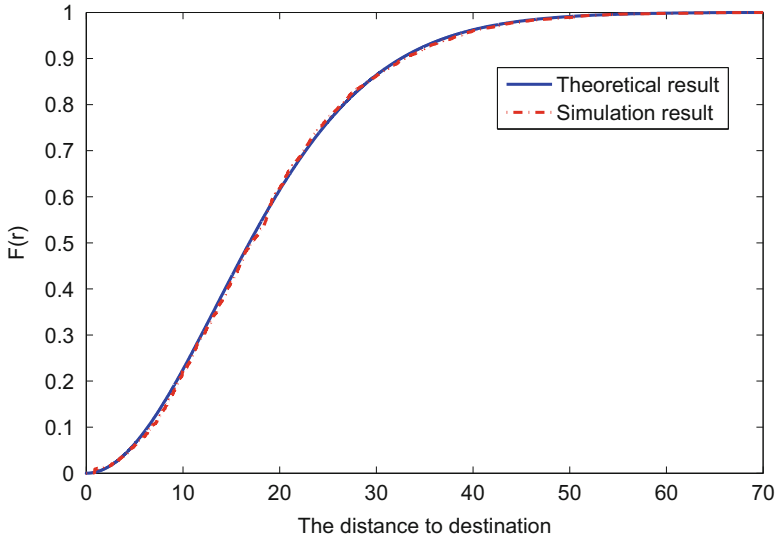


Fig. 3.4 CDF of the distance of the nearest potential relay to the destination

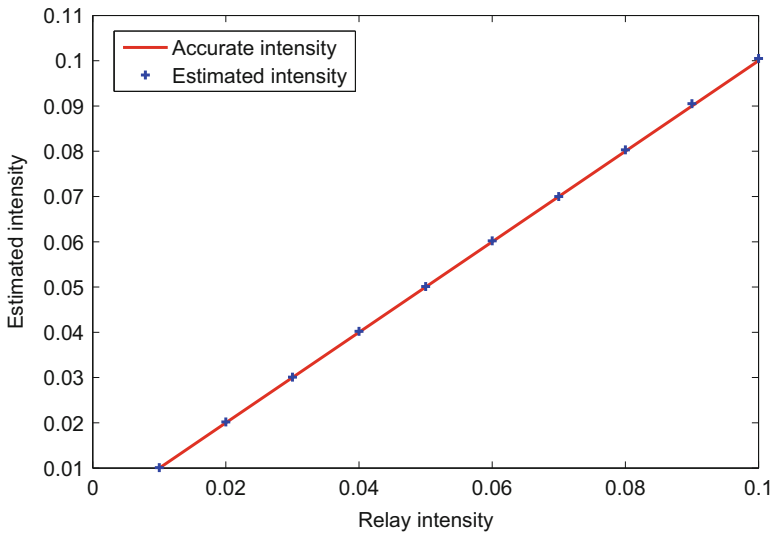


Fig. 3.5 Estimated relay intensity $\tilde{\lambda}$ vs. the exact relay intensity λ

3.5.2 Energy Saving Strategy

Figure 3.6 shows the analytical results of energy consumption (E) against the distance r , where all the relays of a distance to D less than r are active and others are sleeping during the packet transmission. Here, the energy for transmission and that

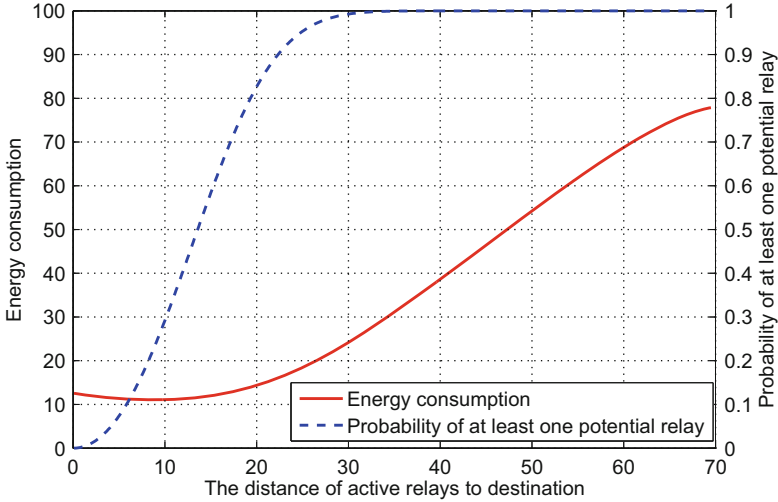


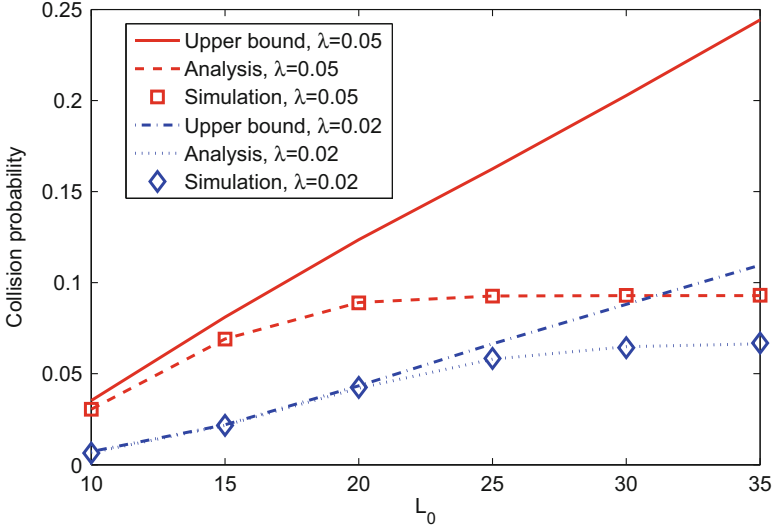
Fig. 3.6 Energy consumption and the probability of at least one potential relay vs. the distance to the destination

for listening/receiving are taken to be a constant [11], and the energy consumption in Fig. 3.6 is in the unit of this constant. Besides, Fig. 3.6 also shows the probability that at least one potential relay lies in the region $\Omega_r (P_{1+})$, which is the upper bound of the transmission success probability. As seen, the energy consumption slightly goes down at the beginning. When r further increases, the energy consumption goes up. This is because the benefit of involving more relays with a greater P_{1+} cannot offset the side effect of higher incurred energy consumption.

Since the transmission success probability is bounded by P_{1+} , there is a trade-off between the transmission success probability and the energy consumption. As seen in Fig. 3.6, the minimum energy consumption is achieved with $L_0 \approx 12$, which can be obtained from (3.26), (3.27), and (3.28). However, the corresponding transmission success probability with such L_0 may be too low to be acceptable for certain loss-sensitive applications. Therefore, a better threshold can be chosen for L_0 so as to satisfy certain required transmission success probability and ensure reasonable energy consumption. For example, by choosing $L_0 = 30$, we have P_{1+} almost 1 and achieve about 70% energy saving compared to $L_0 = L$. If P_{1+} can be relaxed to 0.8, $L_0 = 20$ will be a good choice and almost minimizes the energy consumption. As such, we can achieve a balance between the transmission performance and energy consumption by properly adapting the parameter L_0 based on our preceding analysis in Sect. 3.4.1. For the experiments in Sect. 3.5.3, we use the values in Table 3.3 for L_0 , which ensures a P_{1+} around 0.8.

Table 3.3 L_0 for numerical analysis and simulations.

λ	0.01	0.02	0.03	0.04	0.05
L_0	25.5	20	16.5	14.5	13.5
λ	0.06	0.07	0.08	0.09	0.10
L_0	12.5	11.5	11	10.5	10

**Fig. 3.7** Collision probability P_c vs. L_0

3.5.3 Performance Evaluation

For comparison purposes, we consider an uncoordinated probability-based solution for reference. Similar to the local SNR based scheme proposed in [17], a potential relay R_i forwards an overheard packet with a probability τ_i , given by

$$\tau_i = e^{-\Lambda r_i} \quad (3.36)$$

where r_i is the distance of R_i to D . Thus, τ_i gives the probability that none potential relay in Ω_{r_i} has an average SNR greater than that of R_i .

Figure 3.7 shows the numerical results and simulation results of the collision probability against the threshold L_0 of the energy saving strategy. As seen, the simulation results match closely the analytical results, which validates the accuracy of our analysis. As expected, the collision probability increases with L_0 and λ due to a greater number of potential relays. Also, it is observed that the collision probability is tightly bounded by the upper bound when L_0 is small, and it is much smaller than the bound when L_0 gets larger. As shown in Fig. 3.7, the upper bound increases almost linearly with L_0 . In contrast, the collision probability of the proposed cooperative scheme increases much slower than the linear growth. This is an attractive feature since it means that the collision probability increases slowly when there are more active relays.

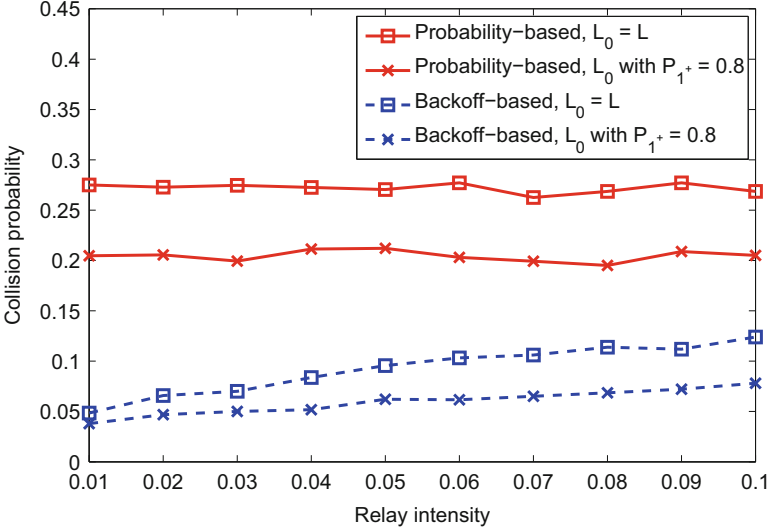


Fig. 3.8 Collision probability P_c vs. the relay intensity λ

Figure 3.8 compares the collision probability of the cooperative scheme proposed in Sect. 3.4.1 to that of the probability-based scheme defined in (3.36). It can be seen that our scheme achieves a much lower collision probability. The proposed energy saving strategy can reduce the collision probability of both schemes, since the number of contending relays is smaller by turning off relays outside the region Ω_{L_0} .

Figure 3.9 shows the transmission success probability of the two cooperative solutions with respect to the relay distribution intensity. We can see that the transmission success probability of the probability-based scheme is bounded by $1/e \approx 0.368$, which matches the observations in [12, 16]. In contrast, the backoff-based solution can achieve a transmission success probability higher than 0.65, because of the low collision probability shown in Fig. 3.8. Moreover, we can find that the transmission success probability of the backoff-based scheme is slightly degraded by considering the energy saving threshold L_0 in Table 3.3, although the threshold L_0 reduces the collision probability, as shown in Fig. 3.8. This is because the transmission success probability is upper bounded by P_{1+} , and we select L_0 here to ensure a P_{1+} around 0.8. It is also observed in Fig. 3.9 that the transmission success probability only vary slightly with the relay intensity. This seems counter-intuitive since there will be more collisions when the relay intensity increases. This is because more potential relays also result in a higher chance of finding good relays, which mitigates packet loss caused by poor channel conditions and offsets the impact of increased packet collisions.

To investigate the energy consumption of the two cooperative schemes, we evaluate the average energy consumption of the relays for a packet against the relay

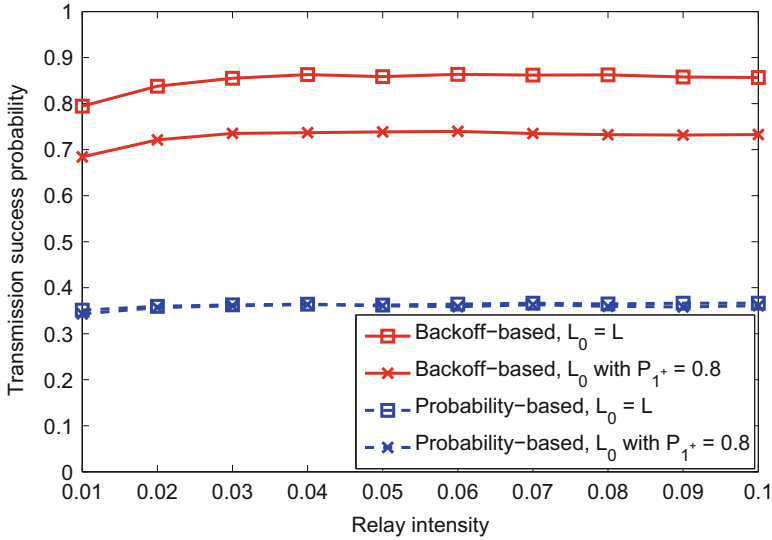


Fig. 3.9 Transmission success probability vs. the relay intensity λ

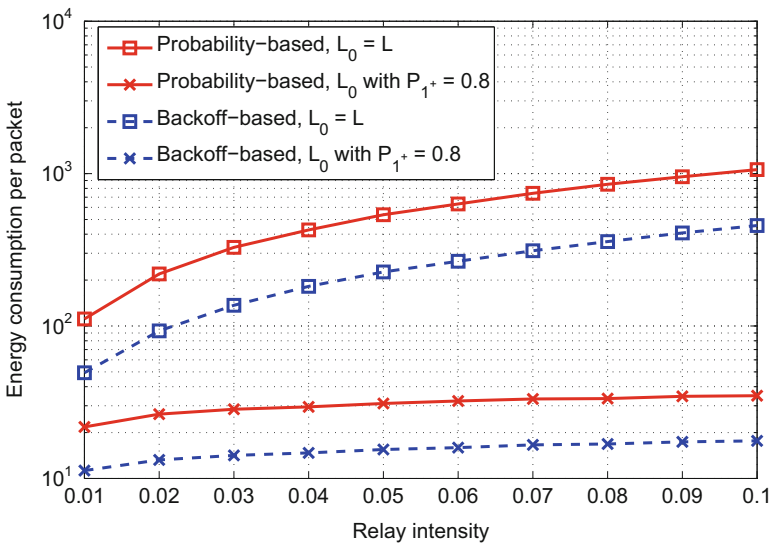


Fig. 3.10 Energy consumption vs. the relay intensity λ

intensity, as shown in Fig. 3.10. Compared to the probability-based scheme, the backoff-based scheme can save around 50% of energy on average, when the energy saving thresholds L_0 in Table 3.3 are applied. This is achieved by taking advantage of the low collision probability and high transmission success probability of the backoff-based scheme. Besides, we find that both schemes can achieve substantial

energy saving as opposed to that with $L_0 = L$. For example, the backoff-based scheme can save more than 75 % of energy, although the transmission success probability is slightly reduced. Therefore, our proposed cooperative scheme is highly energy-efficient.

3.6 Summary

In this chapter, we study distributed cooperative communications between a source-destination pair, where the relays are deployed as a PPP with an *unknown* intensity. Particularly, we focus on a backoff-based cooperative scheme, where the potential relay closest to the destination has the smallest backoff time and wins the contention. To estimate the relay distribution intensity, the PDF and CDF of the distance of the nearest potential relay to the destination are derived, and an iterative estimation algorithm is proposed with the proof of convergence. Although the backoff-based scheme can save considerable energy consumption when compared to the centralized schemes and probability-based schemes, we find that many relays may be active unnecessarily. Hence, we also propose a distributed energy saving strategy, which selectively turns off low-quality relays in certain regions. To evaluate the performance of the proposed scheme with energy saving, we analyze the collision probability and derive an upper bound.

Extensive numerical and simulation results validate our analysis on the probability distribution of the distance of the nearest potential relay to the destination. The proposed estimation algorithm for the relay intensity also shows a high accuracy and a fast convergence speed. In addition, we properly characterize the trade-off between the energy consumption and the transmission success probability. An energy saving threshold can be derived accordingly to guarantee a required transmission success probability and effectively reduce the energy consumption at the same time. The simulation results show that the proposed energy saving strategy can significantly reduce the energy consumption for both the backoff-based and probability-based schemes. Although the transmission success probability of the backoff-based scheme is slightly degraded by the energy saving strategy, it is still much higher than that of the probability-based scheme. Moreover, the backoff-based scheme can save around 50 % of energy on average when compared to the probability-based scheme.

Appendix A: Extended Proof of Lemma 3.2 with N Relays

Let p_1, p_2, \dots, p_N be the probabilities that N relays correctly receive a packet from S , and $\zeta_1, \zeta_2, \dots, \zeta_N$ be the active probabilities of the N relays, respectively. Any unknown ζ_n ($2 \leq n \leq N$) can be determined according to known $\zeta_1, \dots, \zeta_{n-1}$. Thus, $\zeta_1, \zeta_2, \dots, \zeta_N$ can be obtained sequentially so as to minimize the overall energy consumption of these N relays.

The average energy consumption of a packet transmission is given by

$$E = \mathcal{P}_1 \cdot E_t + \mathcal{P}_2 \cdot E_r + \mathcal{P}_3 \cdot E$$

where \mathcal{P}_1 is the probability that at least one active relay correctly overhears the packet from the source, \mathcal{P}_2 is the average number of relays that are active during the packet transmission, and \mathcal{P}_3 is the probability that none of the active relays successfully overhears the packet from the source. For N relays, we have

$$\mathcal{P}_1 = 1 - \prod_{i=1}^N (1 - p_i \zeta_i), \quad \mathcal{P}_2 = \sum_{i=1}^N \zeta_i, \quad \mathcal{P}_3 = 1 - \mathcal{P}_1.$$

Thus, we have

$$E = E_t + \frac{\zeta_1 + \zeta_2 + \cdots + \zeta_N}{1 - (1 - p_1 \zeta_1)(1 - p_2 \zeta_2) \cdots (1 - p_N \zeta_N)} \cdot E_r.$$

Similar to (3.21), (3.22), and (3.23), it can be easily inferred that, given known $\zeta_1, \dots, \zeta_{N-1}$, the active probability ζ_N should be either 0 or 1, so as to minimize the average energy consumption E . The setting of 0 or 1 to ζ_N depends on the successful receiving probability p_N and the status of the other relays.

Appendix B: Proof of (3.34) and (3.35)

The conditional collision probability P_c is given by

$$\begin{aligned} P_c &= \text{P}[r_2 \leq r_1 + w] = 1 - \text{P}[r_2 > r_1 + w] = 1 - \int_0^{L_0-w} \int_{r_1+w}^{L_0} g(r_1, r_2) dr_2 dr_1 \\ &= 1 - \frac{1}{P_{2+}} \int_0^{L_0-w} \left\{ \left[2\lambda r_1 e^{-K(L^2+r_1^2)} \int_0^{\arccos(\frac{r_1}{L})} e^{2KLr_1 \cos \theta} d\theta \right] \right. \\ &\quad \left. \int_{r_1+w}^{L_0} \left[e^{-\Lambda r_2} \left(2\lambda r_2 e^{-K(L^2+r_2^2)} \int_0^{\arccos(\frac{r_2}{L})} e^{2KLr_2 \cos \theta} d\theta \right) \right] dr_2 \right\} dr_1 \\ &= 1 - \frac{1}{P_{2+}} \int_0^{L_0-w} \left\{ \left[2\lambda r_1 e^{-K(L^2+r_1^2)} \int_0^{\arccos(\frac{r_1}{L})} e^{2KLr_1 \cos \theta} d\theta \right] \right. \\ &\quad \left. \cdot \left(e^{-\Lambda r_1} \cdot e^{-\Lambda \Delta w} - e^{-\Lambda L_0} \right) \right\} dr_1 \end{aligned}$$

$$\begin{aligned}
&= 1 - \frac{1}{P_{2+}} \int_0^{\Lambda_{L_0-w}} \left(e^{-\Lambda_{r_1}} \cdot e^{-\Lambda_{\Delta w}} - e^{-\Lambda_{L_0}} \right) d\Lambda_{r_1} \\
&= 1 + \frac{\Lambda_{L_0-w} \cdot e^{-\Lambda_{L_0}}}{P_{2+}} - \frac{1}{P_{2+}} \int_0^{\Lambda_{L_0-w}} e^{-\Lambda_{r_1}} \cdot e^{-\Lambda_{\Delta w}} d\Lambda_{r_1}. \tag{3.37}
\end{aligned}$$

Therefore, (3.34) is proved.

Since $\Lambda_{\Delta w} \leq \Psi$, according to (3.6), we have

$$\begin{aligned}
P_c &\leq 1 + \frac{\Lambda_{L_0-w} \cdot e^{-\Lambda_{L_0}}}{P_{2+}} - \frac{1}{P_{2+}} \int_0^{\Lambda_{L_0-w}} e^{-\Lambda_{r_1}} \cdot e^{-\Psi} d\Lambda_{r_1} \\
&= 1 + \frac{\Lambda_{L_0-w} \cdot e^{-\Lambda_{L_0}}}{P_{2+}} - \frac{e^{-\Psi}}{P_{2+}} \int_0^{\Lambda_{L_0-w}} e^{-\Lambda_{r_1}} d\Lambda_{r_1} \\
&= 1 + \frac{\Lambda_{L_0-w} \cdot e^{-\Lambda_{L_0}}}{P_{2+}} - \frac{e^{-\Psi}}{P_{2+}} \left[(-e^{-\Lambda_{r_1}}) \Big|_0^{\Lambda_{L_0-w}} \right] \\
&= 1 + \frac{\Lambda_{L_0-w} \cdot e^{-\Lambda_{L_0}}}{P_{2+}} - \frac{e^{-\Psi}}{P_{2+}} (1 - e^{-\Lambda_{L_0-w}})
\end{aligned} \tag{3.38}$$

which gives the result in (3.35).

References

1. Bletsas, A., Khisti, A., Reed, D.P., Lippman, A.: A simple cooperative diversity method based on network path selection. *IEEE J. Sel. Areas Commun.* **24**(3), 659–672 (2006)
2. Carofiglio, G., Chiasserini, C., Garetto, M., Leonardi, E.: Route stability in MANETs under the random direction mobility model. *IEEE Trans. Mobile Comput.* **8**(9), 1167–1179 (2009)
3. Chen, Z., Gokeda, G., Yu, Y.: *Introduction to Direction-of-Arrival Estimation*. Artech House, Boston (2010)
4. Du, Q., Zhang, X.: QoS-aware base-station selections for distributed MIMO links in broadband wireless networks. *IEEE J. Sel. Areas Commun.* **29**(6), 1123–1138 (2011)
5. Ganti, R.K., Haenggi, M.: Analysis of uncoordinated opportunistic two-hop wireless ad hoc systems. In: *Proceedings of IEEE International Symposium on Information Theory, Seoul*, pp. 1020–1024 (2009)
6. Jin, A., Song, W., Ju, P., Zhou, D.: An energy-efficient uncoordinated cooperative scheme with uncertain relay distribution intensity. *IEEE Trans. Veh. Technol.* **64**(2), 677–688 (2015)
7. Laneman, J.N., Tse, D.N.C., Wornell, G.W.: Cooperative diversity in wireless networks: efficient protocols and outage behavior. *IEEE Trans. Inf Theory* **50**(12), 3062–3080 (2004)
8. Li, Y., Wang, P., Niyato, D., Zhuang, W.: A hierarchical framework of dynamic relay selection for mobile users and profit maximization for service providers in wireless relay networks. *Wirel. Commun. Mobile Comput.* **14**(12), 1113–1126 (2014)
9. Liu, P., Tao, Z., Narayanan, S., Korakis, T., Panwar, S.S.: CoopMAC: a cooperative MAC for wireless LANs. *IEEE J. Sel. Areas Commun.* **25**(2), 340–354 (2007)
10. Mao, G., Fidan, B., Anderson, B.: Wireless sensor network localization techniques. *Comput. Netw.* **51**, 2529–2553 (2007)

11. Narayanan, S., Panwar, S.S.: To forward or not to forward – that is the question. *Wirel. Pers. Commun.* **43**(1), 65–87 (2007)
12. Ribeiro, A., Sidiropoulos, N.D., Giannakis, G.B.: Optimal distributed stochastic routing algorithms for wireless multihop networks. *IEEE Trans. Wirel. Commun.* **7**(11), 4261–4272 (2008)
13. Shan, H., Cheng, H., Zhuang, W.: Cross-layer cooperative MAC protocol in distributed wireless networks. *IEEE Trans. Wirel. Commun.* **10**(8), 2603–2615 (2011)
14. Song, W., Zhuang, W.: Performance analysis and enhancement of cooperative retransmission strategy for delay-sensitive real-time services. In: *Proceedings of IEEE GLOBECOM, Honolulu* (2009)
15. Stoyan, D., Kendall, W., Mecke, J.: *Stochastic Geometry and Its Applications*, 2nd edn. John Wiley and Sons, Chichester (1996)
16. Xiong, L., Libman, L., Mao, G.: Uncoordinated cooperative communications in highly dynamic wireless networks. *IEEE J. Sel. Areas Commun.* **30**(2), 280–288 (2012)
17. Zhai, C., Zhang, W., Mao, G.: Uncoordinated cooperative communications with spatially random relays. *IEEE Trans. Wirel. Commun.* **11**(9), 3126–3135 (2012)
18. Zorzi, M., Rao, R.R.: Geographic random forwarding (GeRaF) for ad hoc and sensor networks: energy and latency performance. *IEEE Trans. Mobile Comput.* **2**(4), 349–365 (2003)

Chapter 4

Energy-Aware Cooperative MAC with Uncoordinated Group Relays

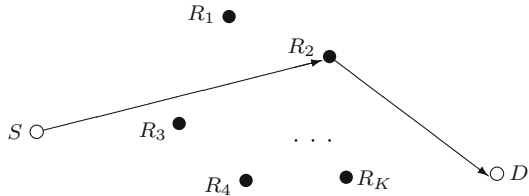
4.1 Motivation and Overview¹

Exploiting spatial diversity, cooperative communications offer a promising low-cost and energy-efficient technique. Taking advantage of the inherent broadcasting nature of the wireless medium, the nodes with good channel conditions can forward the overheard data to facilitate the transmission of one S-D pair, which includes a single source (S) and a single destination (D). As shown in Fig. 4.1, the relay(s) that correctly overhear the packet from S can forward the data to D . Different relaying strategies can be used by the relays, such as amplify-and-forward (AF), decode-and-forward (DF), and coded-cooperation (CC) [8, 13]. Based on this model, the number of relays that participate in each cooperation depends on the channel conditions and the cooperation strategy. It is often assumed that a collision occurs when two or more relays happen to transmit the packet at the same time. Hence, the cooperation gain [7, 10] can vary considerably with the relay selection strategy and the medium access control (MAC) protocol. It is vital to design an effective and efficient cooperation strategy to identify and coordinate the optimal cooperating nodes.

In the centralized solutions such as [5, 9], a central controller (e.g., the source node) needs to acquire the knowledge of the potential relays via additional handshaking messages, and then chooses the optimal relay. The message exchanging may induce unacceptable delay for multimedia services as well as high energy consumption. In contrast, a distributed solution usually does not require such *a priori* information and carries out relay selection in an uncoordinated fashion.

¹Copyright © IEEE (2014). Some content of this chapter is reprinted with permission, from IEEE Transactions on Vehicular Technology (2014) 63(5), 2104–2114, “Energy-aware cooperation strategy with uncoordinated group relays for delay-sensitive services,” A. Jin, W. Song, P. Ju, and D. Zhou [6].

Fig. 4.1 A widely studied network model for cooperative communications



For example, the relays that correctly receive the data from the source can contend to forward the packet to the destination.

For the probability-based uncoordinated cooperation strategies [16–18], each relay that successfully overhears the data independently determines a forwarding probability. Although such strategies involve little signalling overhead, the collision probability can be potentially high when the number of available relays is large. As a consequence, retransmissions will incur high energy consumption as well as long delay. Hence, such cooperation strategies may not be able to accommodate green multimedia services. There is another class of uncoordinated strategies that make use of the relay’s local information to tune a backoff timer [1, 15]. A relay of higher transmission capability is prioritized with shorter backoff time. Such backoff-based uncoordinated strategies can greatly reduce collisions and offer a good match to support green multimedia communications.

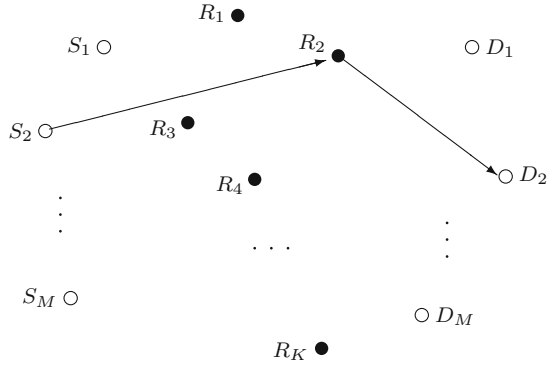
Extending the simple cooperation scenario in Fig. 4.1, we consider a new framework where multiple S-D pairs share a group of relays with energy constraint. To satisfy the quality-of-service (QoS) requirements of multimedia services in a green manner, we propose an energy-aware uncoordinated cooperation strategy based on the backoff timer. Also, its performance is evaluated analytically with respect to the theoretical bounds of the collision probability and the transmission success probability. Extensive simulations are conducted to compare the performance of different uncoordinated strategies and the analytical bounds. The numerical and simulation results demonstrate that our proposed strategy is preferable for the delay-sensitive multimedia services and achieves significant energy saving.

4.2 System Model and Problem Formulation

4.2.1 System Model

Consider a wireless network with M S-D pairs and K relay nodes as illustrated in Fig. 4.2. We assume that the relays are uniformly distributed in a given region and the relay distribution is time-stationary. This assumption is generally valid for a variety of scenarios, e.g., under random direction mobility [2, 12]. The sources refer to the nodes that generate data traffic, while the destinations refer to the nodes that receive data traffic. Relay nodes have no intrinsic traffic demands. Since the relays

Fig. 4.2 An illustration of the system model for cooperative transmission



are shared by multiple S-D pairs, we consider that the relays are energy constrained. When a relay runs out of energy, it is not eligible for future relaying. The sources can communicate with their destinations only through these shared relays using a two-hop DF [8] protocol; other cooperative communication protocols can also be considered in a similar way.

We assume that each node knows its own location, which can be obtained either from a positioning technique based on signal strength, time-of-arrival or angle-of-arrival measurements with nearby nodes [3, 11], or through a GPS receiver that is becoming increasingly ubiquitous in mobile devices. Further, the relay nodes can obtain the locations of the sources and destinations from the piggybacked information within the overheard packets. It should be noted that the sources do not have the knowledge of the locations of the relays, and one relay does not have the location information of other relays either. Besides, we assume that the locations of all the nodes in the network do not change significantly during the short cooperative transmission period, which is a typical assumption that generally holds.

For the data transmission between a transmitter located at x and a receiver located at y , the SNR of the received signal can be written as

$$\gamma_{xy} = \frac{P_0}{N_0} h_{xy} g_{xy} \quad (4.1)$$

where P_0 is the transmit power, N_0 is the power of additive white Gaussian noise (AWGN), and h_{xy} denotes the small-scale channel fading which is exponentially distributed with unit mean. The path-loss effect is captured by $g_{xy} = \|x-y\|^{-\alpha}$, where $\|x-y\|$ is the Euclidean distance, and α is the path-loss exponent. We assume that the receiver is able to correctly decode the received signal only when the instantaneous SNR is no less than a threshold T_0 [18]. Therefore, the probability that a packet is successfully received is given by

$$P_{xy} = \Pr\{\gamma_{xy} \geq T_0\} = \exp\left(-\frac{T_0}{P_0/N_0} \|x-y\|^\alpha\right). \quad (4.2)$$

Since the location information of the sources and destinations is available to the relays, the distances between them can be calculated. Thus, we can estimate the transmission success probabilities from the M sources to the relay R_i by

$$P_{S,R_i} = [P_{S_1R_i}, P_{S_2R_i}, \dots, P_{S_MR_i}], \quad i = 1, 2, \dots, K.$$

Similarly, the transmission success probabilities from the relay R_i to the M destinations are given by

$$P_{R_i,D} = [P_{R_iD_1}, P_{R_iD_2}, \dots, P_{R_iD_M}], \quad i = 1, 2, \dots, K.$$

4.2.2 Problem Formulation

To achieve a high transmission success probability, a centralized relay selection protocol generally identifies the best relay(s) by exploiting the global view of the network. However, additional overhead is usually incurred to exchange the channel state information and results in a large delay. On the other hand, the distributed solutions often require an effective approach to mitigate collisions among multiple potential relays. The probability-based uncoordinated strategies use a forwarding probability that is independently determined for each relay. Nonetheless, when the network scales up, it becomes more difficult to figure out the optimal forwarding probability. Unfortunately, the transmission success probability of these probability-based strategies is upper bounded by $1/e \approx 0.368$ [14, 17] due to high collisions, which also lead to a large delay. In contrast, the backoff-based distributed strategies can handle collisions more effectively and present better performance in terms of the transmission success probability and delay.

In this chapter, we introduce a novel backoff-based uncoordinated cooperation strategy, in which each potential relay sets a backoff timer based on a variety of factors. Considering the group cooperation model in Sect. 4.2.1, we need to effectively address the energy constraint of the relays, which are shared by multiple S-D pairs. The proposed cooperation strategy should not only provide QoS guarantee to the delay-sensitive multimedia services but also perform well in a large-scale network. It is known that the real-time multimedia services are sensitive to delay and delay jitter. In view of the time-varying nature of wireless networks, we consider a statistical QoS guarantee for the delay. That is, the delay outage probability defined in (4.3) is ensured bounded within an acceptable range:

$$P_{out} = \Pr\{\mathcal{D} \geq \mathcal{D}_{max}\} < \varepsilon \quad (4.3)$$

where \mathcal{D} is the packet delay, \mathcal{D}_{max} is the acceptable upper bound, and ε is a small probability that is allowed for QoS violation.

4.3 Energy-Aware Cooperation Strategy

4.3.1 Cooperation Criteria

For a backoff-based cooperation strategy, the determination of the backoff timer is critical to reduce collisions, because a collision may occur when the backoff timers of the first two or more relays expire within an indistinguishable small interval. To improve the achievable performance, the backoff timer is often based on the cooperation capability of the relay. Hence, we need to properly choose the metrics that characterize the cooperation capability, so that the backoff timers of the group of relays can be appropriately scattered to decrease the collision probability.

First, we consider the distance between a relay and a destination, which can be estimated from the location information without incurring extra cost. This distance can capture the transmission success probability of the relay-to-destination channel according to (4.2). This is because we are interested in the potential relays that have correctly overheard the packet from the source and thus only focus on the relay-to-destination channel condition. Denoting the distance between the relay R_i and the destination D_j by d_{ij} , we define the cooperation capability of R_i for D_j with respect to the distance as

$$W_{ij}^d = \begin{cases} 1 - \left(\frac{d_{ij}}{L}\right)^2, & \text{if } d_{ij} \leq L \\ 0, & \text{if } d_{ij} > L \end{cases} \quad (4.4)$$

where L is the largest distance to the destination for a node to be considered as a potential relay. As such, a relay with a smaller distance to the destination is characterized with a greater cooperation capability, because of a higher transmission success probability over the relay-to-destination channel.

Second, the energy status of the relay is also accounted into the estimation of the cooperation capability, since the shared relays are energy constrained. The example in Fig. 4.3 illustrates the importance of incorporating the energy status

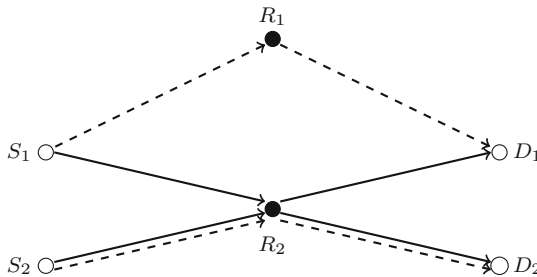


Fig. 4.3 An illustration showing how the energy constraint of the relays affects relay selection. The *solid lines* indicate the cooperative transmissions without considering the energy status; and the *dashed lines* indicate the cooperative transmissions with the energy status taken into account

into the characterization of the cooperation capability. As seen, the relay R_2 is the best relay for both S_1-D_1 and S_2-D_2 pairs, if only the distance to the destination is concerned. Consequently, R_2 will run out of energy quickly. The S_1-D_1 and S_2-D_2 pairs will need to switch to the relay R_1 . The performance of the S_1-D_1 pair will remain almost the same, whereas the S_2-D_2 pair will suffer from a performance degradation since R_1 is far from S_2 and D_2 . On the other hand, if both the distance and the energy status are taken into account, R_1 and R_2 should serve S_1-D_1 and S_2-D_2 , respectively. Thus, the relaying capacities are utilized in a more balanced manner. Therefore, we further consider the energy status of R_i to characterize its cooperation capability by

$$W_i^e = E_i/E_c \quad (4.5)$$

where E_i is the energy level of R_i with an energy upper limit of E_c . Here, we assume that all the relays have the same energy upper limit and their energy levels are uniformly distributed. Therefore, W_i^e follows a uniform distribution between 0 and 1, denoted by $U(0, 1)$. As seen, a relay of a higher energy level thus has a greater cooperation capability.

Based on the two metrics in (4.4) and (4.5), the overall cooperation capability of the relay R_i for the destination D_j is defined as

$$W_{ij} = \theta \cdot W_i^e + (1 - \theta) \cdot W_{ij}^d \quad (4.6)$$

where $\theta \in [0, 1]$ is a weighting parameter to trade-off between the importance of the energy status and that of the distance metric. As seen, $W_{ij} \in [0, 1]$.

4.3.2 Distributed Cooperation Strategy

Table 4.1 presents the proposed energy-aware cooperation strategy in detail. Based on the cooperation capabilities of the relays, the optimal relay for the S_j-D_j pair is defined as

$$R_i = \arg \max_{i \in \{1, \dots, K\}} \{\mathbf{1}_{A_j}(i) \cdot W_{ij}\}$$

where A_j is the set of relays that correctly overhear the data packet from S_j , and

$$\mathbf{1}_{A_j}(i) = \begin{cases} 1, & \text{if } R_i \in A_j \\ 0, & \text{if } R_i \notin A_j. \end{cases}$$

To ensure that the optimal relay has the fastest access to the channel, the relay R_i sets an initial backoff time inversely proportional to its cooperation capability for the S_j-D_j pair as

Table 4.1 Energy-aware cooperation strategy.

```

1: Initialize cooperation capabilities  $W$  of relays according to (4.6)
2: while a new transmission occurs between any  $S_j$ - $D_j$  pair do
3:   for all the relays do
4:     if relay  $R_i$  overhears the packet correctly then
5:       Set the backoff timer of  $R_i$  to  $1 - W_{ij}$ 
6:     end if
7:   end for
8:   for all the relays correctly received the packet do
9:     if backoff timer expires and no relaying sensed then
10:      Forward the packet to  $D_j$ 
11:    end if
12:   end for
13:   if only one relay  $R_i$  transmits within time interval  $c$  then
14:     if  $D_j$  decodes the packet correctly then
15:       Transmission succeeds
16:     else
17:       Transmission fails
18:     end if
19:     // Update  $W$  concerning energy consumption
20:      $W_{ir} \leftarrow W_{ir} - \theta \cdot \eta$ , for  $r = 1, 2, \dots, M$ 
21:   else
22:     Collision happens and transmission fails
23:     for every relay  $R_c$  that transmitted do
24:       // Update  $W$  concerning energy consumption
25:        $W_{cr} \leftarrow W_{cr} - \theta \cdot \eta$ , for  $r = 1, 2, \dots, M$ 
26:       // Update  $W$  concerning collision
27:        $W_{cj} \leftarrow W_{cj} - (1 - \theta) \cdot W_{cj}^d \cdot \eta$ 
28:     end for
29:   end if
30: end while

```

$$T_{ij} = 1 - W_{ij} \quad (4.7)$$

in which the maximum backoff time is taken to be one unit time. As such, the optimal relay of the highest cooperation capability sets the smallest backoff time. If the first two or more relays time out within an indistinguishable small interval c , a collision happens [1].

To account for the energy consumption of packet forwarding of R_i for any S-D pair, we update the cooperation capability of R_i for all S-D pairs as follows

$$W_{ir} = W_{ir} - \theta \cdot \eta, \quad r = 1, 2, \dots, M \quad (4.8)$$

where η is the update step length. This is to yield the forwarding opportunities to other relays and thus balance the energy consumption.

Here comes a problem when a collision happens among the relays. If all the relays involved in the collision update their cooperation capabilities according to (4.8), a collision will happen again in the next transmission. Therefore, we need to penalize these relays by updating their cooperation capabilities to

$$W_{ij} = W_{ij} - (1 - \theta) \cdot W_{ij}^d \cdot \eta, \quad i = c_1, c_2, \dots, c_n \quad (4.9)$$

where c_1, c_2, \dots, c_n are the indices of the relays R_{c_1}, \dots, R_{c_n} that collide when forwarding the packet for the S_j - D_j pair. As a higher W_{ij}^d implies a lower energy level when a collision happens, the corresponding relay is punished more to achieve the energy balance and avoid further collisions.

4.4 Performance Analysis

To satisfy the delay requirements of multimedia services, it is essential to minimize the collision probability so as to maximize the transmission success probability. In this section, we analyze the performance bounds of the proposed cooperation strategy in terms of the collision probability and the transmission success probability. Here, we focus on one S-D pair, since the achievable performance of all S-D pairs is the same, given the homogeneous setting of S-D pairs in the system model.

4.4.1 Upper Bound of Collision Probability

Lemma 4.1. *If the relays are uniformly distributed, the probability density function (PDF) of their distance d to the destination D within L is given by*

$$f(d) = \begin{cases} \frac{2d}{L^2}, & \text{if } d \leq L \\ 0, & \text{otherwise.} \end{cases} \quad (4.10)$$

Proof. Consider the polar coordinate system where D is the origin and an arbitrary relay is located at (d, φ) . The corresponding location of the relay in the Cartesian coordinate system is then (x, y) , where $x = d \cdot \cos(\varphi)$, and $y = d \cdot \sin(\varphi)$. For the relays uniformly distributed within the circle of a radius L and centered at D , the joint PDF of their locations (x, y) is given by

$$f_{X,Y}(x,y) = \begin{cases} \frac{1}{\pi L^2}, & \text{if } \sqrt{x^2 + y^2} \leq L \\ 0, & \text{otherwise.} \end{cases}$$

Since $d = \sqrt{x^2 + y^2}$, according to the Jacobian matrix, we can obtain the PDF of d as shown in (4.10). ■

Lemma 4.2. *If the PDF of the distance of a relay to the destination follows (4.10), the general cooperation capability concerning the distance, W^d defined in (4.4), follows a uniform distribution between 0 and 1.*

Proof. The cumulative distribution function (CDF) of W^d is given by

$$\begin{aligned} \Pr\{W^d \leq w\} &\stackrel{\text{Eq.(4.4)}}{=} \Pr\{1 - (d/L)^2 \leq w\} \\ &= 1 - \Pr\{d \leq L\sqrt{1-w}\} \\ &\stackrel{\text{Eq.(4.10)}}{=} 1 - \int_0^{L\sqrt{1-w}} f(x)dx \\ &= 1 - \frac{d^2}{L^2} \Big|_0^{L\sqrt{1-w}} = w. \end{aligned}$$

Therefore, $W^d \sim U(0, 1)$. ■

Theorem 4.1. *Since $W^e \sim U(0, 1)$ and $W^d \sim U(0, 1)$, the overall cooperation capability defined in (4.6) with $\theta \in (0, 0.2]$ concerning both the distance and the energy status follows a distribution with a PDF*

$$f_W(w) = \begin{cases} \frac{w}{\theta(1-\theta)}, & \text{if } 0 \leq w \leq \theta \\ \frac{1}{1-\theta}, & \text{if } \theta < w \leq 1-\theta \\ \frac{\theta}{\theta(1-\theta)}, & \text{if } 1-\theta < w \leq 1 \\ 0, & \text{otherwise.} \end{cases} \quad (4.11)$$

Proof. Given two continuous random variables U and V , if $V = aU$, the PDFs of U and V are related according to

$$f_V(x) = \left(\frac{1}{a}\right)f_U\left(\frac{x}{a}\right).$$

where $f_U(\cdot)$ and $f_V(\cdot)$ are the PDFs of U and V , respectively. Since $W^e \sim U(0, 1)$ and $W^d \sim U(0, 1)$ (Lemma 4.2), we have

$$X = \theta \cdot W^e \sim U(0, \theta), \quad Y = (1-\theta) \cdot W^d \sim U(0, 1-\theta).$$

Then, for $W = \theta \cdot W^e + (1 - \theta) \cdot W^d = X + Y$, we have

$$\begin{aligned} f_W(w) &= \int_{-\infty}^{\infty} f_X(w-y)f_Y(y)dy \\ &= \frac{1}{1-\theta} \int_0^{1-\theta} f_X(w-y)dy \end{aligned}$$

Only when $0 \leq w - y \leq \theta$, i.e., $w - \theta \leq y \leq w$, $f_X(w - y) = 1/\theta$ and the above integral is not zero. Therefore, we have

$$\begin{aligned} f_W(w) &= \frac{1}{1-\theta} \int_0^w \frac{1}{\theta} dy = \frac{w}{\theta(1-\theta)}, \quad \text{if } 0 \leq w \leq \theta \\ f_W(w) &= \frac{1}{1-\theta} \int_{w-\theta}^w \frac{1}{\theta} dy = \frac{1}{1-\theta}, \quad \text{if } \theta < w \leq 1-\theta \\ f_W(w) &= \frac{1}{1-\theta} \int_{w-\theta}^{1-\theta} \frac{1}{\theta} dy = \frac{1-w}{\theta(1-\theta)}, \quad \text{if } 1-\theta < w \leq 1 \end{aligned}$$

which conclude the proof. ■

According to Theorem 4.1 for $\theta \in (0, 0.2]$, it can be easily shown that the backoff time as defined by (4.7) follows a distribution with a PDF, given by

$$f_T(t) = \begin{cases} \frac{t}{\theta(1-\theta)}, & \text{if } 0 \leq t \leq \theta \\ \frac{1}{1-\theta}, & \text{if } \theta < t \leq 1-\theta \\ \frac{1-t}{\theta(1-\theta)}, & \text{if } 1-\theta < t \leq 1 \\ 0, & \text{otherwise.} \end{cases} \quad (4.12)$$

Assume that N relays (R_{i_1}, \dots, R_{i_N}) correctly overhear the transmitted packet from one particular source. Let $T_1 < T_2 < \dots < T_N$ denote the order statistics of the backoff time of the N relays. According to [1], the collision probability P_c is given by

$$P_c = \Pr\{T_2 < T_1 + c\} = 1 - I_c \quad (4.13)$$

$$I_c = N(N-1) \int_c^1 f_T(t) [1 - F_T(t)]^{N-2} F_T(t-c) dt \quad (4.14)$$

where $f_T(t)$ is the PDF of the backoff time and $F_T(t)$ is the corresponding CDF. Here, c is an indistinguishable small interval and a collision happens when the backoff timers of the first two or more relays time out within c . As one example, the distributed coordination function (DCF) of IEEE 802.11 can choose a maximum

backoff time of 1024 time slots [4]. Then, the interval c can be considered as one time slot. Provided that the maximum backoff time is taken to be one unit time, the interval c can be in the order of 10^{-3} .

When $\theta = 0$, we have $W = W^d$ according to (4.6). Based on Lemma 4.2, this means that the cooperation capability W follows a uniform distribution between 0 and 1. Thus, the backoff time defined in (4.7) is also uniformly distributed with $f_T(t) = 1$ and $F_T(t) = t$ for $0 \leq t \leq 1$. From (4.14), we can easily obtain

$$I_c = (1 - c)^N. \quad (4.15)$$

For $0 < \theta \leq c$, we have

$$I_c = \frac{N(N-1)}{(1-\theta)^N} \left\{ \left(1 - \frac{3}{2}\theta\right)^{N-1} \left(\frac{1-\theta-c}{N-1} - \frac{1-3\theta/2}{N}\right) + \left(\frac{\theta}{2}\right)^{N-1} \left(\frac{2c-c^2/\theta}{2N-2} - \frac{2c}{2N-1}\right) \right\}. \quad (4.16)$$

For $\theta > c$, because a closed-form I_c is not tractable, we derive the following lower bound in Appendix A: Proof of (4.17)

$$I_c > \frac{N(N-1)}{(1-\theta)^N} \left\{ \left(1 - \frac{3}{2}\theta\right)^{N-2} (\theta - c)^3 \left(\frac{1}{8\theta} + \frac{c}{24\theta^2}\right) + \left(1 - \frac{3}{2}\theta\right)^{N-1} \left(\frac{1-\theta-c}{N-1} - \frac{1-3\theta/2}{N}\right) + \left(\frac{\theta}{2}\right)^{N-1} \left(\frac{2c-c^2/\theta}{2N-2} - \frac{2c}{2N-1}\right) \right\}. \quad (4.17)$$

Defining the righthand-side terms in (4.15), (4.16), and (4.17) as I_c^L , we have $I_c \geq I_c^L$ and

$$P_c = 1 - I_c \leq 1 - I_c^L \triangleq P_c^U \quad (4.18)$$

where P_c^U denotes an upper bound of the collision probability.

4.4.2 Lower Bound of Transmission Success Probability

When the traffic load is high, most of the relays will run out of energy quickly, and the distribution of their cooperation capabilities will no longer follow (4.11). Thus, it is hard to theoretically derive a lower or upper bound for the transmission success

probability. Therefore, we focus on a normal traffic load when analyzing the lower bound of the transmission success probability in this section and its upper bound in the next section. In this circumstance, the energy constraint can be relaxed by setting $\theta = 0$. Then, the cooperation capability is only determined by the distance metric and follows a uniform distribution between 0 and 1.

A relay R_i participates in the cooperative relaying for the S_j - D_j pair only if R_i correctly receives the packet from S_j and its cooperation capability W_{ij} is the maximum among the N relays ($R_i, R_{i_1}, \dots, R_{i_{N-1}}$) that overhear this packet successfully. With the largest W_{ij} , R_i sets the shortest backoff time and becomes the first to forward the packet. We have the corresponding occurrence probability

$$\begin{aligned} P_{ij} &= P_{S_j R_i} \cdot \prod_{r=1}^{N-1} \Pr\{W_{ij} > W_{i_r j}\} \\ &= P_{S_j R_i} \cdot (W_{ij})^{N-1}. \end{aligned} \quad (4.19)$$

Besides, the probability that at least one relay successfully overhears and forwards the packet for S_j is given by

$$Q_j = 1 - \prod_{r=1}^K (1 - P_{S_j R_r}). \quad (4.20)$$

Hence, the probability that R_i transmits the packet for S_j in the long term is given by

$$\overline{P}_{ij} = Q_j \cdot \frac{P_{ij}}{\sum_{r=1}^K P_{rj}}. \quad (4.21)$$

Finally, we have the transmission success probability for the S_j - D_j pair

$$\begin{aligned} P_{suc}^{(j)} &= \sum_{r=1}^K \overline{P}_{rj} \cdot P_{R_r D_j} \cdot (1 - P_c) \\ &\geq (1 - P_c^U) \cdot \sum_{r=1}^K \overline{P}_{rj} \cdot P_{R_r D_j} \triangleq P_{suc}^L \end{aligned} \quad (4.22)$$

where P_{suc}^L denotes the lower bound of the transmission success probability.

4.4.3 Upper Bound of Transmission Success Probability

In Sect. 4.4.2, the energy constraint is relaxed to derive the lower bound of the transmission success probability. To obtain the upper bound, we assume no

collisions among the relays in data forwarding. The upper bound of the transmission success probability for an arbitrary S_j - D_j pair is then given by

$$\begin{aligned}
 P_{suc}^U &= P_{S_j R_{(1)}} \cdot P_{R_{(1)} D_j} + (1 - P_{S_j R_{(1)}}) \cdot P_{S_j R_{(2)}} \cdot P_{R_{(2)} D_j} \\
 &+ \cdots + \prod_{r=1}^{K-1} (1 - P_{S_j R_{(r)}}) \cdot P_{S_j R_{(K)}} \cdot P_{R_{(K)} D_j}
 \end{aligned} \tag{4.23}$$

where $P_{R_{(1)} D_j} > P_{R_{(2)} D_j} > \cdots > P_{R_{(K)} D_j}$. The first term in (4.23) represents the case that the best relay $R_{(1)}$ has correctly received the packet from S_j with a probability $P_{S_j R_{(1)}}$, and its forwarding over the relay-to-destination channel to D_j succeeds with a probability $P_{R_{(1)} D_j}$. The second term in (4.23) indicates that the best relay $R_{(1)}$ fails to receive the packet from S_j with a probability $(1 - P_{S_j R_{(1)}})$, while the second best relay $R_{(2)}$ successfully receives and forwards the packet to D_j with a probability $P_{S_j R_{(2)}} \cdot P_{R_{(2)} D_j}$. The other terms in (4.23) can be interpreted in a similar way.

In addition, a relaxed upper bound of the transmission success probability can be obtained as

$$\widetilde{P}_{suc}^U = Q_j \cdot \max_{r \in \{1, 2, \dots, K\}} \{P_{R_r D_j}\} > P_{suc}^U \tag{4.24}$$

where Q_j is given by (4.20). Here, \widetilde{P}_{suc}^U is derived by considering the maximum success probability over the relay-to-destination channel when at least one relay forwards the packet.

4.5 Numerical and Simulation Results

In this section, numerical and simulation results are presented to demonstrate the effectiveness of our proposed cooperation strategy and the analytical bounds. For comparison purposes, we consider an uncoordinated probability-based algorithm, in which each potential relay R_i chooses its forwarding probability according to

$$P_{\tau_i} = \left[1 + \frac{P_0}{N_0 T_0 L^2} \cdot \ln(P_{R_i D}) \right]^{N-1} \tag{4.25}$$

where N is the number of relays that correctly overhear the packet from the source. Here, P_{τ_i} is actually the probability that R_i is the relay with the maximum transmission success probability over the relay-to-destination channel (with $\alpha = 2$). The derivation of (4.25) is given in [Appendix B: Proof of \(4.25\)](#). In the simulation, we further minimize collisions by normalizing P_{τ_i} to

$$P_{\tau}^{(i)} = \frac{P_{\tau_i}}{\sum_{r=1}^N P_{\tau_r}}. \tag{4.26}$$

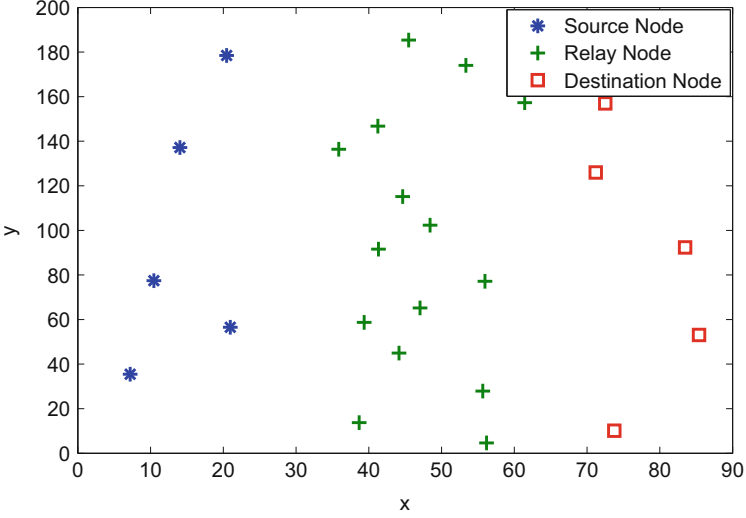


Fig. 4.4 Nodes topology for analysis and simulation

Table 4.2 System parameters

Symbol	Value	Definition
P_0/N_0	40 dB	Transmit SNR
T_0	5	SNR threshold of signal decoding
α	2	Path-loss exponent
L	55 m	Maximum distance of potential relays to a destination
θ	$0 \sim 0.2$	Weighting parameter for distance and energy
η	0.0001	Update step length
c	$0.001 \sim 0.01$	Indistinguishable backoff time interval for collision

In practice, it is not appropriate for a distributed approach to allow a relay to obtain the forwarding probabilities of other relays. Thus, the real performance of the probability-based algorithm can be worse.

In the following experiments, we assume that the nodes are uniformly distributed in a $40 \text{ m} \times 200 \text{ m}$ area, as illustrated by the example in Fig. 4.4. The maximum distance of potential relays to a destination is $L = 55 \text{ m}$, since the transmission success probability over the relay-to-destination channel is lower than 0.25 when $L > 55 \text{ m}$. Assume that all the relays are fully charged at the beginning, and each relay can transmit up to 10^4 packets. More system parameters are given in Table 4.2.

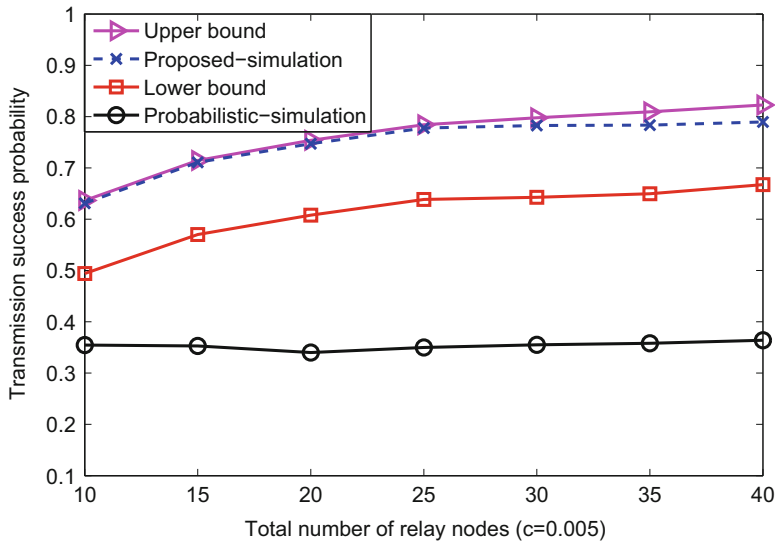


Fig. 4.5 Transmission success probability vs. total number of relay nodes

4.5.1 Transmission Success Probability

Figure 4.5 compares the transmission success probability of different strategies with the analytical bounds. We can see that the transmission success probability of the probability-based algorithm is bounded by $1/e \approx 0.368$, which verifies the conclusions in [14, 17]. In contrast, our proposed backoff-based strategy can easily achieve a transmission success probability higher than 0.6, because of the reduced collision probability. Moreover, we find that the upper bound and the lower bound of the transmission success probability both work well. The proposed strategy approaches the upper bound in a normal traffic load.

Furthermore, it is seen in Fig. 4.5 that the transmission success probability of the proposed strategy increases with a greater number of relays, whereas that of the probability-based algorithm remains almost the same. Though the collision probability of both algorithms increases with the number of relays, the opportunity of finding a good relay increases with more potential relays. Thus, packet loss caused by poor channel conditions can be reduced.

4.5.2 Average Delay and Delay Outage Probability

Figure 4.6 shows the average packet transfer delay of the two algorithms against the packet transmission time. The packet transfer delay represents the time duration from a packet generation to successful transmission, while the packet transmission

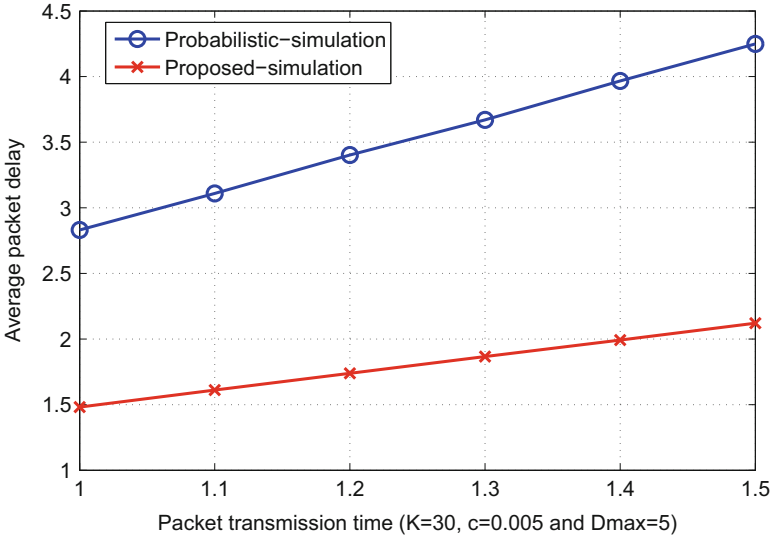


Fig. 4.6 Average packet delay \bar{D} vs. the packet transmission time

time is given by the packet length over the transmission rate. Here, the maximum backoff time is taken to be one unit time. As seen, the average packet delay of the proposed algorithm is much smaller than that of the probability-based algorithm, even though the proposed algorithm requires extra backoff time. This is because the collision probability of the proposed backoff-based algorithm is much lower than that of the probability-based algorithm. As a result, the transmission success probability is improved significantly, as seen in Fig. 4.5. Thus, the average packet transfer delay is reduced accordingly. In addition, we find that the average packet delay of the backoff-based algorithm increases slower than that of the probability-based algorithm, which implies that our proposed algorithm can achieve more gain for a larger packet length.

Figure 4.7 compares the delay outage probability (in log scale) of the two algorithms with respect to the packet transmission time. It can be seen that the backoff-based algorithm has a delay outage probability smaller than 0.01. On the other hand, the delay outage probability of the probability-based algorithm increases faster from 0.12 to 0.21, when the packet transmission time increases from 1 to 1.5. Therefore, our proposed algorithm is preferable for the real-time delay-sensitive services.

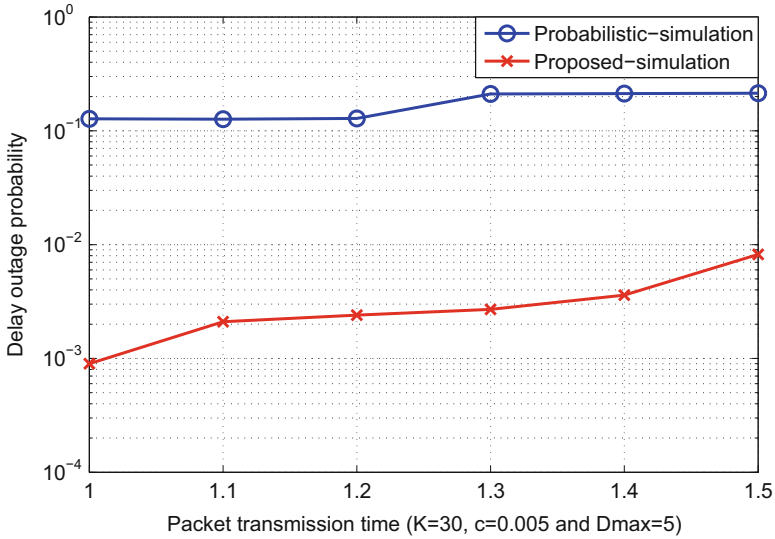


Fig. 4.7 Delay outage probability P_{out} vs. packet transmission time

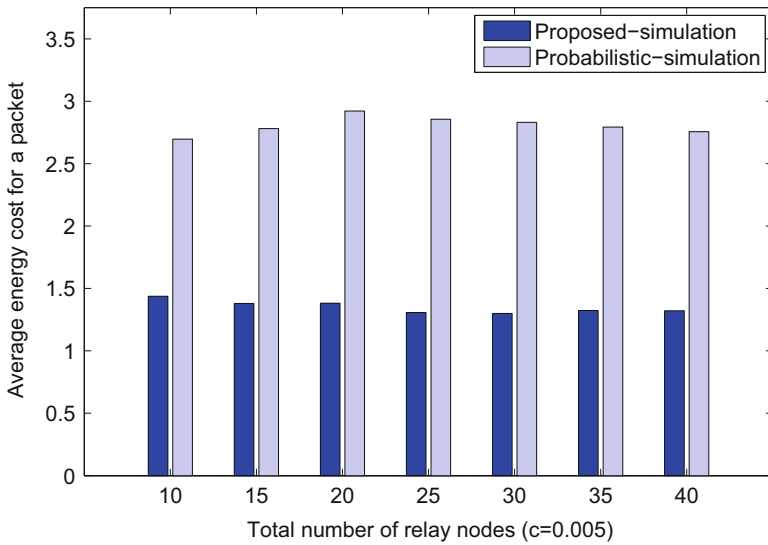


Fig. 4.8 Average energy cost for a packet vs. total number of relay nodes

4.5.3 Energy Saving and Energy Balance

To further investigate the energy consumption of the two algorithms, Fig. 4.8 shows the average energy cost of the relays for a packet with respect to the total number of relays K . Here, the unit of energy cost is the energy consumption of one transmission

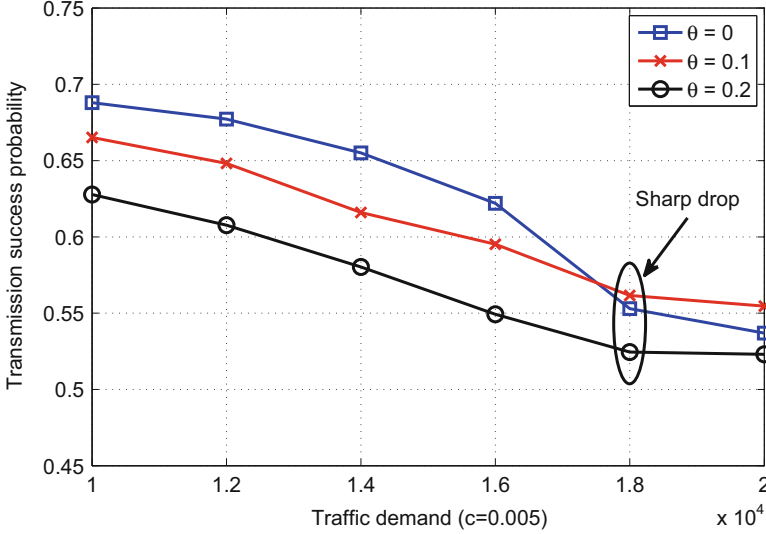


Fig. 4.9 Transmission success probability P_{suc} vs. traffic demand

attempt for a packet with a transmission time of one time unit. As seen in Fig. 4.8, our proposed backoff-based algorithm can save around 50 % of energy on average, compared to the probability-based algorithm. This energy saving is due to the low collision probability and high transmission success probability of the backoff-based algorithm.

In Fig. 4.9, we show the variations of the transmission success probability with the traffic demand of an S-D pair. Here, the traffic demand is the number of packets transmitted for an S-D pair, excluding the retransmitted packets. It is assumed in the simulation that all M S-D pairs have the same traffic demand. As seen, when the traffic demand is low, the highest transmission success probability is achieved at $\theta = 0$. Given a low traffic demand, no relay runs out of energy to satisfy the demand and the relays with the best channel conditions are always available to forward the packets. Hence, the energy constraint does not take effect and it is not necessary to consider energy balance in relay selection.

On the other hand, the situation becomes different with a high traffic demand. As seen in Fig. 4.9, when the traffic demand is greater than 1.8×10^4 , the transmission success probability with $\theta = 0$ is no longer higher than that of $\theta = 0.1$. This is because the energy constraint is not addressed with $\theta = 0$ and consequently the best relay candidates may run out of energy very quickly. In contrast, we can take advantage of energy balance by setting $\theta = 0.1$ for relay selection and thus extend the survival time of the relays. As a result, the average transmission success probability can be improved. Moreover, it is observed in Fig. 4.9 that the transmission success probability with $\theta = 0.2$ is always worse than that of $\theta = 0$ and $\theta = 0.1$. This implies that the weight $\theta = 0.2$ overvalues the importance

of energy status but underestimates that of the relay's distance to the destination. Consequently, the relay selection becomes kind of "blind" to the transmission success probability over the relay-to-destination channel. Therefore, it is usually assumed that $\theta \leq 0.2$.

4.5.4 Scalability

To study the scalability of the proposed algorithm, we vary the total number of relays K and the total number of S-D pairs M in the simulation. Given a fixed number of S-D pairs, $M = 5$, Fig. 4.10a shows that the transmission success probability first increases with the number of relays and then decreases when $K \geq 50$. On one hand, more good relays become available for an S-D pair when the total number of relays is larger. On the other hand, the collision probability also increases correspondingly. At the beginning, the advantage of having more good relays dominates the side effect of collisions. On the contrary, when the number of relays further grows, the collision probability becomes very high and the transmission success probability decreases. For example, the collision probability with $K = 300$ is 20.86 %, which is much higher than 10.34 % with $K = 100$. For the relaying area considered in the simulation, $K = 500$ is an extremely high and rare density in practice. Even so, we still find that the transmission success probability is above 60 % and much larger than that of the probability-based algorithm.

Figure 4.10b shows the transmission success probability vs. the number of S-D pairs M given a fixed number of relays $K = 100$. The two scenarios in comparison have different traffic loads, which are the total number of packets transmitted for each S-D pair, including the retransmitted packets. It is observed that the transmission success probability is above 50 % with a reasonable number of S-D pairs ($M \leq 30$) when the traffic load is normal. This verifies that our proposed algorithm can be deployed in a large-scale network. Moreover, it is seen that the transmission success probability decreases with a larger number of S-D pairs. When more S-D pairs share a group of common relays, the relays with better channel conditions to the destinations will run out of energy quickly. As a result, the transmission success probability goes down, but decreases slower with a lower traffic load. Hence, in order to guarantee the QoS requirements, the amount of traffic that enters the network should be regulated by controlling the number of S-D pairs and/or their admissible traffic loads. In addition, we find that the Jain's fairness index of the transmission success probability among the M S-D pairs is almost 1, which implies that the group of relays are evenly shared by all S-D pairs with the proposed backoff-based algorithm.

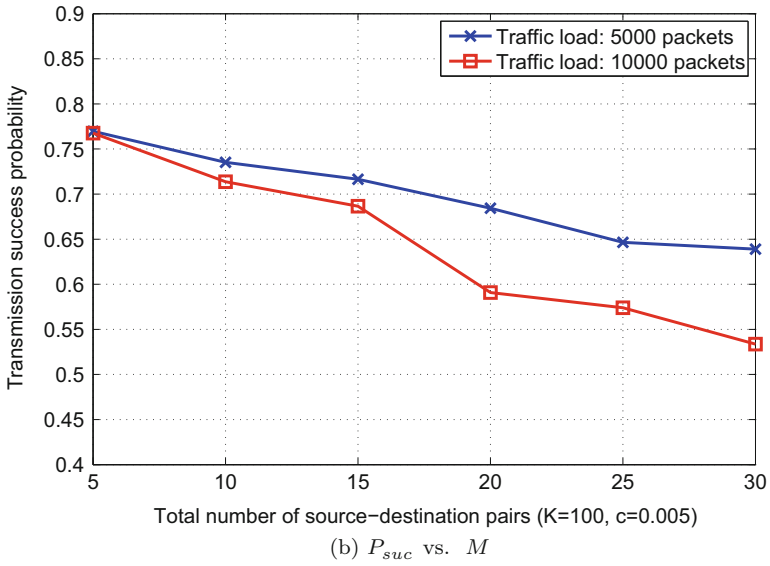
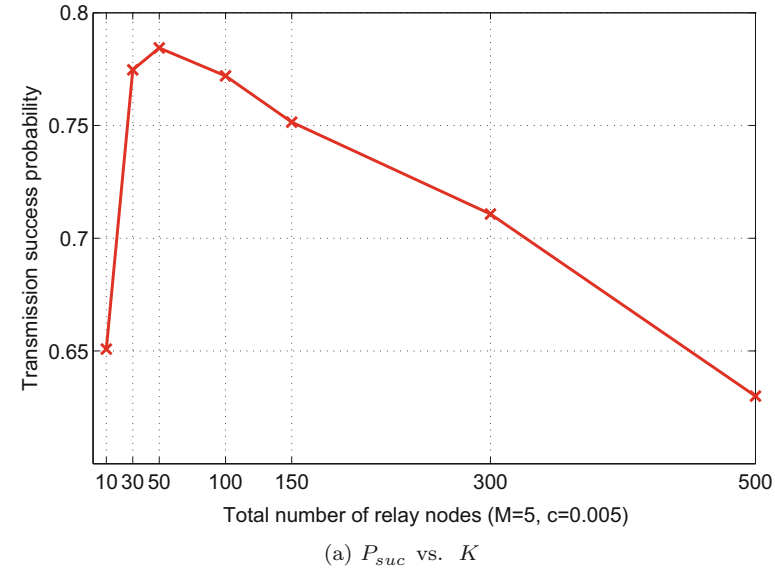


Fig. 4.10 Scalability of the proposed cooperation strategy. (a) P_{suc} vs. K . (b) P_{suc} vs. M

4.6 Summary

In this chapter, we study the uncoordinated cooperative communications between multiple S-D pairs that share a group of energy-constrained relays. A novel cooperation strategy is proposed based on backoff timers. It makes use of the cooperative capability, which is characterized by the distance information and the energy status of the relay. Thus, the relay of a higher cooperative capability ends up with a shorter backoff time. The best relay times out first and wins the contention. However, a collision still happens if the backoff timers of the first two or more relays expire within an indistinguishable time interval. Hence, we also derive the theoretical performance bounds for the proposed strategy with respect to the collision probability and the transmission success probability.

As shown in the numerical results, our proposed strategy can achieve a much lower collision probability and thus a higher transmission success probability, compared to a probability-based reference strategy. We find that the transmission success probability can approach the upper bound in a normal traffic load, which verifies that our algorithm can effectively and efficiently identify the optimal relay in an uncoordinated manner. Besides, our algorithm also outperforms the probability-based strategy in terms of average packet delay, delay outage probability, as well as the energy consumption. By adjusting the weighting parameter θ , we can achieve good performance in the high traffic load condition through energy balance. Therefore, it is safe to conclude that our proposed algorithm can serve as an energy-efficient cooperation strategy for delay-sensitive multimedia services and it is a scalable solution for a large-scale network.

Appendix A: Proof of (4.17)

According to (4.14), when $\theta > c$, we have

$$I_c = N(N-1)(I_{c_1} + I_{c_2} + I_{c_3}) \quad (4.27)$$

where I_{c_1} , I_{c_2} and I_{c_3} are given by

$$I_{c_1} = \int_c^\theta \frac{t}{\theta(1-\theta)} \left[1 - \frac{t^2/2}{\theta(1-\theta)} \right]^{N-2} \frac{(t-c)^2/2}{\theta(1-\theta)} dt \quad (4.28)$$

$$I_{c_2} = \int_\theta^{1-\theta} \frac{1}{1-\theta} \left[1 - \frac{t-\theta/2}{1-\theta} \right]^{N-2} \frac{t-c-\theta/2}{1-\theta} dt \quad (4.29)$$

$$I_{c_3} = \int_{1-\theta}^1 \frac{1-t}{\theta(1-\theta)} \left[\frac{(1-t)^2}{2\theta(1-\theta)} \right]^{N-2} \left[1 - \frac{(1-t+c)^2}{2\theta(1-\theta)} \right] dt. \quad (4.30)$$

As a closed-form expression is not tractable for I_{c_1} , we take $t \leq \theta$ and have

$$\begin{aligned} I_{c_1} &\geq \int_c^\theta \frac{t}{\theta(1-\theta)} \left[1 - \frac{\theta^2/2}{\theta(1-\theta)} \right]^{N-2} \frac{(t-c)^2/2}{\theta(1-\theta)} dt \\ &= \left(\frac{1}{1-\theta} \right)^N \left(1 - \frac{3}{2}\theta \right)^{N-2} (\theta-c)^3 \left(\frac{1}{8\theta} + \frac{c}{24\theta^2} \right). \end{aligned} \quad (4.31)$$

The closed-form expressions of I_{c_2} and I_{c_3} can be obtained as

$$\begin{aligned} I_{c_2} &= \left(\frac{1}{1-\theta} \right)^N \left\{ \frac{1-\theta-c}{N-1} \left[\left(1 - \frac{3}{2}\theta \right)^{N-1} - \left(\frac{\theta}{2} \right)^{N-1} \right] \right. \\ &\quad \left. - \frac{1}{N} \left[\left(1 - \frac{3}{2}\theta \right)^N - \left(\frac{\theta}{2} \right)^N \right] \right\} \end{aligned} \quad (4.32)$$

$$I_{c_3} = \left(\frac{\theta/2}{1-\theta} \right)^N \left(\frac{2}{\theta} \right) \left[\frac{2(1-\theta) - c^2/\theta}{2N-2} - \frac{2c}{2N-1} - \frac{\theta}{2N} \right]. \quad (4.33)$$

The last three equations conclude the proof to (4.17).

Appendix B: Proof of (4.25)

According to (4.2), we obtain the transmission success probability over the relay-to-destination channel with $\alpha = 2$ as

$$P_{RD} = e^{-\phi d^2} \quad (4.34)$$

where $\phi = T_0 N_0 / P_0$. Given the PDF of d in (4.10), we derive the CDF of P_{RD} by

$$\begin{aligned} \Pr\{P_{RD} \leq p\} &= \Pr\{e^{-\phi d^2} \leq p\} = 1 - \Pr\left\{d \leq \sqrt{-\frac{\ln p}{\phi}}\right\} \\ &= 1 - \int_0^{\sqrt{-\frac{1}{\phi} \ln p}} f(x) dx = 1 - \frac{d^2}{L^2} \Big|_0^{\sqrt{-\frac{1}{\phi} \ln p}} \\ &= 1 + \frac{P_0}{N_0 T_0 L^2} \ln p. \end{aligned}$$

Thus, it is easy to show that the probability that a relay has the maximum transmission success probability over the relay-to-destination channel among N candidates is given by (4.25).

References

1. Bletsas, A., Khisti, A., Reed, D.P., Lippman, A.: A simple cooperative diversity method based on network path selection. *IEEE J. Sel. Areas Commun.* **24**(3), 659–672 (2006)
2. Carofiglio, G., Chiasserini, C., Garetto, M., Leonardi, E.: Route stability in MANETs under the random direction mobility model. *IEEE Trans. Mobile Comput.* **8**(9), 1167–1179 (2009)
3. Chen, Z., Gokeda, G., Yu, Y.: Introduction to Direction-of-Arrival estimation. Artech House, Boston (2010)
4. Cheng, Y., Ling, X., Cai, L., Song, W., Zhuang, W., Shen, X., Leon-Garcia, A.: Statistical multiplexing, admission region, and contention window optimization in multiclass wireless LANs. *ACM Wirel. Netw.* **15**(1), 73–86 (2009)
5. Du, Q., Zhang, X.: QoS-aware Base-station selections for distributed MIMO links in broadband wireless networks. *IEEE J. Sel. Areas Commun.* **29**(6), 1123–1138 (2011)
6. Jin, A., Song, W., Ju, P., Zhou, D.: Energy-aware cooperation strategy with uncoordinated group relays for delay-sensitive services. *IEEE Trans. Veh. Technol.* **63**(5), 2104–2114 (2014)
7. Ju, P., Song, W., Zhou, D.: Survey on cooperative medium access control protocols. *IET Commun.* **7**(9), 893–902 (2013)
8. Laneman, J.N., Tse, D.N.C., Wornell, G.W.: Cooperative diversity in wireless networks: efficient protocols and outage behavior. *IEEE Trans. Inf. Theory* **50**(12), 3062–3080 (2004)
9. Li, Y., Wang, P., Niyato, D., Zhuang, W.: A dynamic relay selection scheme for mobile users in wireless relay networks. In: Proceedings of IEEE INFOCOM Workshop (2011)
10. Liu, P., Tao, Z., Narayanan, S., Korakis, T., Panwar, S.S.: CoopMAC: a cooperative MAC for wireless LANs. *IEEE J. Sel. Areas Commun.* **25**(2), 340–354 (2007)
11. Mao, G., Fidan, B., Anderson, B.: Wireless sensor network localization techniques. *Comput. Netw.* **51**, 2529–2553 (2007)
12. Nain, P., Towsley, D., Liu, B., Liu, Z.: Properties of random direction models. In: Proceedings of IEEE INFOCOM, vol. 3, pp. 1897–1907 (2005)
13. Nosratinia, A., Hunter, T.E., Hedayat, A.: Cooperative communication in wireless networks. *IEEE Commun. Mag.* **42**(10), 74–80 (2004)
14. Ribeiro, A., Sidiropoulos, N.D., Giannakis, G.B.: Optimal distributed stochastic routing algorithms for wireless multihop networks. *IEEE Trans. Wirel. Commun.* **7**(11), 4261–4272 (2008)
15. Shan, H., Cheng, H., Zhuang, W.: Cross-layer cooperative MAC protocol in distributed wireless networks. *IEEE Trans. Wirel. Commun.* **10**(8), 2603–2615 (2011)
16. Song, W., Zhuang, W.: Performance analysis and enhancement of cooperative retransmission strategy for delay-sensitive real-time services. In: Proceedings of IEEE GLOBECOM (2009)
17. Xiong, L., Libman, L., Mao, G.: Uncoordinated cooperative communications in highly dynamic wireless networks. *IEEE J. Sel. Areas Commun.* **30**(2), 280–288 (2012)
18. Zhai, C., Zhang, W., Mao, G.: Uncoordinated cooperative communications with spatially random relays. *IEEE Trans. Wirel. Commun.* **11**(9), 3126–3135 (2012)

Chapter 5

Opportunistic Cooperative Relaying with Backoff-Based Contention

5.1 Motivation and Overview¹

To optimize the performance gain with cooperative transmission, it is essential to identify the best relay(s) with a minimum overhead and enable forwarding with a high success probability [1, 7, 11]. Centralized solutions such as [10, 13, 23] need to acquire the knowledge of potential relays usually via additional handshaking messages. Thus, the relays can be short-listed and the best one is chosen in a centralized manner, at the source node for example. On the other hand, distributed solutions [9, 21, 22] do not require a priori information of the relays. The relays that correctly overhear a packet from the source contend in a distributed fashion to forward the packet to the destination. A collision may occur if two or more relays happen to transmit at the same time. Hence, the contention policies should take into account a variety of factors to reduce collisions and improve the relay success probability.

The probabilistic uncoordinated cooperation strategies in [21, 22] have each relay that correctly overhears a packet independently determine a forwarding probability depending on the distance, direction, local signal-to-noise ratio (SNR) [22], or statistical information of the local environment [21]. It is found in [21] that the transmission success probability of the probabilistic strategy is upper bounded by $1/e \approx 0.368$. Although the probabilistic strategies require little signalling overhead, the collision probability can be high and the determination of forwarding probability is critical for the performance.

¹Copyright © IEEE (2015). Some content of this chapter is reprinted with permission, from IEEE Transactions on Vehicular Technology (2015) 64(5), 2023–2036, “Distributed opportunistic two-hop relaying with backoff-based contention among spatially random relays,” by W. Song, P. Ju, A. Jin, and Y. Cheng [18].

There is another class of distributed solutions that make use of local information of relays to tune the backoff timer [2, 17, 24]. Such solutions are also distributed since the backoff time is determined by each individual relay itself based on local information. The relays of a better transmission capability are prioritized with a smaller backoff time. The relay capability can be characterized by the distance to the destination [24], channel estimates for the source-to-relay channel and relay-to-destination channel [2], or a composite cooperative transmission rate [17], which involves the broadcast rate from the source and the data rate from the relay to the destination. As such, the backoff-based solutions naturally rank the relays for access contention according to their transmission capabilities. Collisions are thus greatly reduced but still possible when two or more relays are similar in terms of the defined transmission capabilities and end up with indistinguishable backoff time.

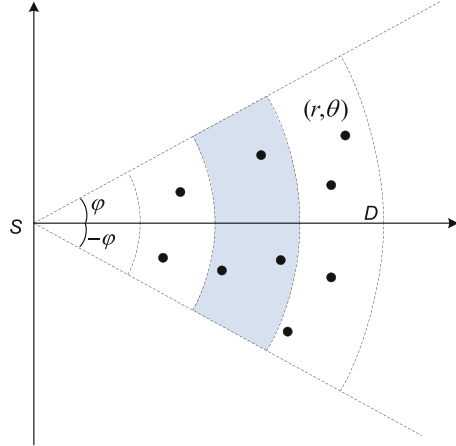
It can be seen that the distributed solutions offer a good match to the opportunistic relaying scenario, where the communication peers do not need a priori global knowledge of the relays. Nonetheless, it is challenging but vital to appropriately coordinate the cooperative contributions of the relays so as to reduce collisions and improve the relay success probability. The existing work usually assumes a certain number of relays that are randomly deployed in a given area. The impact of the spatial distribution of relays is not well understood yet. In fact, the spatial distribution can be exploited in the cooperation strategy to enhance the relaying performance.

In this chapter, we first derive the probability distributions of the average received SNR with the given spatial distribution of random relays. Accordingly, we can obtain the transmission success probability of the potential relays that successfully overhear a packet from the source. Exploiting such statistics and location information, we develop two distributed cooperative relaying schemes, in which each potential relay independently determines a backoff time and/or a forwarding probability. The distributed schemes are compared with a centralized scheme with the pre-selected best relay as an upper bound and a pure probabilistic distributed scheme as a lower bound.

5.2 System Model

Consider a wireless network with a source node S and a destination node D , where the distance between them is fixed at R . The relay nodes are randomly distributed in a given region, following a homogeneous Poisson point process (PPP) with an intensity function λ . We assume that the PPP is time-stationary, which is generally valid under broad assumptions, e.g., the random direction mobility model [3]. Consider a polar coordinate system illustrated in Fig. 5.1, in which S is at the origin and D is at $(R, 0)$. To achieve a higher relay success probability, the packet from S should be directed toward the relays closer to D . Hence, the relays should lie within a symmetric angle interval of $(-\pi/2, \pi/2)$ with respect to the source-

Fig. 5.1 The coordinate system for the source S , the destination D , and the relays which are distributed as a PPP



destination axis [22]. To reduce collisions, the relays within a smaller sector of $(-\phi, \phi)$, $\phi \leq \pi/2$, can be focused on. This sector region is denoted by Ω_{SD} .

We assume that each node knows its own location, which can be obtained either from a locating technique based on signal strength, time-of-arrival or angle-of-arrival measurements with nearby nodes [4, 14], or through a GPS receiver that is becoming increasingly ubiquitous in mobile devices. Further, S can obtain the location of D in advance via a prior handshaking process and piggyback the locations of S and D within the transmitted packet. The relay nodes can thus acquire such information from the overheard packet. It should be noted that S does not know the locations of relays, and the relays do not have the location information of each other.

For the data transmission between a certain transmitter located at x and a certain receiver located at y , considering log-distance path loss and Rayleigh fading, we have the SNR of the received signal, given by

$$\gamma_{xy} = \frac{P_0}{N_0} \|x - y\|^{-\alpha} h_{xy} \quad (5.1)$$

where P_0 is the transmit power, N_0 is the power of the additive white Gaussian noise (AWGN), $\|x - y\|$ is the Euclidean distance, α is the path-loss exponent, and h_{xy} denotes the small-scale channel fading, which is exponentially distributed with unit mean. The receiver is able to successfully decode the received signal only when the local SNR is no less than a threshold T_0 [22]. The transmit SNR P_0/N_0 and decoding threshold T_0 are assumed to be the same for all nodes. Therefore, the probability that a packet is received successfully is given by

$$p_{xy} = \Pr[\gamma_{xy} \geq T_0] = e^{-K_0 \|x-y\|^\alpha}, \quad K_0 = T_0 N_0 / P_0. \quad (5.2)$$

When S broadcasts a data packet to D , it is possible that an intermediate relay correctly overhears it with a probability given by (5.2). We refer to the relays that correctly receive the packet as *potential relays*. Then, the potential relays can follow a distributed cooperation strategy and use decode-and-forward (DF) to transmit the overheard packet to D . The distributed strategy does not require a global knowledge of the relays. Nonetheless, it is assumed that each relay is aware of the spatial distribution parameters of the random relays such as λ and ϕ . Also, since the locations of S and D are piggybacked in the transmitted packet and thus available to the relays, each relay can estimate its transmission success probability to D according to (5.2). Together with the location information and other local estimates, each relay can independently determine a backoff timer and/or a forwarding probability to participate in the relaying.

5.3 Cooperative Relaying Strategies

Based on the system model in Sect. 5.2, the relays that correctly overhear the packet from the source can forward the data to the destination opportunistically. On one hand, the more relays that participate in the cooperative transmission, the higher chance that some promising relays of good channel conditions to the destination can be selected. On the other hand, if two or more relays happen to transmit simultaneously, a collision occurs. In this section, we introduce effective cooperation strategies to select good relays and coordinate their opportunistic forwarding in a distributed fashion. Focusing on the MAC perspective, we assume that a collision causes a transmission failure and aim to minimizing collisions in the first place. Nonetheless, if the signal received from one relay is sufficiently stronger than the interference from the collided signals of other relays, it is still possible for the receiver to successfully recover the data from the collided signals. This capture effect has been analyzed in many previous studies [5, 6, 20] on random access MAC protocols for wireless networks. The above assumption on collision-caused packet loss is actually a worst-case scenario. Due to the capture effect, the achievable relay success probability of the proposed cooperation strategies can be even higher in practice.

There are two types of distributed cooperation solutions. For the probabilistic uncoordinated strategies, each potential relay independently determines a forwarding probability that it will transmit the overheard packet. While the probabilistic strategies offer the benefit of light signalling overhead, the high collision probability often upper bound the success probability by $1/e \approx 0.368$ [16, 21]. For the backoff-based strategies, each potential relay sets a backoff timer depending on its location information and other local estimates. When the backoff timer expires, a potential relay starts to transmit the packet if no forwarding signal is heard from any other relay. The backoff-based strategies can significantly reduce collisions by properly characterizing the transmission capability of relays and mapping that to a backoff time. Nonetheless, a time synchronization overhead is also involved. Based on

the above observations, we propose two distributed cooperation schemes that take advantage of the spatial distribution of random relays to combine the strengths of the probabilistic and backoff-based solutions.

5.3.1 Inter-Group Backoff-Based Contention

To reduce collisions, we consider two-level inter-group and intra-group contentions similar to [17]. As there may exist a large number of potential relays in the entire sector (denoted by Ω_{SD}) in Fig. 5.1, a backoff-based scheme works better for the inter-group contention. Since the potential relays closer to D generally have a higher transmission success probability, a natural idea for grouping is to partition the sector into L strips. The radius boundaries are denoted by a vector $\mathbf{r} = [r_0, r_1, r_2, \dots, r_L]$, where $r_0 = 0$, $r_i < r_j$ for $i < j$ and $0 \leq i, j \leq L$. To prioritize the relays in a strip closer to D , the potential relays in region l (denoted by Ω_l) set a minimum backoff time

$$t_{l,\min} = (L - l + 1) \cdot \Delta, \quad 1 \leq l \leq L \quad (5.3)$$

where Δ is a time constant.

5.3.2 Intra-Group Contention

When the intensity of relay nodes is very high, the collision probability within a group may still be intolerable. Effective intra-group contention strategies are important to further reduce collisions. Firstly, the relays in region Ω_l can choose their backoff time on the basis of the group minimum time $t_{l,\min}$. That is, a relay in the group l sets its backoff time in the range of $[t_{l,\min}, t_{l,\min} + \Delta)$. Secondly, a probabilistic strategy can be used since the number of contending relays in each group is expected to be much smaller. That is, each relay in a certain contention group independently determines a forwarding probability for the cooperative relaying. Although the basic rationale behind these two strategies is that a better relay ends up with a smaller backoff time and/or a higher forwarding probability, the specific algorithms deriving such parameters are critical for the achievable performance.

5.3.2.1 Backoff-Based Strategy

In the first intra-group contention strategy, a potential relay $R_{l,i}$ in region Ω_l first estimates its transmission success probability to D , $p_{l,i}$, according to the location information. Then, on the basis of the group minimum given in (5.3), $R_{l,i}$ can set its backoff time to

$$t_{l,i} = t_{l,\min} + (1 - p_{l,i}) \cdot \Delta. \quad (5.4)$$

As such, $R_{l,i}$ forwards the packet after a backoff time $t_{l,i}$ if there is no forwarding signal overheard, which means that the region of $R_{l,i}$ is the closest to D among all potential relays and its transmission success probability is the highest among the potential relays in the same region.

5.3.2.2 Probabilistic Strategy

Another probabilistic strategy for the intra-group contention is to have each potential relay $R_{l,i}$ in region Ω_l estimate its transmission success probability $p_{l,i}$ and use $p_{l,i}$ to determine a forwarding probability, denoted by $\tau_{l,i}$. That is, after a backoff time $t_{l,\min}$, $R_{l,i}$ forwards the packet with a probability $\tau_{l,i}$, only if no forwarding signal is overheard from the potential relays in regions closer to D ($\Omega_{l+1}, \dots, \Omega_L$), which are supposed to time out earlier. As a result, there is no collision if only one relay in region Ω_l transmits, while none relay in regions ($\Omega_{l+1}, \dots, \Omega_L$) correctly overhears the packet or all potential relays therein are silent.

Intuitively, a potential relay with a higher transmission success probability should end up with a larger forwarding probability. Provided that the statistics of the transmission success probability of potential relays are known, the potential relay $R_{l,i}$ in region Ω_l can set its forwarding probability to

$$\tau_{l,i} = [G_{P,l}(p_{l,i})]^{\lceil \Lambda_l \rceil - 1} \quad (5.5)$$

where Λ_l is the average number of potential relays in region Ω_l , and $G_{P,l}(\cdot)$ is the cumulative distribution function (CDF) of the transmission success probability of the potential relays in region Ω_l . We will derive Λ_l and $G_{P,l}(\cdot)$ in Sect. 5.4.1.

The physical meaning of (5.5) can be interpreted as follows. Supposing that there are M relays ($M \geq 1$) in region Ω_l that correctly overhear the packet, we have $P_{l,(1)} < P_{l,(2)} < \dots < P_{l,(M)}$ denote the M order statistics of the transmission success probability of these potential relays in the group. Then, a given potential relay $R_{l,i}$ has the highest transmission success probability among the M candidates with a probability $[G_{P,l}(p_{l,i})]^{M-1}$. This also means the transmission success probabilities of $(M-1)$ potential relays are all no greater than that of $R_{l,i}$, $p_{l,i}$. Since the relays are not aware of the status of others, the average number of potential relays is used here for approximation.

To further reduce intra-group collisions and augment the forwarding probability of best relays, we can use the generalized logistic function [12] (a.k.a Richards' curve) to adapt $\tau_{l,i}$ in (5.5) as follows:

$$\tilde{\tau}_{l,i} = \frac{1}{[1 + \nu e^{-\mu(\tau_{l,i}-q)}]^{1/\nu}} \quad (5.6)$$

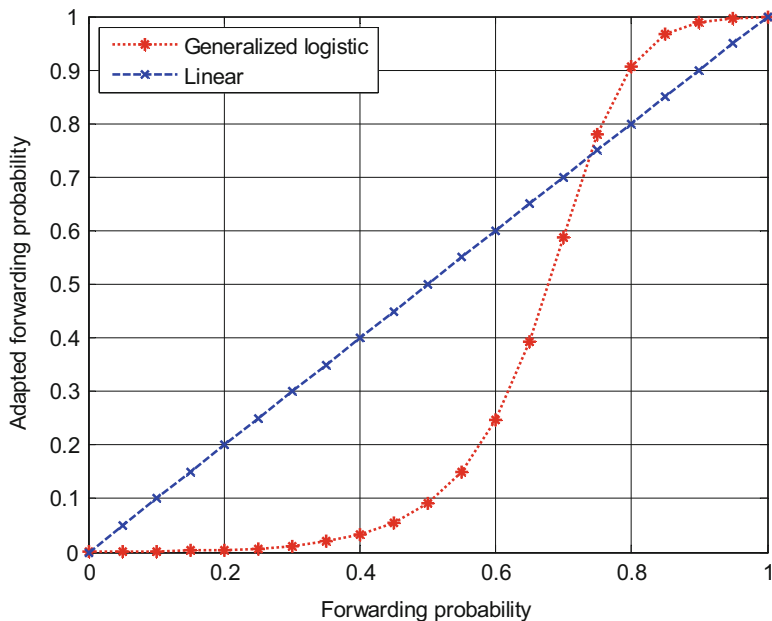


Fig. 5.2 Adaptation of forwarding probability with a generalized logistic function

where μ and ν can be determined so that $\tilde{\tau}_{l,i}$ is bounded within $(0, 1)$. The parameter q indicates the point at which the growth rate is maximum. It is tricky to find the best setting for q and we have referred to the average transmission success probability to adjust this parameter. Figure 5.2 illustrates one example of the logistic function in comparison with the linear case without adaptation. It is expected that, after the forwarding probability is adapted by the logistic function, the bad relays of small transmission success probability are suppressed, while the forwarding probabilities are boosted for good relays of high transmission success probability.

5.4 Performance Analysis

As shown in Sect. 5.3, the intra-group contention parameters highly depend on the location information as well as the transmission success probability of the potential relays and its statistics. The spatial distribution of the relays thus has an essential impact on the determination of the contention parameters and the achievable performance. In this section, we first derive the statistic distributions of the transmission success probability of the potential relays in a region. Then, we develop effective analytical approaches to evaluate the relay performance of the proposed cooperation strategies.

5.4.1 Probability Distributions of Spatial Random Relays

Given the system model in Sect. 5.2, the relays are deployed in the given sector Ω_{SD} between S and D as a homogeneous PPP, denoted by Φ_{SD} . According to (5.2), a relay at the location (r, θ) successfully receives the packet from S and becomes a *potential relay* with a probability

$$p(r) = e^{-K_0 r^\alpha}. \quad (5.7)$$

Considering the inter-group contention strategy in Sect. 5.3.1, we divide all the potential relays into L groups. The potential relays in each region Ω_l ($1 \leq l \leq L$) form a new point process, denoted by Φ_l , from the original PPP Φ_{SD} by retaining a point at (r, θ) with a probability $p(r)$ and deleting the point with a probability $1 - p(r)$. This is referred to as a $p(x)$ -thinning operation in stochastic geometry [19]. In this $p(x)$ -thinning operation, the retention probability that determines a potential relay is independent of the locations and possible retentions of any other points. According to Prekopa's Theorem [19], the distribution of these potential relays in region Ω_l also follows a Poisson distribution with a mean

$$\Lambda_l = \int_{r_{l-1}}^{r_l} \int_{-\phi}^{\phi} p(r) \lambda r \, dr d\theta, \quad 1 \leq l \leq L. \quad (5.8)$$

According to (5.7), we can easily obtain

$$\Lambda_l = \frac{\lambda \phi}{K_0} \left[\exp(-K_0 r_{l-1}^\alpha) - \exp(-K_0 r_l^\alpha) \right]. \quad (5.9)$$

The distribution of the number of *potential relays* in Ω_l is then given by

$$\Pr[\Phi_l = k] = \frac{\Lambda_l^k}{k!} \exp(-\Lambda_l), \quad k = 0, 1, 2, \dots \quad (5.10)$$

Let $P_{RD,l}$ denote the probability that an arbitrary potential relay $R_{l,i}$ in Ω_l forwards the overheard packet to D successfully. Based on (5.2), we write the CDF of $P_{RD,l}$ as

$$\begin{aligned} G_{P,l}(y) &= \Pr[P_{RD,l} \leq y] \\ &= \Pr \left[\exp \left(\frac{-T_0}{P_0/N_0 \|R_{l,i} - D\|^{-\alpha}} \right) \leq y \right]. \end{aligned} \quad (5.11)$$

Letting $\Gamma_{RD,l}$ denote the average received SNR at D for the forwarded signal from a potential relay, that is, $\Gamma_{RD,l} = \frac{P_0}{N_0} \|R_{l,i} - D\|^{-\alpha}$, we rewrite (5.11) as

$$\begin{aligned} G_{P,l}(y) &= \Pr \left[\exp \left(\frac{-T_0}{\Gamma_{RD,l}} \right) \leq y \right] \\ &= \Pr \left[\Gamma_{RD,l} \leq \frac{-T_0}{\ln(y)} \right] \triangleq F_{\Gamma,l} \left(\frac{-T_0}{\ln(y)} \right) \end{aligned} \quad (5.12)$$

where $F_{\Gamma,l}(x)$ denotes the CDF of $\Gamma_{RD,l}$.

Here, $F_{\Gamma,l}(x)$ depends on the spatial distribution of the potential relays as follows:

$$\begin{aligned} F_{\Gamma,l}(x) &= \Pr \left[\frac{P_0}{N_0} \|R_{l,i} - D\|^{-\alpha} \leq x \right] \\ &= \Pr \left[\|R_{l,i} - D\|^\alpha \geq \frac{P_0/N_0}{x} \right]. \end{aligned} \quad (5.13)$$

When $\alpha = 2$, we can further express (5.13) as

$$\begin{aligned} F_{\Gamma,l}(x) &= \iint_{\Omega_l} \exp(-K_0 r^2) \lambda r \\ &\quad \cdot \mathbf{1}_{\mathbb{R}^+} \left(r^2 + R^2 - 2rR \cos \theta - \frac{P_0/N_0}{x} \right) dr d\theta \\ &= \iint_{\Omega_l} \exp(-K_0 r^2) \lambda r dr d\theta \end{aligned} \quad (5.14)$$

where $\mathbf{1}_{\mathbb{R}^+}(\cdot)$ is the indicator function [8] with the set of positive real numbers, \mathbb{R}^+ , given by

$$\mathbf{1}_{\mathbb{R}^+}(y) = \begin{cases} 1, & \text{if } y \in \mathbb{R}^+ \\ 0, & \text{if } y \notin \mathbb{R}^+. \end{cases}$$

The denominator in (5.14) is actually Λ_l derived by (5.9). The ratio in (5.14) defines the fraction of the potential relays in region Ω_l that satisfy the condition $\|R_{l,i} - D\|^\alpha \geq \frac{P_0/N_0}{x}$, for a given average received SNR x . Although there is not a complete closed-form expression to (5.14), it can be more efficiently calculated by the algorithm given in [Appendix: Calculation of the CDF \$F_{\Gamma,l}\(x\)\$ of \$\Gamma_{RD,l}\$](#) .

Based on the CDF $G_{P,l}(y)$ of the transmission success probability of potential relays in region Ω_l , we can easily evaluate the average success probability by

$$\bar{P}_{RD,l} = \int_0^1 [1 - G_{P,l}(y)] dy. \quad (5.15)$$

The average success probability can be interpreted as the ratio of the average number of potential relays that successfully transmit to D to the overall average number of potential relays. Therefore, when $\alpha = 2$, $\bar{P}_{RD,l}$ can also be computed by

$$\begin{aligned} \bar{P}_{RD,l} &= \frac{\int_0^\phi d\theta \int_{r_{l-1}}^{r_l} \exp(-K_0 r^2) \cdot \exp(-K_0(r^2 + R^2 - 2rR \cos \theta)) \lambda r dr}{\int_0^\phi d\theta \int_{r_{l-1}}^{r_l} \exp(-K_0 r^2) \lambda r dr} \\ &= \frac{2K_0 \exp(-K_0 R^2)}{\phi [\exp(-K_0 r_{l-1}^2) - \exp(-K_0 r_l^2)]} \\ &\quad \int_0^\phi \int_{r_{l-1}}^{r_l} \exp(-K_0(2r^2 - 2rR \cos \theta)) r dr d\theta. \end{aligned} \quad (5.16)$$

5.4.2 Performance of Two-Level Backoff-Based Strategy

Combining the backoff-based strategies for both the inter-group and intra-group contentions, we have a two-level backoff-based relaying scheme. That is, a potential relay $R_{l,i}$ in region Ω_l first determines a minimum backoff time based on the location information according to (5.3). Then, $R_{l,i}$ estimates its transmission success probability to the destination D and sets its backoff time according to (5.4).

As seen, the group of potential relays in region Ω_l will have an opportunity to win the inter-group contention and proceed with intra-group contention only if none of the relays in the regions closer to D has correctly received the packet. Similar to (5.8) and (5.9), we see that the number of all potential relays in regions $(\Omega_{l+1}, \dots, \Omega_L)$ is Poisson distributed with a mean

$$\Lambda_{l+} = \frac{\lambda \phi}{K_0} \left[\exp(-K_0 r_l^\alpha) - \exp(-K_0 R^\alpha) \right], \quad 1 \leq l \leq L-1.$$

According to the Poisson distribution, there is no potential relay in these regions with a probability

$$W_l = \begin{cases} \exp(-\Lambda_{l+}), & \text{if } 1 \leq l \leq L-1 \\ 1, & \text{if } l = L. \end{cases} \quad (5.17)$$

This is the probability that the potential relays in region Ω_l win the inter-group contention and are eligible for further intra-group contention.

A potential relay in the winning region Ω_l can estimate the transmission success probability and set its backoff time according to (5.4). Based on the spatial distribution of random relays, the CDF of the transmission success probability of potential relays in region Ω_l , $G_{P,l}(\cdot)$, is analyzed in Sect. 5.4.1. Accordingly, the CDF of the backoff time of potential relays in Ω_l (denoted by T_l) can be obtained as

$$\begin{aligned}
H_{T,l}(t) &= \Pr[T_l \leq t] = \Pr\left[t_{l,\min} + (1 - P_{RD,l}) \cdot \Delta \leq t\right] \\
&= \Pr\left[P_{RD,l} \geq 1 - \frac{t - t_{l,\min}}{\Delta}\right] \\
&= 1 - G_{P,l}\left(1 - \frac{t - t_{l,\min}}{\Delta}\right). \tag{5.18}
\end{aligned}$$

The corresponding probability density function (PDF) of T_l can be easily derived by

$$\begin{aligned}
h_{T,l}(t) &= \left[1 - G_{P,l}\left(1 - \frac{t - t_{l,\min}}{\Delta}\right)\right]' \\
&= \frac{1}{\Delta} g_{P,l}\left(1 - \frac{t - t_{l,\min}}{\Delta}\right) \tag{5.19}
\end{aligned}$$

where $g_{P,l}(y) = G'_{P,l}(y)$ is the PDF of the transmission success probability for region Ω_l .

Supposing that there are M relays ($M \geq 1$) that correctly overhear the packet in region Ω_l , we have the M order statistics of their backoff time, denoted by $T_{l,(1)} < T_{l,(2)} < \dots < T_{l,(M)}$. In [2], the authors derive the joint PDF of the minimum and second minimum of M order statistics and the probability that the difference of the minimum and second minimum is greater than a constant. Based on their conclusion, if the difference of the minimum and second minimum backoff time is greater than a constant c , the probability of no collision is given by

$$\begin{aligned}
I_{l|M} &= \Pr[T_{l,(2)} \geq T_{l,(1)} + c] = M(M-1) \\
&\quad \int_{t_{l,\min}+c}^{t_{l,\min}+\Delta} h_{T,l}(t) [1 - H_{T,l}(t)]^{M-2} H_{T,l}(t-c) dt. \tag{5.20}
\end{aligned}$$

Recall that $P_{l,(1)} < P_{l,(2)} < \dots < P_{l,(M)}$ denote the M order statistics of the transmission success probability of the potential relays in the group. Since the backoff time is chosen inversely proportional to the transmission success probability, the best relay corresponds to the maximum of the order statistics of the transmission success probability, i.e., $P_{l,(M)}$. The CDF of $P_{l,(M)}$ can be written as

$$\tilde{G}_{P,l}(y|M) = \Pr[P_{l,(M)} \leq y|M] = [G_{P,l}(y)]^M, \quad 0 \leq y \leq 1$$

which is actually the probability that all of the M order statistics, $P_{l,(1)}, \dots, P_{l,(M)}$, are no greater than y , since $P_{l,(M)}$ is the maximum. The average transmission success probability of the best relay within the group is then given by

$$\tilde{P}_{RD,l}(M) = \int_0^1 [1 - \tilde{G}_{P,l}(y|M)] dy. \tag{5.21}$$

Thus, the relay success probability of the two-level backoff-based scheme can be expressed as

$$P_{suc}^{bk} = \sum_{l=1}^L \sum_{M=1}^{\infty} \frac{\Lambda_l^M}{M!} e^{-\Lambda_l} \cdot W_l \cdot I_{l|M} \cdot \tilde{P}_{RD,l}(M). \quad (5.22)$$

The terms inside the double summations of (5.22) give the probability that a potential relay in region Ω_l successfully forwards the packet to the destination D without collisions when there are totally M ($M \geq 1$) potential relays in the same group. First, there are M potential relays in region Ω_l with a probability $\frac{\Lambda_l^M}{M!} e^{-\Lambda_l}$. Then, W_l is the probability that no relay is available in the regions ($\Omega_{l+1}, \dots, \Omega_L$) closer to D than Ω_l , given in (5.17); $I_{l|M}$ is the probability of no collision to the best relay in Ω_l with the shortest backoff time, given in (5.20); and $\tilde{P}_{RD,l}(M)$ is the average transmission success probability of the best relay in Ω_l , given in (5.21).

As a potential relay determines its backoff time according to (5.3) and (5.4), intuitively, the collision probability is lower with a larger Δ , whereas a longer backoff delay is involved with the relay selection. To quantify the tradeoff between the collision probability and backoff delay, we evaluate the average backoff delay of the two-level backoff-based scheme by

$$\begin{aligned} D_{sel}^{bk} &= \sum_{l=1}^L W_l \cdot Q_l^{1+} [(L-l+1) + (1 - \bar{P}_{RD,l})] \Delta \\ &\quad + e^{-\Lambda_R} \cdot (F+1) \Delta \\ &= \sum_{l=1}^L W_l \cdot (1 - e^{-\Lambda_l}) [(L-l+1) + (1 - \bar{P}_{RD,l})] \Delta \\ &\quad + e^{-\Lambda_R} \cdot (F+1) \Delta \end{aligned} \quad (5.23)$$

where W_l is the probability that there is no potential relay in the regions closer to D than Ω_l , given in (5.17), and Q_l^{1+} is the probability that there is at least one potential relay in Ω_l , which can be easily obtained according to (5.9). Thus, $W_l \cdot Q_l^{1+}$ is the probability that the potential relays in region Ω_l are selected, while $[(L-l+1) + (1 - \bar{P}_{RD,l})] \Delta$ is the average backoff time taken by these relays. Here, $\bar{P}_{RD,l}$ is the average transmission success probability of potential relays in region Ω_l , given in (5.15). The last term in (5.23) addresses the situation that there is no relay in the entire sector Ω_{SD} that correctly receives the packet from S . In this case, the source does not hear any forwarding signal from the relays and has to retransmit the packet by itself after a maximum backoff time $(F+1)\Delta$. The corresponding occurrence probability is $e^{-\Lambda_R}$, where Λ_R is the intensity measure of potential relays in Ω_{SD} , given by

$$\Lambda_R = \frac{\lambda \phi}{K_0} \left[1 - \exp(-K_0 R^\alpha) \right]. \quad (5.24)$$

5.4.3 Performance of Hybrid Relaying Strategy

When the backoff-based inter-group contention is considered with the probabilistic intra-group contention, we have a hybrid cooperation scheme. A potential relay $R_{l,i}$ in region Ω_l first determines a backoff time based on the location information according to (5.3). When the backoff timer expires and no transmission signal is overheard, $R_{l,i}$ forwards the packet to D with the probability defined in (5.5). According to the hybrid scheme, a relay $R_{l,i}$ in region Ω_l forwards to D successfully, only if the relays in regions $(\Omega_{l+1}, \dots, \Omega_L)$ closer to D are all silent and $R_{l,i}$ is the only relay in Ω_l that transmits and the transmission succeeds.

Let Q_l^0 denote the probability that there is no potential relay in region Ω_l or all potential relays in Ω_l if any remain silent. Then, the probability that there is no forwarding from the relays in $(\Omega_{l+1}, \dots, \Omega_L)$ is given by $\sum_{j=l+1}^L Q_j^0$. Provided that all except one relay in Ω_l are silent, with the occurrence probability denoted by \tilde{Q}_l^0 , we represent the probability that one potential relay exists in Ω_l and transmits successfully to D by P_l^1 . Thus, the relay success probability of the hybrid scheme can be expressed as

$$P_{suc}^{hyb} = \sum_{l=1}^L \left(\sum_{j=l+1}^L Q_j^0 \right) \cdot \tilde{Q}_l^0 \cdot P_l^1. \quad (5.25)$$

In the following, we derive Q_l^0 , \tilde{Q}_l^0 , and P_l^1 , using an approach similar to that of [22].

Consider a sufficiently small arc region centered at (r, θ) in Ω_l of an area $\delta A = r\delta r\delta\theta$. The probability that a potential relay exists in this small region and it forwards the overheard packet is given by

$$q(r, \theta) = \lambda p(r) \tau_l(r, \theta) \delta A = \lambda e^{-K_0 r^\alpha} [G_{P,l}(e^{-K_0 r_d^\alpha})]^{\lceil \Lambda_l \rceil - 1} \delta A$$

where $p(r)$ is given by (5.7) and $\tau_l(r, \theta)$ refers to the forwarding probability in (5.5). Here, we revise the notation of $\tau_{l,i}$ to highlight its dependance on the location of the potential relay (r, θ) . According to (5.5), we have $\tau_l(r, \theta) = [G_{P,l}(e^{-K_0 r_d^\alpha})]^{\lceil \Lambda_l \rceil - 1}$, where r_d is the distance of the potential relay at (r, θ) to D , given by $r_d = \sqrt{r^2 + R^2 - 2rR \cos \theta}$. Then, we obtain

$$\begin{aligned} Q_l^0 &= \lim_{\delta A \rightarrow 0} \prod_{(r, \theta)} \left[1 - \lambda p(r) \tau_l(r, \theta) \delta A \right] \\ &= \lim_{\delta A \rightarrow 0} \exp \left\{ \sum_{(r, \theta)} \log \left[1 - \lambda p(r) \tau_l(r, \theta) \delta A \right] \right\} \\ &= \lim_{\delta A \rightarrow 0} \exp \left[\sum_{(r, \theta)} -\lambda p(r) \tau_l(r, \theta) \delta A \right] \\ &= \exp \left\{ - \iint_{\Omega_l} \lambda p(r) \tau_l(r, \theta) r dr d\theta \right\}. \end{aligned} \quad (5.26)$$

Comparing the definitions of Q_l^0 and \tilde{Q}_l^0 , we see that Q_l^0 assumes no forwarding from any potential relay in region Ω_l , while \tilde{Q}_l^0 assumes all but one potential relay are silent. Considering the infinitesimal impact of excluding a single point from a continuous space [22], we have $\tilde{Q}_l^0 = Q_l^0$.

Given that no relay in $(\Omega_{l+1}, \dots, \Omega_L)$ is forwarding and all except one relay in Ω_l are silent, we can derive the probability that one relay in Ω_l transmits to D successfully by

$$P_l^1 = \iint_{\Omega_l} \lambda p(r) \tau_l(r, \theta) e^{-K_{\text{or}} r} r \, dr d\theta. \quad (5.27)$$

Applying (5.26) and (5.27) to (5.25), we can obtain the relay success probability of the hybrid scheme. Likewise, the backoff delay of the hybrid scheme can be evaluated by

$$D_{sel}^{hyb} = \sum_{l=1}^L \left(\sum_{j=l+1}^L Q_j^0 \right) \cdot (1 - \tilde{Q}_l^0) \cdot [(L - l + 1)\Delta] + e^{-\Lambda_R} \cdot (F + 1)\Delta. \quad (5.28)$$

Here, the potential relays in region Ω_l win the contention for forwarding only if the relays in the closer regions are all silent and at least one potential relay in region Ω_l transmits after a backoff time $(L - l + 1)\Delta$. The first condition happens with a probability $\sum_{j=l+1}^L Q_j^0$, while the occurrence probability of the second condition is $(1 - \tilde{Q}_l^0)$. The last term in (5.28) is the same as the last term in (5.23), which addresses the case that there is no potential relay in the entire sector Ω_{SD} .

5.5 Numerical Results and Discussions

In this section, we first present analysis and simulation results to validate the derivation of the CDF of transmission success probability of potential relays in Sect. 5.4.1. Then, we introduce two reference cooperation schemes, including a centralized scheme with the pre-selected best relay and a pure probabilistic scheme. The performance achieved by the two reference schemes are considered as an upper bound and a lower bound for comparison purposes. The two reference schemes are compared with the two cooperation strategies proposed in Sect. 5.3 in various system settings with respect to relay success probability as well as backoff delay of relay selection.

5.5.1 CDF of Transmission Success Probability

In Sect. 5.4.1, we introduce an analytical approach to evaluate the CDF of the transmission success probability of potential relays in a region. This CDF can be efficiently calculated by the algorithm in [Appendix: Calculation of the CDF \$F_{\Gamma,l}\(x\)\$ of \$\Gamma_{RD,l}\$](#) . As the forwarding probability and the performance analysis depend on this CDF, we need to validate the accuracy of the calculation algorithm. Considering the system parameters in Table 5.1, we conduct extensive numerical analysis and computer simulations by MATLAB 8.1.0 (R2013a) [15].

Taking the entire sector between S and D , Ω_{SD} , as an example, we can get the CDF $Y_P(y)$, $0 \leq y \leq 1$. Figure 5.3 shows the distribution that the transmission success probability of potential relays, P_{RD} , falls into small intervals within $[10^{-3}, 1]$. For example, the probability that $y_1 \leq P_{RD} \leq y_2$ is given by $Y_P(y_2) - Y_P(y_1)$. As such, we can clearly compare the analysis results with the simulation results. As seen in Fig. 5.3, they match quite well. The average difference is around 4.5%. Since we run the simulations for 100 rounds to remove the randomness effect, the minor difference is mainly due to the errors with the numerical evaluation of the integrals in (5.38) and (5.40) without closed-form expressions.

Similarly, we can evaluate the CDF $G_{P,l}(y)$ of transmission success probability $P_{RD,l}$ for each strip region Ω_l . Based on $G_{P,l}(y)$, the average transmission success probability $\bar{P}_{RD,l}$ of potential relays in Ω_l can be computed by (5.15). Figure 5.4 shows $\bar{P}_{RD,l}$ of each contention region. As seen, the analysis results are validated by the simulation results. The small calculation error is bounded within the range (0.27%, 1.88%). It is worth mentioning that Fig. 5.4 is based on segmentations that partition the entire sector into concentric arcs of an equal area. The equal-area segmentation is also used in Figs. 5.5, 5.6, 5.7 and 5.9.

Table 5.1 System parameters

Symbol	Value	Definition
λ	0.001 ~ 0.025	Intensity function of relay distribution
P_0/N_0	40 dB	Transmit SNR
T_0	4	Decoding SNR threshold
R	50 ~ 90 m	Source-destination distance
ϕ	30° ~ 90°	Directional angle toward destination
L	1 ~ 16	Number of region partitions of the sector between S and D
Δ	4 ~ 22	Backoff time unit for inter-group contention
c	1	Collision threshold for backoff time of intra-group contention
q	0.7	Point of maximum growth rate of generalized logistic function
μ	22.2326	Parameter of generalized logistic function
ν	2.1780	Parameter of generalized logistic function

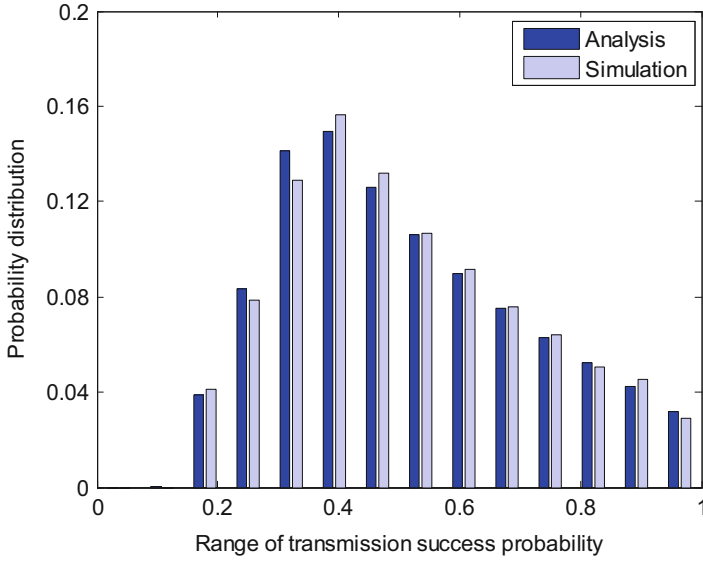


Fig. 5.3 Distribution of transmission success probability of potential relays in Ω_{SD} ($\lambda = 10^{-2}$, $R = 70$, and $\phi = 45^\circ$)

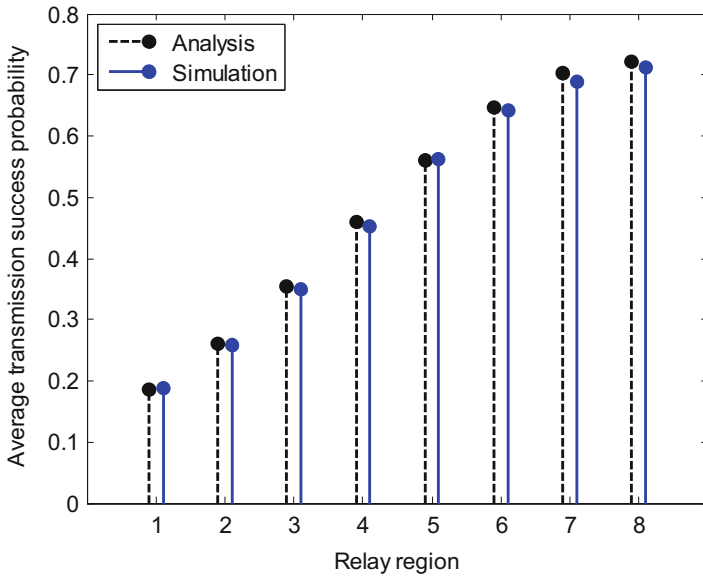


Fig. 5.4 Average transmission success probability of potential relays in each region Ω_l ($\lambda = 10^{-2}$, $R = 70$, $\phi = 45^\circ$, and $L = 8$)

5.5.2 Performance Upper and Lower Bounds

While the distributed solutions can reduce the coordination overhead for cooperative transmission, it is also vital to ensure a high success probability. Jointly considering the inter-group and intra-group contentions, we propose two distributed cooperation strategies in Sect. 5.3, which exploit both the location information and local estimate of transmission success probability. The first one is a two-level backoff-based scheme, whose relay success probability can be analytically evaluated by (5.22). The second one is a hybrid scheme with backoff-based inter-group contention and probabilistic intra-group contention. The relay success probability of the hybrid scheme is analyzed by (5.25).

In the following, we further introduce two reference schemes. The first scheme achieves a performance upper bound with the pre-selected best relay given the global knowledge of potential relays. The second scheme of pure probabilistic forwarding without grouping is considered as a lower bound due to more collisions.

In the first reference scheme, among all potential relays in the entire sector Ω_{SD} , only the relay with the highest transmission success probability to D forwards the overheard packet. The relay success probability of this centralized scheme can be evaluated similarly by the approach in Sect. 5.4.2. In this case, $L = 1$ with $r_0 = 0$ and $r_L = R$.

The CDF of the transmission success probability P_{RD} of all potential relays, denoted by $Y_P(y)$, can be calculated in the same manner as in Sect. 5.4.1. With the pre-selection of the best relay, there is no collision and the relay success probability only depends on the transmission success probability of the best relay. The CDF of the transmission success probability of the best relay among M potential candidates is $[Y_P(y)]^M$. Thus, we obtain the relay success probability as

$$P_{suc}^{\max} = \sum_{M=1}^{\infty} \frac{\Lambda_R^M}{M!} e^{-\Lambda_R} \int_0^1 [1 - (Y_P(y))^M] dy \quad (5.29)$$

where the integral term gives the average transmission success probability of the pre-selected best relay and Λ_R is the intensity measure of the potential relays in the entire sector Ω_{SD} , given in (5.24).

In the second reference scheme, we consider pure probabilistic forwarding without partitioning the sector for grouping. Similar to (5.5), a potential relay R_i in the sector Ω_{SD} independently sets its forwarding probability to:

$$\tau_i = [Y_P(p_i)]^{\lceil \Lambda_R \rceil - 1} \quad (5.30)$$

where Λ_R is given by (5.24) and p_i is the local estimate of R_i for its transmission success probability to D . A collision happens if more than one relay forwards the packet. Obviously, the collision probability can be much higher since all potential relays in the entire sector contend for forwarding. Hence, we consider the performance of this pure probabilistic scheme as a lower bound.

Following the analytical approach in Sect. 5.4.3, we can evaluate the relay success probability of the pure probabilistic scheme by

$$P_{suc}^{prob} = \tilde{Q}_R^0 \cdot P_R^1 \quad (5.31)$$

where \tilde{Q}_R^0 is the probability that all but one potential relay in the sector Ω_{SD} remain silent, and P_R^1 is the transmission success probability of the only potential relay in Ω_{SD} . Similar to (5.26), we derive \tilde{Q}_R^0 by

$$\begin{aligned} \tilde{Q}_R^0 &= Q_R^0 = \exp \left\{ \iint_{\Omega_{SD}} -\lambda p(r) \tau(r, \theta) r \, dr d\theta \right\} \\ &= \exp \left\{ \iint_{\Omega_{SD}} -\lambda e^{-K_0 r^\alpha} [Y_P(e^{-K_0 r^\alpha})]^{[\Lambda_R]-1} r \, dr d\theta \right\}. \end{aligned}$$

Likewise, P_R^1 is obtained from (5.27) as

$$\begin{aligned} P_R^1 &= \iint_{\Omega_{SD}} \lambda p(r) \tau(r, \theta) e^{-K_0 r^\alpha} r \, dr d\theta \\ &= \iint_{\Omega_{SD}} \lambda e^{-K_0 r^\alpha} [Y_P(e^{-K_0 r^\alpha})]^{[\Lambda_R]-1} e^{-K_0 r^\alpha} r \, dr d\theta. \end{aligned}$$

5.5.3 Relay Success Probability

Figure 5.5 shows the analysis results and simulation results of the two proposed schemes and the two reference schemes. Note that the relay success probability in Fig. 5.5 only accounts for the forwarding success via potential relays. The overall packet success probability can be even higher considering the successful direct transmission from S to D . Since the cooperative relaying strategies only differ in the forwarding phase via the relays, we focus on the relay success probability to highlight the difference of these relaying strategies. As seen, the analysis and simulation results match well and our analytical approaches are quite accurate.

Besides, Fig. 5.5 compares the performance of the proposed schemes with the upper and lower bounds of the reference schemes with respect to the relay intensity. As seen, the proposed cooperation schemes greatly outperform the pure probabilistic scheme, whose maximum relay success probability is limited to 0.3496. On average, the relay success probability of the two-level backoff-based scheme is 1.07 times higher than that of the pure probabilistic scheme, while the average performance gain of the hybrid scheme with adaptation is 85.3 %.

Moreover, it is observed in Fig. 5.5 that the two-level backoff-based scheme achieves a stable relay success probability and well outperforms the hybrid scheme when the relay intensity is relatively low. In particular, the relay success probability of the two-level backoff-based scheme first increases fast with the relay intensity and then decreases slightly. When the relay intensity is larger, there are more contending

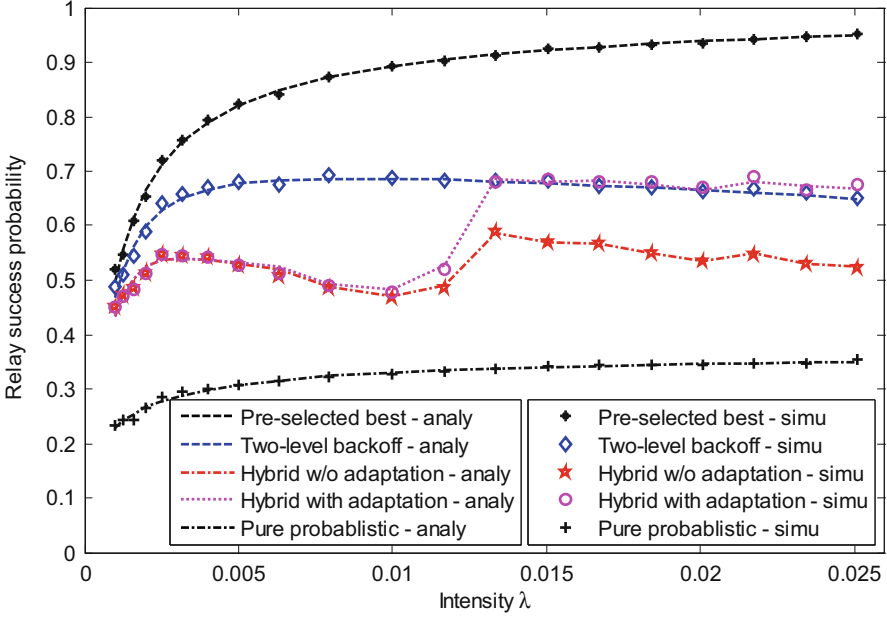


Fig. 5.5 Relay success probability of different schemes vs. relay intensity λ ($R = 70, \phi = 45^\circ, L = 8,$ and $\Delta = 16$)

potential relays in each group. On one hand, more relays of good channel conditions to the destination likely exist. On the other hand, the contention among more relays can lead to a higher collision probability. Hence, when the relay intensity is sufficiently high, the gain of locating good relays is offset by the increased collisions and the relay success probability even decreases slightly with λ .

It is also noticed in Fig. 5.5 that the performance of the hybrid scheme does not vary with the relay intensity as smoothly as the other schemes. This is not due to the randomness effect since we run the simulations for 100 rounds and the simulation results match well the validated analysis results. This fluctuation is mainly because each relay determines its forwarding probability based on the average number of contending potential relays in a region (Λ_l). The forwarding probability $\tau_{l,i}$ in (5.5) uses the ceiling function to Λ_l and causes the truncation effect. The performance can be improved if each relay knows the exact number of relays in contention. However, extra overhead will be introduced to acquire such information, which also harms the distributed nature of the cooperation strategy.

In addition, Fig. 5.5 clearly illustrates the difference of two cases of the hybrid scheme with and without using the logistic function in (5.6) to adapt the forwarding probability. As seen, the relay success probability of both cases is much lower than that of the two-level backoff-based scheme when the relay intensity is relatively low. This implies that the relays are over-conservative with a small forwarding probability in such scenarios. By using the logistic function to adapt the forwarding probability, the hybrid scheme approaches and even slightly exceeds the high

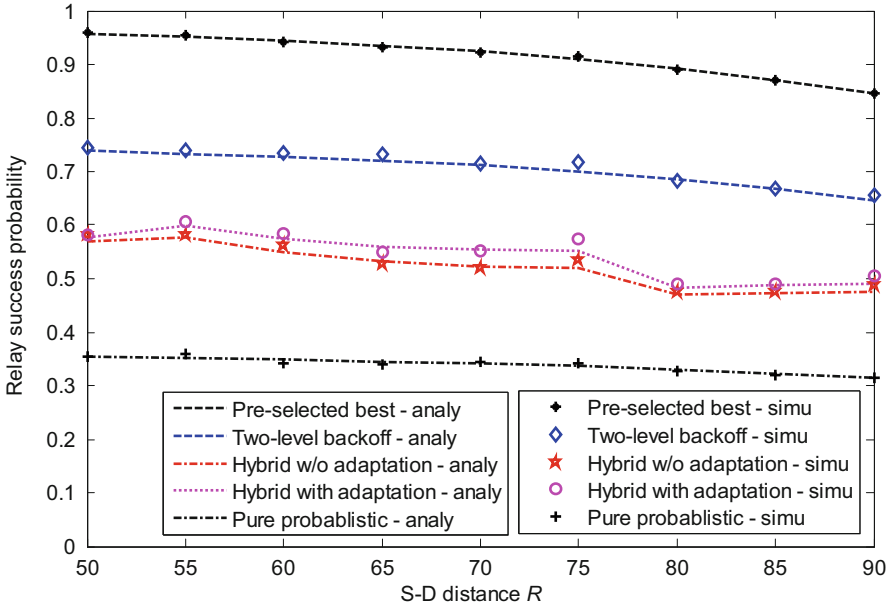


Fig. 5.6 Relay success probability of different schemes vs. S - D distance R ($\lambda = 10^{-2}$, $\phi = 45^\circ$, $L = 8$, and $\Delta = 16$)

performance of the two-level backoff-based scheme when $\lambda > 0.0134$. As shown in Fig. 5.2, the logistic function can suppress the forwarding probability of poor relays of low transmission success probability and promote the forwarding probability of good relays. Consequently, the adaptation can ensure a high forwarding probability for very selective good relays and thus mitigate the collisions among a large number of contending relays.

Figure 5.6 shows the variation of the four relaying schemes with respect to the S - D distance R . As seen, the relay success probability of all schemes slowly degrades with the increase of R . This is intuitive since a larger S - D distance results in a higher path loss.

Figure 5.7 shows the variation of the four schemes with the directional angle ϕ for the sector Ω_{SD} . As expected, the pre-selected best relay scheme and the pure probabilistic scheme are insensitive to ϕ , given the relay spatial distribution as a homogenous PPP. The two-level backoff-based scheme has a higher relay success probability with a smaller ϕ . This is because, when the relay region is more narrowly tuned toward the destination, the potential relays are closer to D and there are less collisions with fewer relays in the smaller arc region. Nonetheless, Fig. 5.7 considers a relatively high relay intensity and it is not always true that the smaller ϕ the better. When the relay intensity is low, there may not be sufficient good relays in the small region, which can degrade the relay success probability. The hybrid scheme without adaptation using the logistic function also shows a decreasing trend with ϕ in the long run. Meanwhile, there is slight fluctuation due to the truncation effect of the

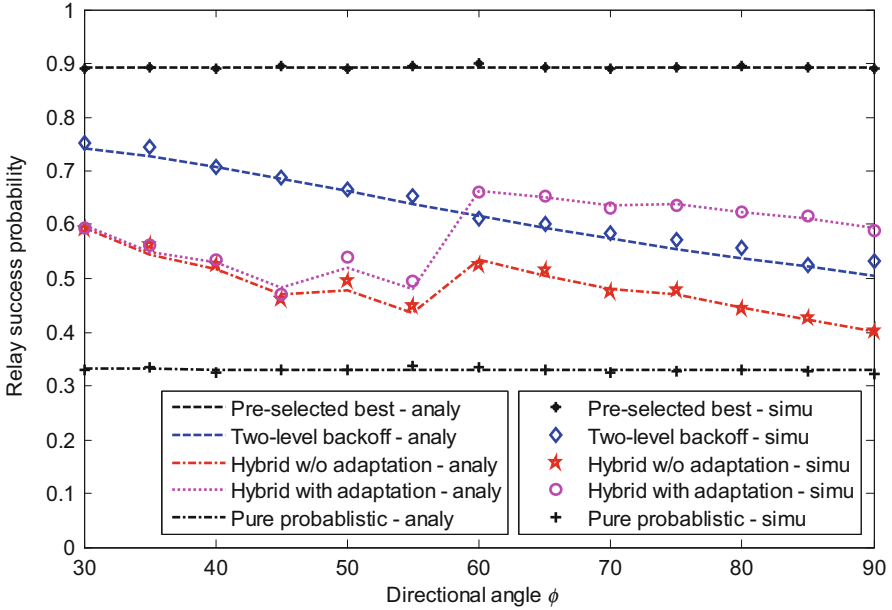


Fig. 5.7 Relay success probability of different schemes vs. directional angle ϕ ($\lambda = 10^{-2}$, $R = 70$, $L = 8$, and $\Delta = 16$)

ceiling function for the forwarding probability. When the logistic function is used to adapt the forwarding probability, the relay success probability first decreases with ϕ , then increases fast to the highest at $\phi = 60^\circ$, and last decreases slowly beyond that. This is because the logistic function takes better effect when there are more relay candidates in a larger relay region with a larger ϕ . The analytical approaches in Sect. 5.4 can characterize the impact of various system parameters on the achievable performance and be used to adjust the setting of ϕ .

The performance of the proposed cooperation schemes not only varies with the system parameters λ , R , and ϕ , but also depends on the region segmentation $\mathbf{r} = [r_0, r_1, r_2, \dots, r_L]$. As given in Sect. 5.3, we partition the entire sector Ω_{SD} into L groups, whose radius boundaries are defined by the vector \mathbf{r} . In addition to the equal-area segmentation considered above, another natural idea for grouping is to divide the source-destination distance R into L equal-length segments. Figure 5.8 compares the relay success probability of the two different configurations. As seen, for the two-level backoff-based scheme, the equal-area segmentation achieves a higher relay success probability than the equal-length segmentation. Intuitively, the number of potential relays in each region should be comparable since the contention interval Δ for each region is the same. As the relays are deployed in the sector Ω_{SD} as a homogeneous PPP of an intensity λ , the number of relays in a region is proportional to the region area. Hence, the equal-area segmentation is preferable for the two-level backoff-based scheme. On the other hand, the hybrid scheme with equal-length segmentation outperforms the equal-area segmentation when the relay intensity is

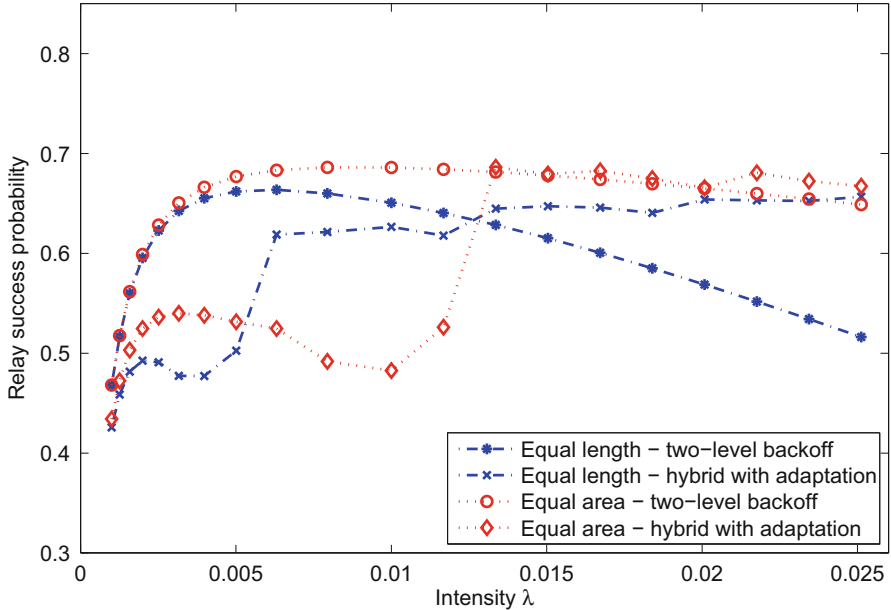


Fig. 5.8 Relay success probability of the proposed cooperation schemes with different region segmentations

in the middle range of (0.005, 0.0117). In contrast, when the relay intensity is very low and very high, the hybrid scheme with equal-area segmentation achieves a relay success probability higher than that of the equal-length segmentation.

5.5.4 Backoff Delay of Relay Selection

As seen in Sect. 5.5.3, the relay success probability varies with the system parameters λ , R , ϕ and \mathbf{r} in different manners. In Sect. 5.4, we also analyze another aspect of the relay performance in terms of the average backoff delay of relay selection. Figure 5.9 shows the analysis and simulation results for the backoff delay of the proposed cooperation schemes. As seen, the analysis results match well the simulation results, which validates the accuracy of our analytical approaches.

Moreover, it is found in Fig. 5.9 that, when the relay intensity is low, the hybrid scheme takes a shorter backoff time before any potential relay or the source starts the retransmission. This is because the backoff delay is mainly attributed to the backoff-based inter-group contention since the hybrid scheme uses the probabilistic strategy for the intra-group contention. Nonetheless, it is observed in Fig. 5.5 that the hybrid scheme achieves a smaller relay success probability when the relay intensity is low. Hence, we can see the tradeoff between the relay success probability and the

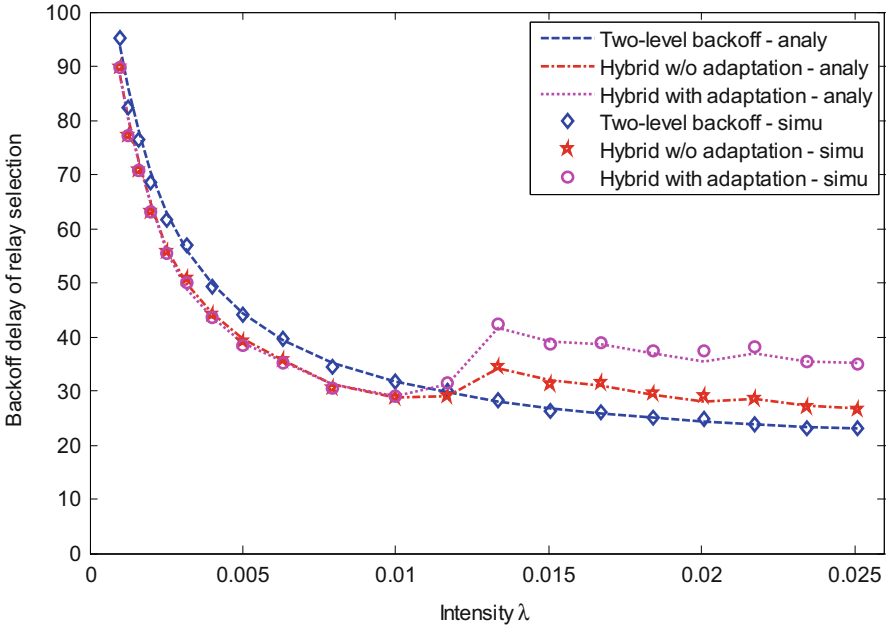


Fig. 5.9 Average backoff delay of relay selection of different schemes vs. relay intensity λ ($R = 70, \phi = 45^\circ, L = 8,$ and $\Delta = 16$)

backoff delay. On the other hand, when there is a high relay intensity, the hybrid scheme involves a backoff delay longer than that of the two-level backoff-based scheme, while the relay success probability of the hybrid scheme with adaptation is very close to that of the two-level backoff-based scheme. This implies that the hybrid scheme does not guarantee the winning relay is located in a region closer to the destination with a shorter backoff time. Even so, the logistic function can adapt the forwarding probability of the relays so that only few best relays can maintain high forwarding probabilities, which ensures less collisions and more successful transmissions.

In addition, Fig. 5.10 compares the backoff delay of the proposed cooperation schemes with two different region segmentations. Similar to Fig. 5.8, we consider the equal-area segmentation and the equal-length segmentation. As observed in Fig. 5.10, the equal-area segmentation results in a larger backoff delay. Compared to the equal-length segmentation, the equal-area segmentation allocates more relays to the groups farther away from the destination, which take a longer backoff time. As a result, the backoff delay of equal-area segmentation is larger on average. On the other hand, the backoff delay of the hybrid scheme exhibits a trend which is opposite to that of the relay success probability in Fig. 5.8 regarding the two segmentations.

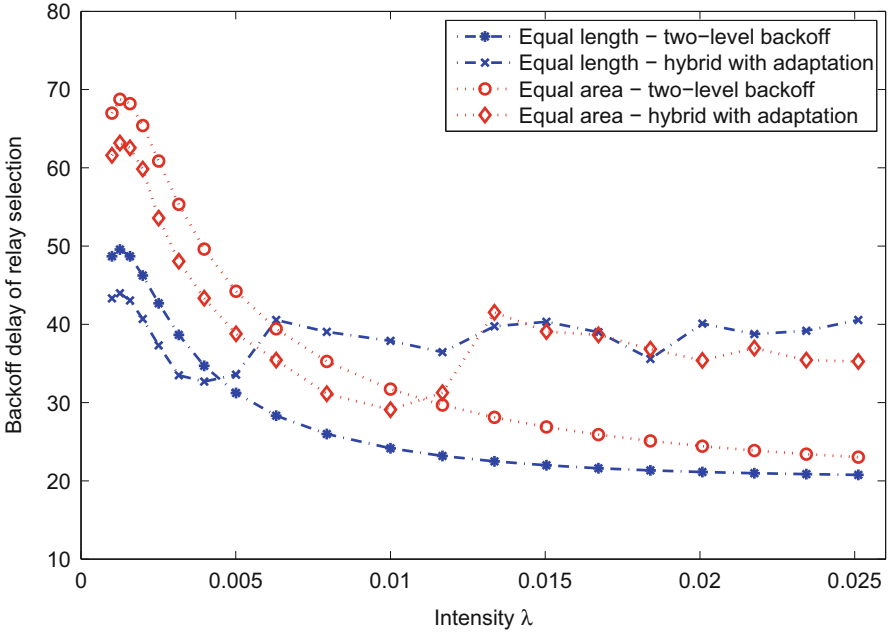


Fig. 5.10 Average backoff delay of the proposed cooperation schemes with different region segmentations

5.6 Summary

In this chapter, we study the opportunistic cooperative relaying with spatially random relays. In particular, we derive the probability distributions of the transmission success probability of spatially distributed relays, and propose two distributed relaying strategies that exploit such statistics. In the two-level backoff-based scheme, each relay independently sets a backoff time according to the location information and its transmission success probability to D . In the other hybrid backoff and probabilistic scheme, each relay first determines a backoff time according to the location information and then a forwarding probability based on its transmission success probability to D . The forwarding probability can be further adapted with a generalized logistic function so as to suppress poor relays and promote good ones.

In addition, we analytically evaluate the performance of the proposed schemes in terms of the relay success probability and average backoff delay of relay selection. The analysis accuracy is well validated by simulations. We also consider a centralized scheme with the pre-selected best relay as an upper bound and a pure probabilistic scheme as a lower bound. The proposed schemes are compared to the two reference schemes in a variety of system settings and significant performance gain is observed over the pure probabilistic scheme. The proposed analytical approaches can be used to determine appropriate configurations that balance the tradeoff between relay success probability and backoff delay.

Appendix: Calculation of the CDF $F_{\Gamma_I}(x)$ of $\Gamma_{RD,I}$

The CDF of the average received SNR at D for the forwarded signal from a potential relay in region Ω_I is defined in (5.14), which can be rewritten as

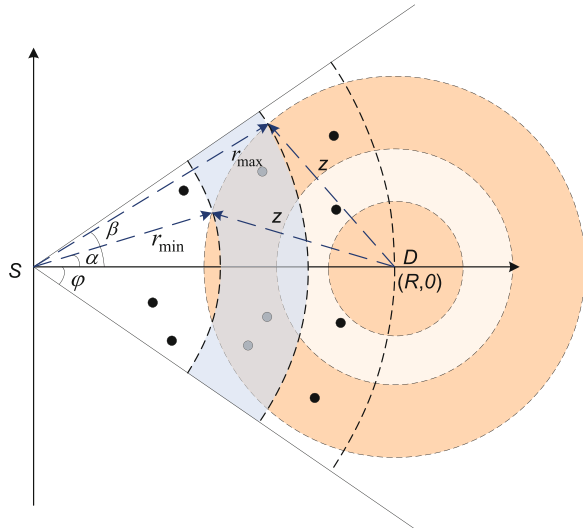
$$F_{\Gamma_I}(x) = \frac{1}{\Lambda_I} \iint_{\Omega_I} \exp(-K_0 r^2) \lambda r \cdot \mathbf{1}\left(r^2 + R^2 - 2rR \cos \theta \geq \frac{P_0/N_0}{x}\right) drd\theta. \tag{5.32}$$

Since region Ω_I is symmetric to the x axis, we can focus on the half strip above the x axis for $0 \leq \theta \leq \phi$ and define the above double integral as $2A_\Gamma(x)$.

As illustrated in Fig. 5.11, we refer to a circle centered at D of a radius $z = \sqrt{\frac{P_0/N_0}{x}}$ as D_z and define $r_{\min} = r_{I-1}$ and $r_{\max} = r_I$. According to the indicator function in (5.32), $A_\Gamma(x)$ depends on the area of region Ω_I outside the circle D_z . The shaded blue strip in Fig. 5.11 represents a specific region Ω_I under consideration. There are three cases of this region Ω_I with respect to r_{\min} , r_{\max} , and $R - z$. They are illustrated by the three dashed circles centered at D , from the smallest to the largest, respectively. Firstly, when $R - z \geq r_{\max}$, obviously $F_{\Gamma_I}(x) = 1$, since the entire circle D_z is outside Ω_I . Secondly, when $r_{\min} \leq R - z \leq r_{\max}$, the circle D_z overlaps with the right arc of region Ω_I and its angle to the origin falls within $[\alpha, \beta]$, where $\alpha = 0$ and

$$\beta = \arccos\left(\frac{R^2 + r_{\max}^2 - z^2}{2Rr_{\max}}\right). \tag{5.33}$$

Fig. 5.11 An illustration for the calculation of $F_{\Gamma_I}(x)$



Thirdly, when $R - z \leq r_{\min}$, the dashed arrow lines illustrate the corresponding situation with r_{\min} , r_{\max} , and z . Different from the second case, D_z overlaps with both arcs of Ω_l and the overlapped arc of D_z has an angle to the origin within $[\alpha, \beta]$, where β is defined in (5.33) and α is given by

$$\alpha = \arccos\left(\frac{R^2 + r_{\min}^2 - z^2}{2Rr_{\min}}\right). \quad (5.34)$$

In the following, we derive $A_\Gamma(x)$ for $r_{\min} \leq R - z \leq r_{\max}$ and $R - z \leq r_{\min}$, assuming $\phi \geq \max(\alpha, \beta)$. The same approach can be easily used to analyze other cases of ϕ . On one hand, when $\alpha \leq \beta$, for example, $\alpha = 0 \leq \beta$ if $r_{\min} \leq R - z \leq r_{\max}$, we have

$$\begin{aligned} A_\Gamma(x) &= \int_{\beta}^{\phi} d\theta \int_{r_{\min}}^{r_{\max}} \exp(-K_0 r^2) \lambda r dr \\ &\quad + \int_{\alpha}^{\beta} d\theta \int_{r_{\min}}^{r(\theta)} \exp(-K_0 r^2) \lambda r dr \end{aligned} \quad (5.35)$$

where $r(\theta)$ depicts the arc of D_z inside Ω_l and it satisfies

$$z^2 = R^2 + r^2 - 2Rr \cos \theta. \quad (5.36)$$

Solving this quadratic equation, we have

$$r(\theta) = \begin{cases} R \cos \theta - \sqrt{z^2 - R^2 \sin^2 \theta}, & \text{if } \alpha \leq \beta \\ R \cos \theta + \sqrt{z^2 - R^2 \sin^2 \theta}, & \text{if } \alpha > \beta. \end{cases} \quad (5.37)$$

Then, Eq. (5.35) can be expressed as

$$\begin{aligned} A_\Gamma(x) &= \frac{\lambda(\phi - \beta)}{2K_0} \left[\exp(-K_0 r_{\min}^2) - \exp(-K_0 r_{\max}^2) \right] \\ &\quad + \int_{\alpha}^{\beta} \frac{\lambda}{2K_0} \exp(-K_0 r_{\min}^2) d\theta \\ &\quad - \int_{\alpha}^{\beta} \frac{\lambda}{2K_0} \exp(-K_0 r^2(\theta)) d\theta \\ &= \frac{\lambda(\phi - \alpha)}{2K_0} \exp(-K_0 r_{\min}^2) - \frac{\lambda(\phi - \beta)}{2K_0} \exp(-K_0 r_{\max}^2) \\ &\quad - \int_{\alpha}^{\beta} \frac{\lambda}{2K_0} \exp\left(-K_0(z^2 + R^2 \cos(2\theta))\right) \\ &\quad \quad \exp\left(K_0(2R \cos \theta \sqrt{z^2 - R^2 \sin^2 \theta})\right) d\theta. \end{aligned} \quad (5.38)$$

On the other hand, it is possible that $\alpha > \beta$ when $R - z \leq r_{\min}$. Similarly, we can write $A_{\Gamma}(x)$ as

$$A_{\Gamma}(x) = \int_{\alpha}^{\phi} d\theta \int_{r_{\min}}^{r_{\max}} \exp(-K_0 r^2) \lambda r dr + \int_{\beta}^{\alpha} d\theta \int_{r(\theta)}^{r_{\max}} \exp(-K_0 r^2) \lambda r dr. \quad (5.39)$$

Referring to (5.37) for $r(\theta)$ when $\alpha > \beta$, we simplify (5.39) to

$$\begin{aligned} A_{\Gamma}(x) &= \frac{\lambda(\phi - \alpha)}{2K_0} \left[\exp(-K_0 r_{\min}^2) - \exp(-K_0 r_{\max}^2) \right] \\ &\quad - \int_{\beta}^{\alpha} \frac{\lambda}{2K_0} \exp(-K_0 r_{\max}^2) d\theta \\ &\quad + \int_{\beta}^{\alpha} \frac{\lambda}{2K_0} \exp(-K_0 r^2(\theta)) d\theta \\ &= \frac{\lambda(\phi - \alpha)}{2K_0} \exp(-K_0 r_{\min}^2) - \frac{\lambda(\phi - \beta)}{2K_0} \exp(-K_0 r_{\max}^2) \\ &\quad + \int_{\beta}^{\alpha} \frac{\lambda}{2K_0} \exp\left(-K_0(z^2 + R^2 \cos(2\theta))\right) \\ &\quad \quad \exp\left(-K_0(2R \cos \theta \sqrt{z^2 - R^2 \sin^2 \theta})\right) d\theta. \end{aligned} \quad (5.40)$$

As Eqs. (5.39) and (5.40) can efficiently evaluate $A_{\Gamma}(x)$, we have the CDF of the average received SNR of potential relays given by $F_{\Gamma,l}(x) = 2A_{\Gamma}(x)$. Then, according to (5.12), we can obtain the CDF of the transmission success probability of potential relays in region Ω_{l} , i.e., $G_{P,l}(y)$.

References

1. Atapattu, S., Jing, Y., Jiang, H., Tellambura, C.: Relay selection schemes and performance analysis approximations for two-way networks. *IEEE Trans. Wirel. Commun.* **61**(3), 987–998 (2013)
2. Bletsas, A., Khisti, A., Reed, D.P., Lippman, A.: A simple cooperative diversity method based on network path selection. *IEEE J. Sel. Areas Commun.* **24**(3), 659–672 (2006)
3. Carofiglio, G., Chiasserini, C., Garetto, M., Leonardi, E.: Route stability in MANETs under the random direction mobility model. *IEEE Trans. Mobile Comput.* **8**(9), 1167–1179 (2009)
4. Chen, Z., Gokeda, G., Yu, Y.: *Introduction to Direction-of-Arrival Estimation*. Artech House, Boston (2010)
5. Daneshgaran, F., Laddomada, M., Mesiti, F., Mondin, M.: Unsaturated throughput analysis of IEEE 802.11 in presence of non ideal transmission channel and capture effects. *IEEE Trans. Wirel. Commun.* **7**(4), 1276–1286 (2008)

6. Daneshgaran, F., Laddomada, M., Mesiti, F., Mondin, M., Zanolo, M.: Saturation throughput analysis of IEEE 802.11 in the presence of non ideal transmission channel and capture effects. *IEEE Trans. Commun.* **56**(7), 1178–1188 (2008)
7. Hao, Y., Tang, J., Cheng, Y.: Secure cooperative data downloading in vehicular ad hoc networks. *IEEE J. Sel. Areas Commun.* **31**(9), 132–141 (2013)
8. Hunter, J.K.: *Measure Theory*. Department of Mathematics, University of California, Davis. https://www.math.ucdavis.edu/~hunter/measure_theory/measure_theory.html (2011)
9. Jin, A., Song, W., Ju, P., Zhou, D.: Energy-aware cooperation strategy with uncoordinated group relays for delay-sensitive services. *IEEE Trans. Veh. Technol.* **63**(5), 2104–2114 (2014)
10. Ju, P., Song, W., Zhou, D.: An enhanced cooperative MAC protocol based on perceptron training. In: *Proceedings of the IEEE WCNC, Shanghai* (2013)
11. Ju, P., Song, W., Zhou, D.: Survey on cooperative medium access control protocols. *IET Commun.* **7**(9), 893–902 (2013)
12. Jukić, D., Scitovski, R.: The existence of optimal parameters of the generalized logistic function. *Appl. Math. Comput.* **77**(2–3), 281–294 (1996)
13. Liu, P., Tao, Z., Narayanan, S., Korakis, T., Panwar, S.S.: CoopMAC: a cooperative MAC for wireless LANs. *IEEE J. Sel. Areas Commun.* **25**(2), 340–354 (2007)
14. Mao, G., Fidan, B., Anderson, B.: Wireless sensor network localization techniques. *Comput. Netw.* **51**, 2529–2553 (2007)
15. MathWorks: MATLAB R. <http://www.mathworks.com> (2013)
16. Ribeiro, A., Sidiropoulos, N.D., Giannakis, G.B.: Optimal distributed stochastic routing algorithms for wireless multihop networks. *IEEE Trans. Wirel. Commun.* **7**(11), 4261–4272 (2008)
17. Shan, H., Cheng, H., Zhuang, W.: Cross-layer cooperative MAC protocol in distributed wireless networks. *IEEE Trans. Wirel. Commun.* **10**(8), 2603–2615 (2011)
18. Song, W., Ju, P., Jin, A., Cheng, Y.: Distributed opportunistic two-hop relaying with backoff-based contention among spatially random relays. *IEEE Trans. Veh. Technol.* **64**(5), 2023–2036 (2015)
19. Stoyan, D., Kendall, W., Mecke, J.: *Stochastic Geometry and its Applications*, 2nd edn. John Wiley and Sons, Chichester (1996)
20. Wang, L.C., Chen, A., Huang, S.Y.: A cross-layer investigation for the throughput performance of CSMA/CA-based WLANs with directional antennas and capture effect. *IEEE Trans. Veh. Technol.* **56**(5), 2756–2766 (2007)
21. Xiong, L., Libman, L., Mao, G.: Uncoordinated cooperative communications in highly dynamic wireless networks. *IEEE J. Sel. Areas Commun.* **30**(2), 280–288 (2012)
22. Zhai, C., Zhang, W., Mao, G.: Uncoordinated cooperative communications with spatially random relays. *IEEE Trans. Wirel. Commun.* **11**(9), 3126–3135 (2012)
23. Zhu, H., Cao, G.: rDCF: A relay-enabled medium access control protocol for wireless ad hoc networks. *IEEE Trans. Mobile Comput.* **5**(9), 1201–1214 (2006)
24. Zorzi, M., Rao, R.R.: Geographic random forwarding (GeRaF) for ad hoc and sensor networks: energy and latency performance. *IEEE Trans. Mobile Comput.* **2**(4), 349–365 (2003)

Chapter 6

Diversity Relaying with Spatially Random Mobile Relays

6.1 Motivation and Overview¹

Cooperative communications [18, 19] enable cooperation among mobile terminals to form virtual antennas and achieve spatial diversity via cooperation. Specifically, the cooperating helper nodes can relay the overheard signal from the source by various schemes, such as amplify-and-forward (AF) and decode-and-forward (DF). A variety of cooperative communication techniques were studied for wireless sensor networks [22], wireless local area networks [13], and wireless ad hoc networks [1].

Generally speaking, the cooperation among wireless nodes, which brings spatial diversity gain, can be performed in a centralized or distributed manner. In centralized cooperation, the source gathers the knowledge about the helpers and selects the best helper(s) for cooperation. The analysis of the diversity gain often needs certain a priori deterministic knowledge of the network, such as the number of helpers, and their locations and characteristics of received signal strength [3, 4, 17]. The collection of such knowledge is reasonable when the network topology is static. It becomes challenging, however, with a varying topology, e.g., when the nodes are moving and their locations are changing. In such circumstances, the received signal strength of helpers (e.g., the expectation of the received signal-to-noise ratio) presents dynamic variations which are related to the locations of helpers. Hence, the collected network knowledge can be out-of-date quickly with fast movements [12]. As a result, the selected relay may not be the best due to lack of accurate network information, which undermines the achievable cooperation gain at the physical layer and/or the media access control (MAC) layer.

¹Copyright © Elsevier (2014). Reprinted with permission from Journal of Network and Computer Applications (2014), 46, P. Ju, W. Song, A. Jin, and D. Zhou, “Performance analysis and enhancement for a cooperative wireless diversity network with spatially random mobile helpers,” pp. 305–314 [11].

On the other hand, a distributed approach requires minimum a priori knowledge of the helpers and thus is robust to network variations. Nonetheless, it is more complex to analyze the diversity gain of a distributed approach, especially in the case of multiple helpers where the spatial diversity gain of cooperation can be potentially high. From the physical-layer point of view, the more helpers, the higher the diversity gain. Meanwhile, more coordination delay may also be involved at the MAC layer. Hence, it is important to balance the tradeoff between the physical-layer diversity gain and MAC-layer delay.

Based on the above observations, this chapter aims to address the following key questions:

- When the helpers are moving, the fading characteristics of the received signal strength is not static but varying with the node locations. In such a case, how can we analyze the diversity gain?
- Considering node mobility, the spatial distribution of potential helpers is random depending on the overheard signal quality. In particular, the number of potential helpers becomes a random variable. How can the spatially random distribution of helpers impact on the diversity gain?
- Intuitively, there is a tradeoff between the physical-layer diversity gain and MAC-layer delay when multiple helpers are available. Nonetheless, the exact scaling relationship depends on the spatial distribution of helpers. How can we mathematically quantify the tradeoff and obtain an optimal balance point in this tradeoff relationship?

To answer the above questions, we focus on a wireless diversity system with multiple helpers based on a distributed cooperation strategy. Each node independently decides to cooperate as a helper or not based on its local estimates of signal-to-noise ratio (SNR) between the source, the destination, and itself. As such, each node does not need to acquire a global knowledge of other helper candidates and their channel characteristics. Moreover, the potential helpers are assumed subject to random direction (RD) mobility [16]. As a result, the spatial distribution of helpers becomes random. Hence, we apply stochastic geometry [8, 21] to model the random locations of potential helper nodes and analyze the aggregate cooperative performance with multiple helpers.

First, assuming that the spatial random locations of all nodes, except the source and the destination, follow a Poisson point process (PPP), we analyze the helper set with $p(x)$ -thinning [21] and derive the exact form and approximation forms of the probability distribution of the upper bound of the total combined SNR. Then, based on the SNR upper bound, we further obtain the unconditional success probability of the multi-helper cooperation strategy. This is the probability that the received SNR is above a given threshold and it is also the complement of the outage probability. The success probability is proved to be approximately linear with the number of helpers and the helper intensity under certain conditions. To evaluate the tradeoff between the success probability and delay, we consider two medium access control (MAC) schemes to coordinate multiple helpers, i.e., an ALOHA-like scheme and a timer-based random backoff scheme. It is shown that the delay of the ALOHA scheme

increases exponentially with the number of helpers, whereas the delay of the timer-based scheme increases more slowly. To characterize the tradeoff, we further define a success/delay ratio, which can be maximized by adapting the intensity measure of selected helpers.

6.2 System Model

6.2.1 Channel Model

We consider a two-dimensional circle Borel area $\mathbb{B}(o, B)$ as shown in Fig. 6.1 with an origin o and radius B . The source node $s(-R, 0)$ and the destination node $d(0, R)$ are fixed, where $R < B$. A Rayleigh fading channel is considered between any data transmitter x and receiver y . The received instantaneous SNR, γ_{xy} , can be modelled by an exponential distribution [7] with a PDF conditional on the average SNR $\bar{\gamma}_{xy}$, given by

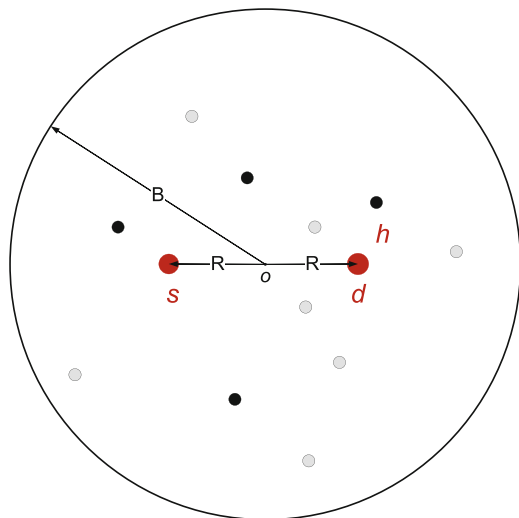
$$f_{\gamma_{xy}}(\gamma|\bar{\gamma}_{xy}) = \frac{1}{\bar{\gamma}_{xy}} e^{-\frac{\gamma}{\bar{\gamma}_{xy}}}, \quad \gamma \geq 0. \quad (6.1)$$

Here, the PDF characteristic $\bar{\gamma}_{xy}$ depends on log-distance path loss, given by

$$\bar{\gamma}_{xy} = K_0 \|x - y\|^{-\alpha} \quad (6.2)$$

where $\|\cdot\|$ is the Euclidean distance operator, α is the path-loss exponent, and $K_0 = P_0/N_0$ is the ratio of transmit power to additive white Gaussian noise (AWGN)

Fig. 6.1 System topology. *Black* nodes represent eligible helpers while *gray* ones are not helpers



power. Specifically, when $\alpha = 2$, $\bar{\gamma}_{sd} = \frac{K_0}{4R^2}$. It should be noticed that, in a system with randomly distributed mobile helpers, $\bar{\gamma}_{xy}$ itself is a random variable depending on the locations of the nodes. Denoting the PDF of $\bar{\gamma}_{xy}$ by $f_{\bar{\gamma}_{xy}}(\gamma)$, we have the unconditional PDF of γ_{xy} , given by $f_{\gamma_{xy}}(\gamma|\bar{\gamma}_{xy})f_{\bar{\gamma}_{xy}}(\gamma)$.

6.2.2 Mobility Model and Poisson Point Process

We refer to all the nodes in $\mathbb{B}(o, B)$ except s and d as *potential helpers*. All the potential helpers are assumed subject to random direction (RD) mobility [16]. For the RD mobility model, a helper is uniformly placed at an initial position in $\mathbb{B}(o, B)$ at time $t = 0$ and then chooses a direction and a speed that are uniformly distributed, with a wrapping around assumption when it hits the boundary. According to [16], at any following time instant $t > 0$, the position of the helper preserves a uniform distribution. Thus, the location of a potential helper z in a polar coordination system, denoted by (r_{oz}, θ_z) , follows the PDF expressed as

$$f_{r_{oz}}(r) = \frac{2r}{B^2}, \quad 0 \leq r \leq B \quad (6.3)$$

$$f_{\theta_z}(\theta) = \frac{1}{2\pi}, \quad 0 \leq \theta \leq 2\pi. \quad (6.4)$$

We further assume that the number of potential helpers in $\mathbb{B}(o, B)$, N_B , follows a Poisson distribution with a probability mass function (PMF):

$$\Pr[N_B = n] = \frac{\lambda_B^n}{n!} e^{-\lambda_B}, \quad n = 0, 1, \dots \quad (6.5)$$

where the intensity measure $\lambda_B = \lambda\pi B^2$ and λ is a constant. Combining the location distribution in (6.3) and (6.4) and the distribution of the number of potential helpers in (6.5), we see that the mobile potential helpers can be modeled by a homogeneous Poisson point process (PPP), denoted by Φ_B .

6.2.3 Distributed Cooperative Transmission

Here, we consider a distributed cooperative transmission strategy. Whenever the source node s has a packet to transmit, it first sends a ready-to-send (RTS) message and waits for a clear-to-send (CTS) response from the destination d . Based on the overheard RTS and CTS packets, a *potential helper* z can estimate the SNR between itself and s and d , denoted by γ_{sz} and γ_{zd} , respectively. Node z is automatically activated as a *helper* as long as $\gamma_{sz} \geq \Gamma_s$ and $\gamma_{zd} \geq \Gamma_d$. Here, Γ_s and Γ_d are thresholds pre-defined according to the quality-of-service (QoS) requirement. They can be the

same constants for all potential helpers or vary with the actual locations of the potential helpers. For example, the potential helpers relatively far from s and d can use low thresholds to allow more nodes to participate in cooperative transmission.

Based on the above distributed helper selection, all helpers selected from Φ_B constitute a new point process defined by

$$\Phi_H = \{z | z \in \Phi_B, \gamma_{sz} \geq \Gamma_s, \gamma_{zd} \geq \Gamma_d\}. \quad (6.6)$$

We show in Sect. 6.2.2 that the number of *potential helpers* in Φ_B and their locations are random variables. As a result of (6.6), the number of *helpers* (denoted by N) and their locations are also random variables for each cooperation. On receiving *CTS*, s transmits its data packet and the helpers that overhear the data packet successfully also relay the packet to d . Since multiple helpers may contribute to the relaying, we consider certain coordination schemes specified in Sect. 6.2.4 to minimize collisions among the helpers. Finally, d combines all the received signals based on MRC (to be discussed in Sect. 6.2.5). If the total SNR is above a decoding threshold γ_0 , an *ACK* message is returned. Otherwise, the data transmission fails and s retransmits the packet after timeout or a *NACK* message is received.

6.2.4 MAC for Multi-Helper Coordination

Due to the opportunistic behavior of the distributed helper selection described in Sect. 6.2.3, it is possible that multiple helpers are eligible for cooperative transmission. Thus, multiple helpers need to be properly coordinated with an effective MAC scheme to minimize collisions among their cooperative transmissions. We assume that the transmission channel is time-slotted and each packet takes one time slot to transmit. An error-free broadcast feedback channel exists between d and all participating helpers, so that d returns an *ACK* or *NACK* message after each transmission to indicate whether the relayed signal is successfully received or not. Based on the feedback, the helpers who have experienced collisions can schedule retransmission attempts according to certain MAC schemes. The above assumptions are typical for the analysis of cooperative MAC protocols [6, 9] and can be supported by simple techniques such as busy tone [20].

First, we consider an ALOHA-like MAC scheme for comparison purposes. If a packet from s is overheard by a potential helper z that satisfies $\gamma_{sz} \geq \Gamma_s$ and $\gamma_{zd} \geq \Gamma_d$ in one time slot, z becomes a helper and accesses the channel in the next slot with a probability p to forward this packet. If more than one helper transmits at the same time slot, a collision happens and the collided helpers re-access the channel with the probability p in the next slot. A helper will remain silent once it has successfully occupied the channel for a transmission until all the helpers have made their cooperative contributions without collisions. After that, s starts to transmit a new packet.

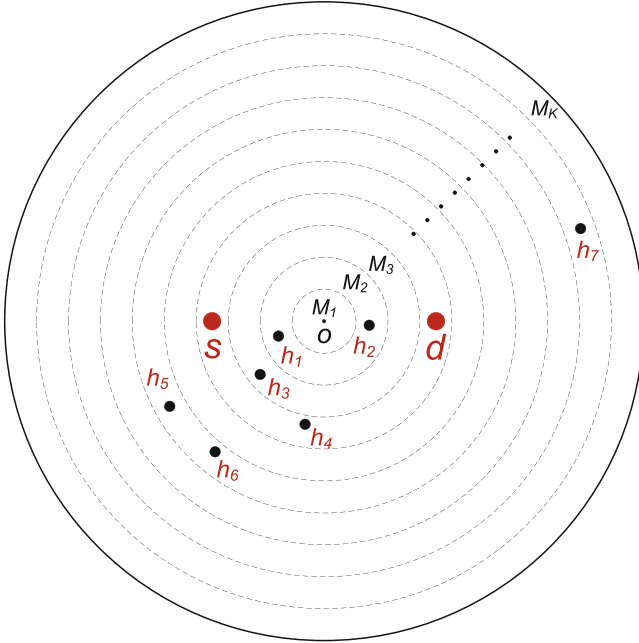


Fig. 6.2 Timer-based random backoff scheme

In practice, the ALOHA scheme is not realistic since the delay increases exponentially with the number of participating helpers. Hence, we further propose a timer-based random backoff scheme, which adopts distributed coordination and perfectly complements the distributed cooperative transmission procedure in Sect. 6.2.3. As shown later in Sect. 6.3.4, the timer-based backoff scheme exhibits a good delay property.

Consider the circle area $\mathbb{B}(o, B)$ in Fig. 6.1. We divide this area into K rings as illustrated in Fig. 6.2. Each region M_i , $i = 1, \dots, K$, is associated with a timer of a length $\Delta_i = i\delta$, where δ is a time constant. Take the example in Fig. 6.2. The helpers h_1 and h_2 in M_2 will relay their overheard signals after a backoff time 2δ , while the helper h_3 in M_3 will start its forwarding after a backoff time 3δ . Apparently, a collision will occur since there are two valid helpers in M_2 that transmit at the same time. When a collision happens a *NACK* message is broadcast, so that not only the collided helpers but also the helpers who expect to transmit after their backoff time are informed of the failed transmission. Similar to IEEE 802.11, the timer space of the region where the collided helpers are located is doubled, while the timers of the regions farther from the origin are deferred accordingly.

6.2.5 MRC and Upper Bound of Total SNR

Based on the distributed helper selection in Sect. 6.2.3, some potential helpers become active helpers and they are coordinated with the MAC schemes in Sect. 6.2.4 and relay their overheard signals using an AF scheme [14, 17]. At the destination node d , all the received signals are combined with MRC and the total SNR is given by [14]

$$\gamma_{tot} = \gamma_{sd} + \sum_{i=1}^N \frac{\gamma_{si}\gamma_{id}}{\gamma_{si} + \gamma_{id} + 1} \quad (6.7)$$

where the number of helpers (N), the SNR between s , d , and each helper i (γ_{sd} , γ_{si} , and γ_{id}), are all random variables, which depend on the topology defined in Sect. 6.2.1.

In practice, because (6.7) is often not tractable, the upper bound of (6.7) can be used instead. An upper bound of γ_{tot} is proposed in [2, 10], given by

$$\gamma_{ub} = \gamma_{sd} + \sum_{i=1}^N \gamma_i \quad (6.8)$$

where $\gamma_i = \min(\gamma_{si}, \gamma_{id})$. It is worth mentioning that a lower bound can be formulated by defining $\gamma_i = \min(\gamma_{si}, \gamma_{id})/2$ [2]. According to (6.1), it is easy to show that γ_i also follows an exponential distribution with a PDF

$$f_{\gamma_i}(\gamma|\tau_i) = \frac{1}{\tau_i} e^{-\frac{\gamma}{\tau_i}}, \quad \gamma \geq 0 \quad (6.9)$$

where

$$\tau_i = \frac{\bar{\gamma}_{si}\bar{\gamma}_{id}}{\bar{\gamma}_{si} + \bar{\gamma}_{id}}. \quad (6.10)$$

In [17], the non-i.i.d. PDF of γ_{ub} conditional on τ_1, \dots, τ_N is obtained as

$$f_{\gamma_{ub}}(\gamma|\tau_1, \tau_2, \dots, \tau_N) = \frac{\beta_0}{\bar{\gamma}_{sd}} e^{-\frac{\gamma}{\bar{\gamma}_{sd}}} + \sum_{i=1}^N \frac{\beta_i}{\tau_i} e^{-\frac{\gamma}{\tau_i}} \quad (6.11)$$

where

$$\beta_0 = \prod_{i=1}^N \left(1 - \frac{\tau_i}{\bar{\gamma}_{sd}}\right)^{-1}$$

$$\beta_i = \left(1 - \frac{\bar{\gamma}_{sd}}{\tau_i}\right)^{-1} \prod_{k=1, k \neq i}^N \left(1 - \frac{\tau_k}{\tau_i}\right)^{-1}, \quad i = 1, \dots, N.$$

6.3 Unconditional Success Probability and Delay

In this section, we first derive the distribution of the number of helpers (N) in the random set defined in (6.6). Then, we obtain the PDF of the locations of the random helpers. After that, the unconditional counterpart of (6.11) is obtained for a given number of helpers n . Two simplified approximations are also proposed for the unconditional PDF of the SNR upper bound. Based on these preparation steps, we eventually provide the analysis for the unconditional success probability, which is the complement of the unconditional outage probability. At the end, we analyze the delay involved with different MAC schemes and evaluate the outage-delay tradeoff.

6.3.1 Exact Unconditional PDF of SNR Upper Bound

For any potential helper z in Φ_B , its SNR of the channel from s to z and the SNR of the channel from z to d (i.e., γ_{sz} and γ_{zd}) are independent. According to (6.1), (6.2) and (6.6), the probability that a potential helper z is an eligible helper can be written as

$$\begin{aligned}
 P_z &= \Pr[\gamma_{sz} \geq \Gamma_s, \gamma_{zd} \geq \Gamma_d] \\
 &= \int_{\Gamma_s}^{\infty} \int_{\Gamma_d}^{\infty} f_{\gamma_{sz}}(\gamma_1 | \bar{\gamma}_{sz}) f_{\gamma_{zd}}(\gamma_2 | \bar{\gamma}_{zd}) d\gamma_1 d\gamma_2 \\
 &= \exp\left(\frac{-\Gamma_s \|s - z\|^\alpha - \Gamma_d \|z - d\|^\alpha}{K_0}\right). \tag{6.12}
 \end{aligned}$$

As seen in (6.12), whether a node is an eligible helper or not is related to its location. Thus, the helper set Φ_H can be generated from Φ_B by retaining z in Φ_B with a probability P_z and deleting it with a probability $(1 - P_z)$. The resulting point process of remaining nodes forms Φ_H . This is actually the result of an independent $p(x)$ -thinning operation to Φ_B . The $p(x)$ -thinning operation defines a retention probability $p(x)$ for each point x of a PPP and yields a thinned point process by deleting the point x with a probability $1 - p(x)$ [21]. According to *Prekopa's Theorem* [21], the number of eligible helpers is still Poisson distributed with a parameter λ_H , given by

$$\lambda_H = \int_0^B \int_0^{2\pi} \exp\left(\frac{-\Gamma_s \|s - z\|^\alpha - \Gamma_d \|z - d\|^\alpha}{K_0}\right) \frac{\lambda_B}{\pi B^2} r dr d\theta. \tag{6.13}$$

We consider the following location-dependent thresholds for helper selection:

$$\Gamma_s = \Gamma_d = \frac{K_0 \ln(2r_{oz})}{2(r_{oz}^2 + R^2)} \tag{6.14}$$

where r_{oz} is the distance between a potential helper z and the origin and $\ln(\cdot)$ is the natural logarithm. As such, when $\alpha = 2$, we have

$$\lambda_H = \frac{\lambda_B}{B}. \quad (6.15)$$

Thus, the number of helpers in Φ_H is Poisson distributed with the PMF

$$\Pr[N = n] = \frac{\lambda_H^n}{n!} e^{-\lambda_H}, \quad n = 0, 1, \dots \quad (6.16)$$

Proposition 6.1. *For a given $N = n$, when the selection thresholds are defined in (6.14) and $\alpha = 2$, the distance between a helper in Φ_H and the origin (denoted by r_{oh}) follows a uniform distribution with the normalized PDF:*

$$f_{r_{oh}}(r) = \frac{1}{B}, \quad 0 \leq r \leq B. \quad (6.17)$$

Proof. Here, r_{oz} denotes the distance between a potential helper z and the origin o , while r_{oh} is the distance between an eligible helper h and the origin. Based on the relationship of r_{oz} and r_{oh} , we can obtain

$$\begin{aligned} \Pr[r_{oh} \leq r] &= \Pr[r_{oz} \leq r \text{ and } z \text{ is selected as } h | r_{oz}] \\ &= \int_0^r f_{r_{oz}}(x) P_z(x) dx. \end{aligned} \quad (6.18)$$

Substituting $f_{r_{oz}}$ and P_z in (6.18) by (6.3) and (6.12), respectively, we can easily prove (6.17). ■

Proposition 6.2. *When $\alpha = 2$ and the thresholds of helper selection are defined as (6.14), any random variable τ_i in (6.10) has a PDF given by*

$$f_\tau(t) = \frac{K_0}{4Bt^2} \left(\frac{K_0}{2t} - R^2 \right)^{-\frac{1}{2}}, \quad \frac{K_0}{2(B^2 + R^2)} < t < \frac{K_0}{2R^2}. \quad (6.19)$$

Proof. According to Apollonius' theorem, we combine (6.2) and (6.10) and have

$$\begin{aligned} \frac{1}{\tau_i} &= \frac{\|s - h\|^2 + \|h - d\|^2}{K_0} \\ &= 2(r_{oh}^2 + R^2)/K_0 \end{aligned} \quad (6.20)$$

where r_{oh} is the distance of any helper h in Φ_H to the origin o . From Proposition 6.1, we know that r_{oh} follows a uniform distribution. Based on (6.17) and (6.20), it is straightforward to obtain (6.19) for the PDF of any τ_i . ■

Applying the PDF of τ_i , we can remove the conditions of τ_1, \dots, τ_N in (6.11). The unconditional PDF of the upper bound of total SNR when $N = n$ can be expressed as

$$f_{\gamma_{ub}}(\gamma) = \underbrace{\int \cdots \int}_n f_{\gamma_{ub}}(\gamma|t_1, t_2, \dots, t_n) \cdot f_{\tau_1}(t_1) \cdots f_{\tau_n}(t_n) dt_1 \cdots dt_n. \quad (6.21)$$

Lemma 6.1. *For a given $N = n$, the exact form of the unconditional PDF of γ_{ub} is expressed as*

$$f_{\gamma_{ub}}(\gamma) = \underbrace{\frac{C^n}{\bar{\gamma}_{sd}} e^{-\frac{\gamma}{\bar{\gamma}_{sd}}}}_{F_1} + n \underbrace{\int_{\mathbb{I}} W(\gamma, t) U(t)^{n-1} dt}_{F_2} \quad (6.22)$$

where \mathbb{I} is the interval $\left(\frac{K_0}{2(B^2+R^2)}, \frac{K_0}{2R^2}\right)$ and

$$C = 1 + \frac{R}{B} \ln \left(\frac{B-R}{B+R} \right)$$

$$W(\gamma, t) = \frac{e^{-\frac{\gamma}{t}}}{t - \bar{\gamma}_{sd}} f_{\tau}(t)$$

$$U(t) = 1 + \frac{K_0}{4B\sqrt{tY}} \ln \left(\frac{Bt - \sqrt{tY}}{Bt + \sqrt{tY}} \right), \quad Y = \frac{K_0}{2} - R^2 t.$$

Proof. The proof of Lemma 6.1 is given in [Appendix: Proof of Lemma 6.1](#). ■

6.3.2 Approximate Unconditional PDF of SNR Upper Bound

In (6.22), F_2 is very complicated and a closed-form expression is not tractable. Besides, the exact form does not shed much insight on deriving the success or outage probability. Hence, we propose to use the Newton-Cotes formula [5] of the open type to approximate (6.22). Specifically, redefining the integral interval $\mathbb{I} = \left(\frac{K_0}{2(B^2+R^2)}, \frac{K_0}{2R^2}\right)$ as (a, b) , we have the i th Newton-Cotes sampling point of m degree as $x_{mi} = a + \frac{i(b-a)}{m}$. Then, (6.22) can be approximated by

$$f_{\gamma_{ub}}(\gamma) \approx \frac{C^n}{\bar{\gamma}_{sd}} e^{-\frac{\gamma}{\bar{\gamma}_{sd}}} + n \sum_{i=1}^{m-1} A_{mi} W(\gamma, x_{mi}) U(x_{mi})^{n-1} \quad (6.23)$$

where A_{mi} is the i th coefficient of the Newton-Cotes formula of m degree. When $B \gg R$, it is obvious that $C \approx 1$ and $U(t) \approx 1$. As a result, (6.23) can be further simplified as

$$f_{\gamma_{ub}}(\gamma) \approx \frac{1}{\bar{\gamma}_{sd}} e^{-\frac{\gamma}{\bar{\gamma}_{sd}}} + n \sum_{i=1}^{m-1} A_{mi} W(\gamma, x_{mi}). \quad (6.24)$$

6.3.3 Approximation of Unconditional Success Probability

The success probability, which is the complement of the outage probability, is defined as the probability that γ_{ub} is above a certain threshold γ_0 when $N = n$, which can be expressed as

$$P_s(n) = \int_{\gamma_0}^{\infty} f_{\gamma_{ub}}(\gamma) d\gamma. \quad (6.25)$$

Lemma 6.2. For a given $N = n$, the success probability of the cooperative wireless system as described in Sect. 6.2.1 can be approximated by

$$P_s(n) \approx C^n e^{-\frac{\gamma_0}{\bar{\gamma}_{sd}}} + n \sum_{i=1}^{m-1} x_{mi} A_{mi} W(\gamma_0, x_{mi}) U(x_{mi})^{n-1} \quad (6.26)$$

where x_{mi} and A_{mi} are the i th Newton-Cotes sampling point and coefficient of m degree, respectively. If $B \gg R$, (6.26) can be further simplified as

$$P_s(n) \approx E + nA \quad (6.27)$$

where E and A are constants given by

$$E = e^{-\frac{\gamma_0}{\bar{\gamma}_{sd}}} \quad (6.28)$$

$$A = \sum_{i=1}^{m-1} x_{mi} A_{mi} W(\gamma_0, x_{mi}). \quad (6.29)$$

Proof. It can be easily proved that $W(\gamma, t)$ satisfies the following property

$$\int_{\gamma_0}^{\infty} W(\gamma, t) d\gamma = tW(\gamma_0, t). \quad (6.30)$$

Applying this property to (6.23) and (6.25), we have

$$\begin{aligned}
 P_s(n) &\approx \int_{\gamma_0}^{\infty} \frac{C^n}{\bar{\gamma}_{sd}} e^{-\frac{\gamma}{\bar{\gamma}_{sd}}} d\gamma + n \sum_{i=1}^{m-1} A_{mi} U(x_{mi})^{n-1} \int_{\gamma_0}^{\infty} W(\gamma, x_{mi}) d\gamma \\
 &= C^n e^{-\frac{\gamma_0}{\bar{\gamma}_{sd}}} + n \sum_{i=1}^{m-1} A_{mi} U(x_{mi})^{n-1} \cdot x_{mi} W(\gamma_0, x_{mi}) \\
 &= C^n e^{-\frac{\gamma_0}{\bar{\gamma}_{sd}}} + n \sum_{i=1}^{m-1} x_{mi} A_{mi} W(\gamma_0, x_{mi}) U(x_{mi})^{n-1}.
 \end{aligned}$$

Thus, (6.26) is proved. Similarly, (6.27) can be derived by using the property in (6.30) to (6.24) and (6.25). ■

Theorem 6.1. *The unconditional success probability of the wireless diversity system that uses the distributed cooperative transmission with spatially random helpers as described in Sect. 6.2.1 is given by*

$$\mathcal{P}_s = \sum_{i=1}^{\infty} \frac{\lambda_H^i}{i!} e^{-\lambda_H} P_s(n). \quad (6.31)$$

When $\alpha = 2$ and $B \gg R$, (6.31) can be approximated by

$$\mathcal{P}_s \approx E + \lambda_H A \quad (6.32)$$

where λ_H is the intensity measure of Φ_H given in (6.13), and E and A are constants given in (6.28) and (6.29), respectively.

Proof. Equation (6.31) provides the unconditional expectation of the success probability. It can be easily obtained by averaging $P_s(n)$ with the PMF of N , which follows the Poisson distribution in (6.16). Equation (6.32) is a straightforward result of (6.27) and (6.31), since the mean of N is equal to the intensity λ_H . ■

6.3.4 Delay Analysis of MAC Coordination Schemes

As discussed in Sect. 6.2.4, we consider both an ALOHA-like MAC scheme and a timer-based random backoff scheme to coordinate multiple available helpers. These MAC schemes may introduce different levels of collisions, which have a direct impact on the cooperative transmission. In this section, we analyze the delay of the two MAC schemes, which is another important performance metric in addition to the success probability evaluated in Sect. 6.3.3.

In the ALOHA-like MAC scheme, an eligible helper accesses the channel with a probability p to forward the overheard packet. Given n eligible helpers in total, if i ($1 \leq i \leq n$) helpers have not made their relaying contributions, the probability that the channel is successfully occupied by only one of these helpers is given by

$$P_a(i) = \binom{i}{1} p(1-p)^{i-1}, \quad i = 1, \dots, n. \quad (6.33)$$

Let L denote the number of wasted time slots before a slot is successfully occupied by one of the i helpers. Obviously, L follows a geometric distribution with the parameter $P_a(i)$ and has a PMF

$$\Pr[L = l|i] = [1 - P_a(i)]^{l-1} P_a(i), \quad l = 1, 2, \dots \quad (6.34)$$

Thus, the average number of time slots before one of the i helpers successfully captures the channel and relays the packet is given by

$$\bar{L}(i) = \frac{1}{P_a(i)}.$$

The same contention process repeats until each of the n helpers has successfully occupied the channel and relayed the packet. Therefore, we can obtain the total delay as

$$D_A(n) = \sum_{i=1}^n \frac{\xi}{ip(1-p)^{i-1}} \quad (6.35)$$

where ξ is the time slot for a packet transmission.

As shown later in Sect. 6.4, $D_A(n)$ increases exponentially with n . To simplify the calculation in (6.35), we can approximate the delay by

$$\tilde{D}_A(n) = \varepsilon \zeta^n \quad (6.36)$$

where the coefficients ε and ζ can be determined by fitting two sample values $D_A(1)$ and $D_A(\tilde{n})$ with (6.36). Thus, we have

$$\varepsilon = D_A(1), \quad \zeta = \left[\frac{D_A(\tilde{n})}{D_A(1)} \right]^{\frac{1}{\tilde{n}}}. \quad (6.37)$$

Combining (6.16) and (6.35), we further obtain the average delay with the ALOHA scheme as

$$\bar{D}_A = \sum_{i=1}^{\infty} \frac{\lambda_H^n}{n!} e^{-\lambda_H} \tilde{D}_A(n) = \varepsilon e^{\lambda_H(\zeta-1)}. \quad (6.38)$$

For the timer-based backoff scheme, it is intractable to derive a closed-form expression for the delay. Therefore, we provide a numerical approximation based on the observation of the simulation results. In particular, the delay of the timer-based backoff scheme is approximated by

$$\tilde{D}_T(n) = \mu_2 n^2 + \mu_1 n + \mu_0 \quad (6.39)$$

where the coefficients μ_2 , μ_1 , and μ_0 can be obtained by using three delay sample values when the number of helpers is 1, $\frac{\tilde{n}}{2}$, and \tilde{n} , which are denoted by $D_T(1)$, $D_T(\frac{\tilde{n}}{2})$, and $D_T(\tilde{n})$, respectively. Then, based on the Lagrange numerical analytical expression [15], we have

$$\mu_2 = \frac{D_T(1)}{(1 - \tilde{n}/2)(1 - \tilde{n})} - \frac{D_T(\frac{\tilde{n}}{2})}{(\tilde{n}/2 - 1)\tilde{n}/2} + \frac{D_T(\tilde{n})}{(\tilde{n} - 1)\tilde{n}/2} \quad (6.40)$$

$$\mu_1 = -\frac{(3\tilde{n}/2)D_T(1)}{(1 - \tilde{n}/2)(1 - \tilde{n})} + \frac{(1 + \tilde{n})D_T(\frac{\tilde{n}}{2})}{(\tilde{n}/2 - 1)\tilde{n}/2} - \frac{(1 + \tilde{n}/2)D_T(\tilde{n})}{(\tilde{n} - 1)\tilde{n}/2} \quad (6.41)$$

$$\mu_0 = \frac{\tilde{n}^2 D_T(1)}{2(1 - \tilde{n}/2)(1 - \tilde{n})} - \frac{\tilde{n} D_T(\frac{\tilde{n}}{2})}{(\tilde{n}/2 - 1)\tilde{n}/2} + \frac{\tilde{n} D_T(\tilde{n})}{2(\tilde{n} - 1)\tilde{n}/2}. \quad (6.42)$$

We further combine (6.16) and (6.39) to evaluate the average delay of the timer-based backoff scheme by

$$\bar{D}_T = \sum_{i=1}^{\infty} \frac{\lambda_H^i}{i!} e^{-\lambda_H} \tilde{D}_T(i) = \mu_2 \lambda_H^2 + (\mu_2 + \mu_1) \lambda_H + \mu_0. \quad (6.43)$$

6.3.5 Outage-Delay Tradeoff

As the complement of success probability, the outage probability, denoted by \mathcal{P}_o , is the probability that the total SNR at d falls below the decoding threshold γ_0 , which means that a data transmission fails. When the direct channel between s and d is poor, more helpers should be involved for a higher diversity gain. On the other hand, a larger overhead of coordination delay may also be introduced due to collisions among more helpers. As seen, there is a tradeoff between the outage probability and the delay.

In Sect. 6.3.3, the success probability \mathcal{P}_s is derived and given in (6.32). Hence, the outage probability can be written as $\mathcal{P}_o = 1 - \mathcal{P}_s$. The delay of the two MAC schemes is analyzed in Sect. 6.3.4 and given in (6.38) and (6.43). For the ALOHA-like scheme, we can relate the delay to the outage probability as follows:

$$\bar{D}_A = \varepsilon \exp\left(\frac{1 - E - \mathcal{P}_o}{A}(\zeta - 1)\right). \quad (6.44)$$

According to (6.32), we have $\lambda_H = \frac{1-E-\mathcal{P}_o}{A}$, which can be applied to (6.38) to obtain (6.44). Similarly, the outage-delay tradeoff for the timer-based backoff scheme can be expressed as

$$\overline{\mathcal{D}}_T = \mu_2 \left(\frac{1-E-\mathcal{P}_o}{A} \right)^2 + (\mu_2 + \mu_1) \left(\frac{1-E-\mathcal{P}_o}{A} \right) + \mu_0. \quad (6.45)$$

Considering the overall system performance, we are interested in the ratio of the success probability to the delay, defined by

$$\mathcal{B} = \frac{\mathcal{P}_s}{\mathcal{D}} \quad (6.46)$$

in which the delay \mathcal{D} can be interpreted as the price paid to achieve certain success probability \mathcal{P}_s . When the ALOHA scheme is used, based on (6.32) and (6.38), the success/delay ratio is written as

$$\mathcal{B}_A = \frac{E + \lambda_H A}{\varepsilon e^{\lambda_H(\xi-1)}}. \quad (6.47)$$

Taking the first-order derivative of (6.47) with respect to λ_H , we can find that the success/delay ratio is maximized when

$$\lambda_H = \hat{\lambda}_A = \frac{1}{\xi-1} - \frac{E}{A}. \quad (6.48)$$

Likewise, for the timer-based backoff scheme, the success/delay ratio can be obtained from (6.32) and (6.43) as

$$\mathcal{B}_T = \frac{E + \lambda_H A}{\mu_2 \lambda_H^2 + (\mu_2 + \mu_1) \lambda_H + \mu_0}. \quad (6.49)$$

Similarly, the success/delay ratio is maximized when

$$\lambda_H = \hat{\lambda}_T = \frac{-\mu_2 E + \sqrt{(\mu_2 E)^2 + \mu_2 \mu_0 A^2 - \mu_2 (\mu_1 + \mu_2) A E}}{\mu_2 A}. \quad (6.50)$$

6.4 Numerical and Simulation Results

In this section, we first validate the accuracy of the linear approximation of Lemma 6.2. Then, we compare the numerical results and simulation results for the unconditional success probability \mathcal{P}_s derived in Theorem 6.1 and the delay of the ALOHA scheme and the backoff timer-based scheme, $\overline{\mathcal{D}}_A$ and $\overline{\mathcal{D}}_T$, given in (6.38) and (6.43). Finally, we present numerical results demonstrating the outage-delay tradeoff. The main system parameters are given in Table 6.1.

Table 6.1 System parameters

Definition	Symbol	Value
Intensity measure of Φ_B	λ_B	500
Location parameter of nodes s and d	R	5
Circle area radius	B	40
Transmit SNR	K_0	14.7 dB
Decoding SNR threshold	γ_0	$2\bar{\gamma}_{sd}$
Path loss exponent	α	2
ALOHA channel access probability	p	0.4
Number of contention regions	K	10
Time slot length	ξ	1

6.4.1 Analysis Validation

Figure 6.3a shows how the success probability $P_s(n)$ varies with the number of helpers n . As seen, the simulation results exhibit an apparent linear tendency and our analysis results have a good approximation accuracy. Figure 6.3a further shows the analysis error versus the approximation degree m . As expected, the higher the degree m , the closer the approximation. For example, when $m = 6$, the relative error is as low as 4 %.

Figure 6.3b compares the numerical results and simulation results to verify the conclusion in Theorem 6.1. If the nodes are located according to the system model in Sect. 6.2.2 and the helpers are selected by the distributed algorithm in Sect. 6.2.3, the number of helpers follows a Poisson distribution of a parameter λ_H . It is clearly shown in Fig. 6.3b that the unconditional success probability varies linearly with λ_H , which confirms Eq. (6.32).

Figure 6.4a shows the numerical and simulation results of delay with the ALOHA scheme and the timer-based backoff scheme. As seen, the simulation results match well the numerical approximations in (6.36) and (6.39). Here, the coefficients of the delay approximation for the ALOHA scheme are $\varepsilon = 2.50$ and $\zeta = 1.44$, given that the access probability $p = 0.4$. In this case, the delay increases exponentially with the number of helpers due to collisions. On the other hand, for the timer-based backoff scheme, we choose the parameter $\tilde{n} = 15$ and determine the coefficients of the delay approximation as $\mu_2 = 0.075$, $\mu_1 = 1.46$, and $\mu_0 = 3.98$. Apparently, the timer-based backoff scheme performs much better in terms of delay when the number of helpers are potentially large. This observation is also verified by Fig. 6.4b, which shows the numerical results of (6.38) and (6.43). It is seen that when the nodes are densely deployed with a large λ_H , the timer-based backoff scheme is more effective in handling collisions and mitigating the delay overhead.

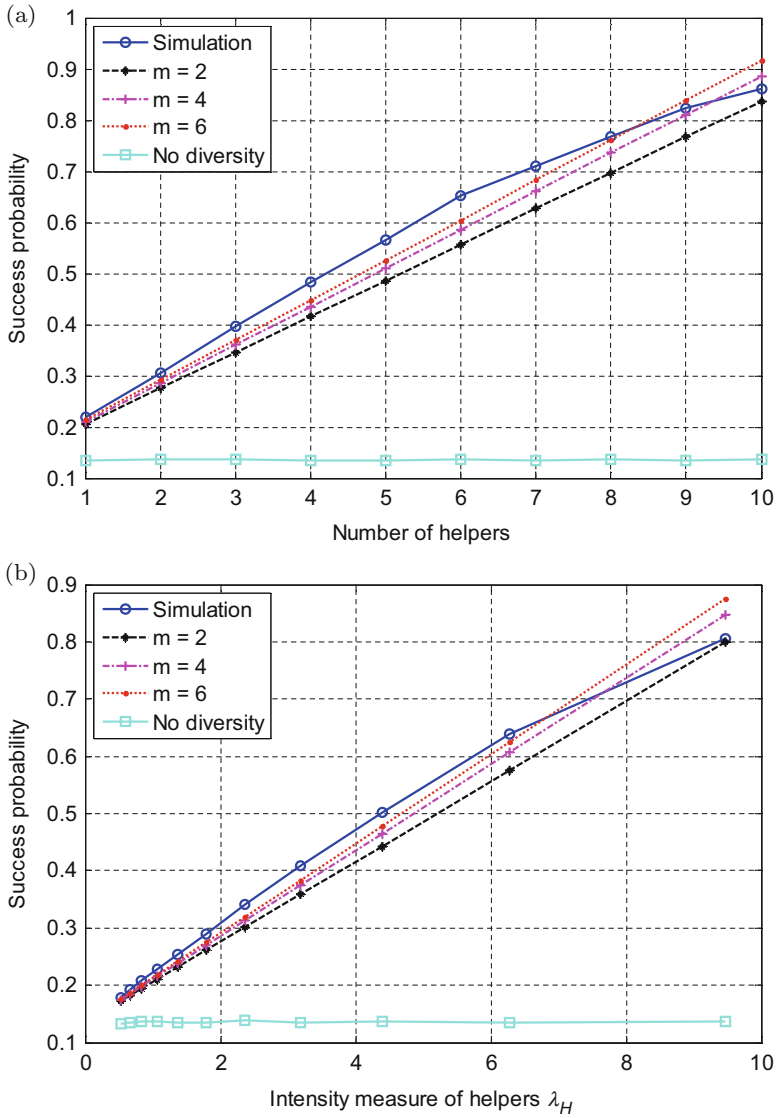


Fig. 6.3 Success probability. (a) Success probability vs. the number of helpers (b) Success probability vs. the intensity measure λ_H

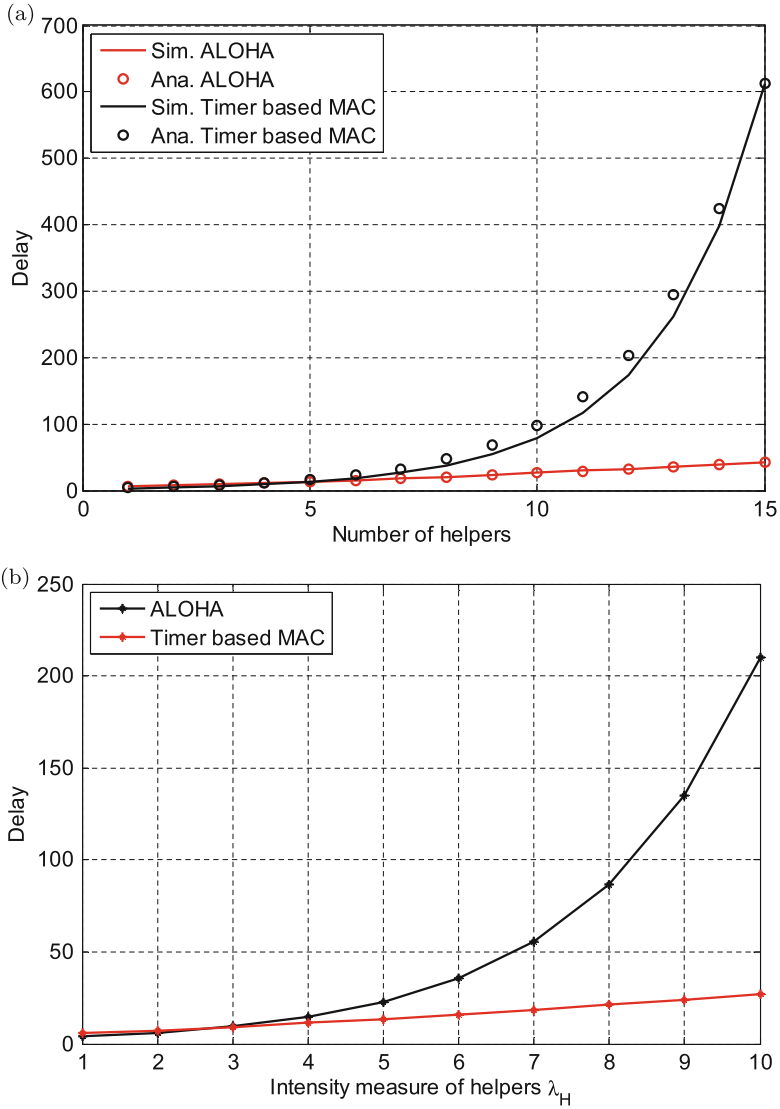


Fig. 6.4 Delay performance. (a) Delay vs. the number of helpers. (b) Delay vs. the intensity measure λ_H

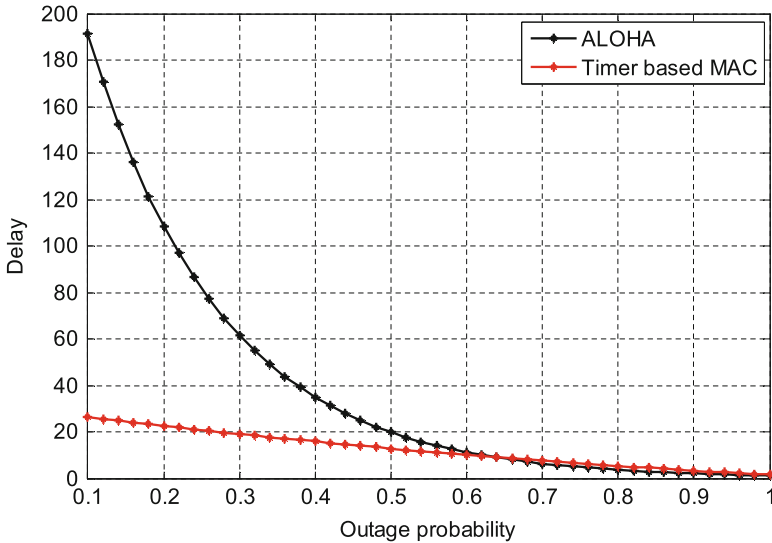


Fig. 6.5 Outage-delay tradeoff ($m = 6$)

6.4.2 Outage-Delay Tradeoff

While the success probability presents a linear increase with the number of helpers, the delay also increases fast due to the multi-helper coordination. Figure 6.5 shows the numerical results of (6.44) and (6.45), which demonstrates the tradeoff between the outage probability and the delay. As observed in Fig. 6.5, when the QoS requirement of the outage probability is very low, there is a much larger delay overhead with the ALOHA scheme compared to the timer-based backoff scheme. As the outage requirement is further relaxed, the difference between these two MAC schemes diminishes.

Figure 6.6 shows the variation of the success/delay ratio defined in (6.47) and (6.49) with the intensity measure λ_H . This success/delay ratio can be interpreted as the price paid in terms of delay to achieve certain required success probability. As seen, the success/delay ratio of the ALOHA scheme drops dramatically after the ratio reaches the maximum when the helper intensity measure $\lambda_H = \hat{\lambda}_A = 0.69$, which is obtained from (6.48). In contrast, the timer-based backoff scheme experiences much smaller fluctuation. The success/delay ratio is maximal when $\lambda_H = \hat{\lambda}_T = 2.8$ as calculated by (6.50). It means that the timer-based backoff scheme also performs well in a dense network. Since the intensity measure of helpers λ_H is related to that of potential helpers λ_B according to (6.15), we can use pre-selection to adapt λ_H so that the success/delay ratio is maximized.

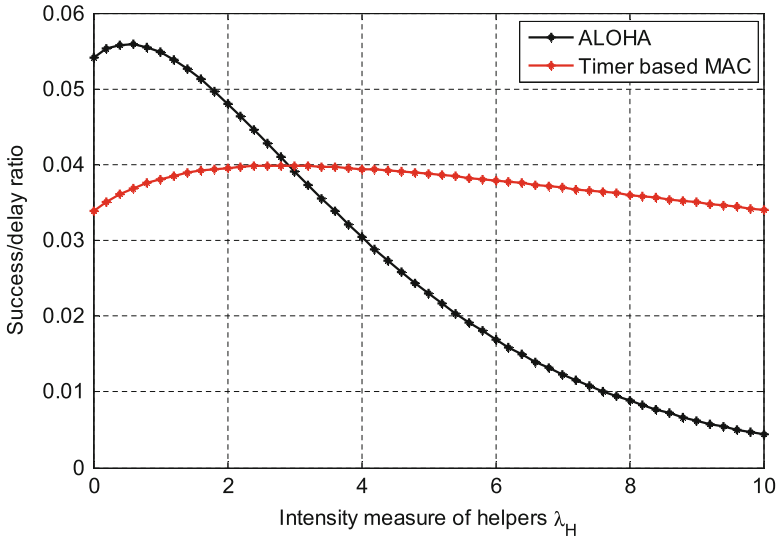


Fig. 6.6 Success/delay ratio vs. the intensity measure λ_H

6.5 Summary

In this chapter, we considered a wireless diversity system with multiple mobile helpers using a distributed cooperation strategy. As the helpers are assumed to be randomly deployed in certain area, the number of helpers and their spatial locations are not deterministic or known in advance. Taking into account the spatial random characteristics of helpers, we analyzed the cooperative transmission success probability. We found that the success probability is linear with the number of helpers when the system covers a sufficiently large area. Further, because the number of eligible helpers is random itself, the unconditional success probability is only related to the intensity measure of the point process of helpers. Considering an ALOHA-like MAC scheme and a timer-based random backoff scheme, we quantified the tradeoff between the success probability and delay, and defined the performance metric success/delay ratio. The ratio can be maximized by adapting the helper intensity λ_H which is linearly related to the overall node intensity λ_B .

The conclusions and analysis results are not only mathematically proved but also validated by simulations. The approximations of the success probability simplify the performance evaluation and exhibit a high accuracy. A basic framework is also built to analyze wireless diversity systems with distributed cooperation. Exploiting the mobility models defined with stochastic geometry, we can naturally involve more mobility patterns of nodes in the analysis.

Appendix: Proof of Lemma 6.1

Proof. The original expression of the unconditional PDF of γ_{ub} is given in (6.21). Based on (6.11), (6.21) can be divided into the following two parts:

$$F_1 = \underbrace{\int_{\mathbb{I}} \cdots \int_{\mathbb{I}}}_{n} \frac{\beta_0}{\gamma_{sd}} e^{-\frac{\gamma}{\gamma_{sd}}} f_{\tau_1}(t_1) \cdots f_{\tau_n}(t_n) dt_1 \cdots dt_n \quad (6.51)$$

$$F_2 = \underbrace{\int_{\mathbb{I}} \cdots \int_{\mathbb{I}}}_{n} \sum_{i=1}^n \frac{\beta_i}{t_i} e^{-\frac{\gamma}{t_i}} f_{\tau_1}(t_1) \cdots f_{\tau_n}(t_n) dt_1 \cdots dt_n. \quad (6.52)$$

For F_1 , since τ_i ($i = 1, \dots, n$) are independent of each other, and $e^{-\frac{\gamma}{\gamma_{sd}}}$ is separable from β_0 and $f_{\tau}(t_i)$, we rewrite (6.51) as

$$F_1 = \frac{1}{\gamma_{sd}} e^{-\frac{\gamma}{\gamma_{sd}}} \left[\int_{\mathbb{I}} \left(1 - \frac{t}{\gamma_{sd}}\right)^{-1} f_{\tau}(t) dt \right]^n = \frac{C^n}{\gamma_{sd}} e^{-\frac{\gamma}{\gamma_{sd}}}$$

where

$$C = \int_{\mathbb{I}} \left(1 - \frac{t}{\gamma_{sd}}\right)^{-1} f_{\tau}(t) dt = 1 + \frac{R}{B} \ln \left(\frac{B-R}{B+R} \right).$$

Since $t_1 \cdots t_n$ are symmetric for the integral in (6.52), the following equation holds for any $i \neq j$:

$$\underbrace{\int_{\mathbb{I}} \cdots \int_{\mathbb{I}}}_{n} \frac{\beta_i}{t_i} e^{-\frac{\gamma}{t_i}} f_{\tau_1}(t_1) \cdots f_{\tau_n}(t_n) dt_1 \cdots dt_n = \underbrace{\int_{\mathbb{I}} \cdots \int_{\mathbb{I}}}_{n} \frac{\beta_j}{t_j} e^{-\frac{\gamma}{t_j}} f_{\tau_1}(t_1) \cdots f_{\tau_n}(t_n) dt_1 \cdots dt_n.$$

Thus, (6.52) can be derived as follows:

$$\begin{aligned} F_2 &= \underbrace{\int_{\mathbb{I}} \cdots \int_{\mathbb{I}}}_{n} \sum_{i=1}^n \frac{\beta_i}{t_i} e^{-\frac{\gamma}{t_i}} f_{\tau_1}(t_1) \cdots f_{\tau_n}(t_n) dt_1 \cdots dt_n \\ &= \sum_{i=1}^n \underbrace{\int_{\mathbb{I}} \cdots \int_{\mathbb{I}}}_{n} \frac{\beta_i}{t_i} e^{-\frac{\gamma}{t_i}} f_{\tau_1}(t_1) \cdots f_{\tau_n}(t_n) dt_1 \cdots dt_n \\ &= n \underbrace{\int_{\mathbb{I}} \cdots \int_{\mathbb{I}}}_{n} \frac{\beta_1}{t_1} e^{-\frac{\gamma}{t_1}} f_{\tau_1}(t_1) \cdots f_{\tau_n}(t_n) dt_1 \cdots dt_n. \end{aligned}$$

It is further noticed that, the above integral has two separate parts which depend on either t_1 or t_i ($i = 2, \dots, n$). Therefore, replacing t_1 by t and t_i ($i = 2, \dots, n$) by s and considering τ_i ($i = 2, \dots, n$) are independent of each other, we can simplify (6.53) as follows:

$$\begin{aligned} F_2 &= n \underbrace{\int_{\mathbb{I}} \cdots \int_{\mathbb{I}}}_{n} \frac{\beta_1}{t_1} e^{-\frac{\gamma}{t_1}} f_{\tau_1}(t_1) \cdots f_{\tau_n}(t_n) dt_1 \cdots dt_n \\ &= n \int_{\mathbb{I}} \frac{e^{-\frac{\gamma}{t}}}{t - \bar{\gamma}_{sd}} f_{\tau}(t) \left[\int_{\mathbb{I}} \left(1 - \frac{s}{t}\right)^{-1} f_{\tau}(s) ds \right]^{n-1} dt \\ &= n \int_{\mathbb{I}} W(\gamma, t) U(t)^{n-1} dt \end{aligned}$$

where we define

$$\begin{aligned} W(\gamma, t) &\triangleq \frac{e^{-\frac{\gamma}{t}}}{t - \bar{\gamma}_{sd}} f_{\tau}(t) \\ U(t) &\triangleq \int_{\mathbb{I}} \left(1 - \frac{s}{t}\right)^{-1} f_{\tau}(s) ds = 1 + \frac{K_0}{4B\sqrt{tY}} \ln \left(\frac{Bt - \sqrt{tY}}{Bt + \sqrt{tY}} \right) \end{aligned}$$

and $Y \triangleq \frac{K_0}{2} - R^2t$. Thus, Lemma 6.1 is proved. ■

References

1. Al-Sultan, S., Al-Doori, M.M., Al-Bayatti, A.H., Zedan, H.: A comprehensive survey on vehicular ad hoc network. *J. Netw. Comput. Appl.* **37**, 380–392 (2014)
2. Anghel, P.A., Kaveh, M.: Exact symbol error probability of a cooperative network in a Rayleigh-fading environment. *IEEE Trans. Wirel. Commun.* **3**(5), 1416–1421 (2004)
3. Avestimehr, A.S., Tse, D.N.C.: Outage capacity of the fading relay channel in the low-SNR regime. *IEEE Trans. Inf. Theory* **53**(4), 1401–1415 (2007)
4. Beaulieu, N.C., Hu, J.: A closed-form expression for the outage probability of decode-and-forward relaying in dissimilar Rayleigh fading channels. *IEEE Commun. Lett.* **10**(12), 813–815 (2006)
5. Davis, P.J., Rabinowitz, P.: *Methods of Numerical Integration*, 2nd edn. Academic Press, Orlando (1984)
6. Gokturk, M.S., Ercetin, O., Gurbuz, O.: Throughput analysis of ALOHA with cooperative diversity. *IEEE Commun. Lett.* **12**(6), 468–470 (2008)
7. Goldsmith, A.: *Wireless Communications*, 1st edn. Cambridge University Press, Cambridge (2005)
8. Haenggi, M., Andrews, J.G., Fran, Baccelli, F., Dousse, O., Franceschetti, M.: Stochastic geometry and random graphs for the analysis and design of wireless networks. *IEEE J. Sel. Areas Commun.* **27**(7), 1029–1046 (2009)

9. Hong, Y.W.P., Lin, C., Wang, S.: Exploiting cooperative advantages in slotted ALOHA random access networks. *IEEE Trans. Inf. Theory* **56**(8), 3828–3846 (2010)
10. Ikki, S., Ahmed, M.H.: Performance analysis of cooperative diversity wireless networks over Nakagami-m fading channel. *IEEE Commun. Lett.* **11**(4), 334–336 (2007)
11. Ju, P., Song, W., Jin, A., Zhou, D.: Performance analysis and enhancement for a cooperative wireless diversity network with spatially random mobile helpers. *J. Netw. Comput. Appl.* **46**, 305–314 (2014)
12. Ju, P., Song, W., Zhou, D.: Survey on cooperative medium access control protocols. *IET Commun.* **7**(9), 893–902 (2013)
13. Kumar, D.S., Nagarajan, N.: Relay technologies and technical issues in IEEE 802.16j mobile multi-hop relay (MMR) networks. *J. Netw. Comput. Appl.* **36**(1), 91–102 (2013)
14. Laneman, J.N., Tse, D.N.C., Wornell, G.W.: Cooperative diversity in wireless networks: efficient protocols and outage behavior. *IEEE Trans. Inf. Theory* **50**(12), 3062–3080 (2004)
15. Li, H.: *Numerical Analysis*, 1st edn. Huazhong University of Science and Technology Press, Wuhan (2003)
16. Nain, P., Towsley, D., Liu, B., Liu, Z.: Properties of random direction models. In: *Proceedings of the IEEE INFOCOM*, Miami, vol. 3, pp. 1897–1907 (2005)
17. Nechiporenko, T., Phan, K.T., Tellambura, C., Nguyen, H.H.: on the capacity of Rayleigh fading cooperative systems under adaptive transmission. *IEEE Trans. Wirel. Commun.* **8**(4), 1626–1631 (2009)
18. Sendonaris, A., Erkip, E., Aazhang, B.: User cooperation diversity—part I: system description. *IEEE Trans. Commun.* **51**(11), 1927–1938 (2003)
19. Sendonaris, A., Erkip, E., Aazhang, B.: User cooperation diversity—part II: implementation aspects and performance analysis. *IEEE Trans. Commun.* **51**(11), 1939–1948 (2003)
20. Shan, H., Wang, P., Zhuang, W., Wang, Z.: Cross-layer cooperative triple busy tone multiple access for wireless networks. In: *Proceedings of the IEEE GLOBECOM*, New Orleans (2008)
21. Stoyan, D., Kendall, W., Mecke, J.: *Stochastic Geometry and Its Applications*, 2nd edn. John Wiley & Sons, Chichester (1996)
22. Tarnq, H., Chuang, B., Liu, P.: A relay node deployment method for disconnected wireless sensor networks: applied in indoor environments. *J. Netw. Comput. Appl.* **32**(3), 652–659 (2009)

Chapter 7

Conclusions and Future Directions

7.1 Conclusions

MAC protocols in cooperative networks not only need to fulfill the function of a regular MAC protocol which is to coordinate multiple nodes sharing the wireless medium and alleviate the effect of hidden and exposed terminals, but also need to address several fundamental problems, such as when to cooperate and whom to cooperate with. In this book brief, we investigate cooperative MAC protocols with energy saving taking into account spatially random mobile relays. The main results are summarized and highlighted in the following.

- ***Energy-efficient cooperative MAC for single S-D pair.*** We first introduced an algorithm to estimate the unknown intensity of relay distribution, which is critical to properly engage cooperating nodes. The convergence and accuracy of the estimation algorithm have been theoretically and numerically justified. Although the backoff-based scheme can save considerable energy consumption when compared to the centralized schemes and probability-based schemes, we found that many relays may be active unnecessarily. Hence, we further proposed a distributed energy saving scheme to minimize energy consumption while maintaining satisfactory transmission success probability. To evaluate the performance of the proposed cooperative scheme with energy saving, we analyzed the collision probability and derived an upper bound. Moreover, the simulation results showed that the energy saving scheme can significantly reduce the energy consumption.
- ***Energy-efficient cooperative MAC for multiple S-D pairs.*** Extending the widely studied single S-D pair scenario, we considered a new framework where multiple S-D pairs share a group of relays with energy constraint. To satisfy the QoS requirement of multimedia services in a green manner, we proposed an energy-aware distributed cooperative scheme. Besides, we derived the theoretical performance bounds for the proposed scheme with respect to the collision

probability and transmission success probability. Extensive simulations were conducted to compare the performance of different distributed schemes and the analytical bounds. As shown in the simulation results, by adjusting the weighting parameter, we can achieve good performance in the high traffic load condition through energy balance. Moreover, the theoretical and simulation results demonstrated that our proposed scheme can achieve much energy saving.

- ***Opportunistic cooperative relaying with backoff-based contention.*** We studied the opportunistic cooperative relaying with spatially random relays. In particular, we derived the probability distributions of the transmission success probability of spatially distributed relays, and proposed two distributed relaying strategies that exploit such statistics. In addition, we analytically evaluated the performance of the proposed schemes in terms of the relay success probability and average backoff delay of relay selection. The analysis accuracy is well validated by simulations. The proposed analytical approaches can be used to determine appropriate configurations that balance the tradeoff between relay success probability and backoff delay.
- ***Relay selection in the multiple-helper diversity mobile scenario.*** We focused on a wireless diversity system with multiple helpers and distributed cooperation. Each node independently decides whether to cooperate as a helper or not based on its local estimates of SNR. Moreover, considering random direction mobility, we obtained the unconditional success probability of multi-helper diversity cooperation, which is proven to be approximately linear with the number of helpers and the helper intensity under certain conditions. To further evaluate the tradeoff between the success probability and delay, we investigated an ALOHA-like scheme and a timer-based random backoff scheme. It was shown that the delay of the ALOHA scheme increases exponentially with the number of helpers, whereas the delay of the timer-based scheme increases more slowly. Based on our analysis, we are able to adapt the intensity measure of the selected helpers to optimize the success/delay ratio.

7.2 Future Work

The cooperative wireless networks as a very large area keep posing new challenges when cooperation becomes more deeply involved. On one hand, many possible extensions are worth investigating for the scenarios studied in this brief. On the other hand, new cooperation scenarios are arising and bring up interesting new problems.

- ***Enhancement to energy efficiency in cooperative MAC.*** The proposed energy-efficient scheme in Chap. 3 is not optimal, since we set bias for the relays close to destination due to their high transmission success probability. If we take into account the transmission success probability over the relay-destination channel, the energy consumption can be further reduced. To determine the optimal active

probability for each relay, global information of the relays is prerequisite, and more complex reasoning is required. Extending the widely studied single S-D pair to multiple S-D pairs in Chap. 4, we focused on the energy perspective, and thus defined the cooperation capability based on the energy level and the distance metric. Actually, depending on the design objective for the multiple S-D pairs scenario, the cooperation capability can be adapted accordingly. For example, to maximize the throughput of each source, the instantaneous channel state information should be incorporated into the cooperation capability.

- **Full duplexity consideration.** Half-duplexity is a fundamental assumption for the studies on cooperative communications in the literature. In recent years, full-duplex wireless communications become a hot topic as the hardware and signal processing techniques are improving. Full-duplexity will have a deep impact on both relay selection and incentive design. For relay selection, the handshaking and data transmission procedure will be fairly different. Since the nodes can retrieve information from the packets in a timely manner, the metadata of the packets would be more accurate.
- **Advanced mobility models and analysis.** Spatial diversity is related to the location of helpers nodes. Mobility is also an essential aspect of wireless nodes that cannot be neglected. In the literature, many works that involve mobility models are based on simulations, mainly because mobility in the real world is too complex to have good mathematical models that are capable of characterizing the diverse properties. To enable theoretical analysis, however, a tractable mobility model is vital. How to provide a good interface between simulation engineering and mathematical analysis for mobility models is a very challenging problem. Besides, a mobility model itself is very dependent on actual scenarios. For indoor environments, a random mobility model may be more suitable. For vehicular networks, there may be complex mobility trace patterns with low speed in the urban environment. In contrast, mobility in the suburban environment can be simpler but with higher speed. Under those different scenarios, the design of cooperative MAC protocols should be adjusted.